



The Global Methane Budget: 2000-2012

Marielle Saunois¹, Philippe Bousquet¹, Ben Poulter², Anna Peregon¹, Philippe Ciais¹, Josep G. Canadell³, Edward J. Dlugokencky⁴, Giuseppe Etiope⁵, David Bastviken⁶, Sander Houweling^{7,8}, Greet Janssens-Maenhout⁹, Francesco N. Tubiello¹⁰, Simona Castaldi^{11,12}, Robert B. Jackson¹³, Mihai Alexe⁹,
5 Vivek K. Arora¹⁴, David J. Beerling¹⁵, Peter Bergamaschi⁹, Donald R. Blake¹⁶, Gordon Brailsford¹⁷,
Victor Brovkin¹⁸, Lori Bruhwiler⁴, Cyril Crevoisier¹⁹, Patrick Crill²⁰, Charles Curry²¹, Christian
Frankenberg²², Nicola Gedney²³, Lena Höglund-Isaksson²⁴, Misa Ishizawa²⁵, Akihiko Ito²⁵, Fortunat
Joos²⁶, Heon-Sook Kim²⁵, Thomas Kleinen¹⁸, Paul Krummel²⁷, Jean-François Lamarque²⁸, Ray
Langenfelds²⁷, Robin Locatelli¹, Toshinobu Machida²⁵, Shamil Maksyutov²⁵, Kyle C. McDonald²⁹, Julia
10 Marshall³⁰, Joe R. Melton³¹, Isamu Morino²⁵, Simon O'Doherty³², Frans-Jan W. Parmentier³³, Prabir K.
Patra³⁴, Changhui Peng³⁵, Shushi Peng¹, Glen P. Peters³⁶, Isabelle Pison¹, Catherine Prigent³⁷, Ronald
Prinn³⁸, Michel Ramonet¹, William J. Riley³⁹, Makoto Saito²⁵, Ronny Schroeder^{29,40}, Isobel J. Simpson¹⁶,
Renato Spahni²⁶, Paul Steele²⁷, Atsushi Takizawa⁴¹, Brett F. Thornton²⁰, Hanqin Tian⁴², Yasunori
Tohjima²⁵, Nicolas Viovy¹, Apostolos Voulgarakis⁴³, Michiel van Weele⁴⁴, Guido van der Werf⁴⁵, Ray
15 Weiss⁴⁶, Christine Wiedinmyer²⁸, David J. Wilton¹⁵, Andy Wiltshire⁴⁷, Doug Worthy⁴⁸, Debra B.
Wunch⁴⁹, Xiyan Xu³⁹, Yukio Yoshida²⁵, Bowen Zhang⁴², Zhen Zhang^{2,50}, and Qian Zhu⁵¹.

¹Laboratoire des Sciences du Climat et de l'Environnement, LSCE-IPSL (CEA-CNRS-UVSQ), Université Paris-Saclay 91191 Gif-sur-Yvette, France

20 ²Institute on Ecosystems and Department of Ecology, Montana State University, Bozeman, MT 59717, USA

³Global Carbon Project, CSIRO, Marine and Atmospheric Research, Canberra, ACT 2601, Australia

⁴NOAA ESRL, 325 Broadway, Boulder, Colorado 80305, USA

⁵Istituto Nazionale di Geofisica e Vulcanologia, Sezione Roma 2, via V. Murata 605 00143 Roma

⁶Department of Thematic Studies – Environmental Change, Linköping University, SE-581 83 LINKÖPING, Sweden

25 ⁷Netherlands Institute for Space Research (SRON), Sorbonnelaan 2, 3584 CA Utrecht, The Netherlands

⁸Institute for Marine and Atmospheric Research Sorbonnelaan 2, 3584 CA, Utrecht, The Netherlands

⁹European Commission, Joint Research Centre, Institute for Environment and Sustainability, Air and Climate Unit, Ispra, Italy

30 ¹⁰Statistics Division, Food and Agriculture Organization of the United Nations (FAO), Viale delle Terme di Caracalla, Rome 00153, Italy

¹¹Department of Environmental Sciences, Second University of Naples, via Vivaldi 43, 81100 Caserta, Italy

¹²Centro Euro-Mediterraneo sui Cambiamenti Climatici (CMCC), via Augusto Imperatore 16, 73100 Lecce, Italy

¹³School of Earth, Energy & Environmental Sciences, Stanford University, Stanford, CA 94305-2210, USA

35 ¹⁴Canadian Centre for Climate Modelling and Analysis, Climate Research Division, Environment and Climate Change Canada, Victoria, BC, V8W 2Y2, Canada

¹⁵Department of Animal and Plant Sciences, University of Sheffield, Sheffield S10 2TN, UK

¹⁶University of California Irvine, 570 Rowland Hall, Irvine, California 92697, USA

¹⁷NIWA Turangi, 22 Turanga Place, Turangi 3334, New Zealand

¹⁸Max Planck Institute for Meteorology, Bundesstrasse 53, 20146 Hamburg, Germany

40 ¹⁹Laboratoire de Météorologie Dynamique, LMD-IPSL, Ecole Polytechnique, 91120 Palaiseau, France

²⁰Department of Geological Sciences and Bolin Centre for Climate Research, Svante Arrhenius väg 8, SE-106 91 Stockholm, Sweden

²¹School of Earth and Ocean Sciences, University of Victoria, PO Box 1700 STN CSC, Victoria, BC, Canada V8W 2Y2

²²Jet Propulsion Laboratory, M/S 183-601, 4800 Oak Grove Drive, Pasadena, CA 91109, USA



- ²³Met Office Hadley Centre, Joint Centre for Hydrometeorological Research, Maclean Building, Wallingford OX10 8BB, UK
- ²⁴Air Quality and Greenhouse Gases program (AIR), International Institute for Applied Systems Analysis (IIASA), A-2361 Laxenburg, Austria
- ²⁵Center for Global Environmental Research, National Institute for Environmental Studies (NIES), Onogawa 16-2, Tsukuba, Ibaraki 305-8506, Japan
- ²⁶Climate and Environmental Physics, Physics Institute and Oeschger Center for Climate Change Research, University of Bern, Sidlerstr. 5, CH-3012 Bern, Switzerland
- ²⁷CSIRO Oceans and Atmosphere, Aspendale, Victoria 3195 Australia
- ²⁸NCAR, PO Box 3000, Boulder, Colorado 80307-3000, USA
- ²⁹Department of Earth and Atmospheric Sciences, City University of New York, New York, NY 10031, USA
- ³⁰Max Planck Institute for Biogeochemistry, Hans Knoell Str. 10, 07745 Jena, Germany
- ³¹Climate Research Division, Environment and Climate Change Canada, Victoria, BC, V8W 2Y2, Canada
- ³²School of Chemistry, University of Bristol, Cantock's Close, Clifton, Bristol BS8 1TS
- ³³Department of Physical Geography and Ecosystem Science, Lund University, Sölvegatan 12, SE-223 62, Lund, Sweden
- ³⁴Department of Environmental Geochemical Cycle Research, JAMSTEC, 3173-25 Showa-machi, Kanazawa-ku, Yokohama, 236-0001, Japan
- ³⁵Department of Biology Sciences, Institute of Environment Science, University of Quebec at Montreal, Montreal, QC H3C 3P8, Canada
- ³⁶Center for International Climate and Environmental Research – Oslo (CICERO), Pb. 1129 Blindern, 0318 Oslo, Norway
- ³⁷CNRS/LERMA, Observatoire de Paris, 61 Ave. de l'Observatoire, 75014 Paris, France
- ³⁸Massachusetts Institute of Technology (MIT), Building 54-1312, Cambridge, MA 02139, USA
- ³⁹Earth Sciences Division, Lawrence Berkeley National Lab, 1 Cyclotron Road, Berkeley, CA 94720, USA
- ⁴⁰Institute of Botany, University of Hohenheim 70593 Stuttgart, Germany
- ⁴¹Japan Meteorological Agency (JMA), 1-3-4 Otemachi, Chiyoda-ku, Tokyo 100-8122, Japan
- ⁴²International Center for Climate and Global Change Research, School of Forestry and Wildlife Sciences, Auburn University, 602 Duncan Drive, Auburn, AL 36849, USA
- ⁴³Space & Atmospheric Physics, The Blackett Laboratory, Imperial College London, London SW7 2AZ, U.K.
- ⁴⁴KNMI, PO Box 201, 3730 AE, De Bilt, Netherlands
- ⁴⁵VU University Amsterdam, Faculty of Earth and Life Sciences, Earth and Climate Cluster, Amsterdam, The Netherlands
- ⁴⁶Scripps Institution of Oceanography (SIO), University of California San Diego, La Jolla, CA 92093, USA
- ⁴⁷Met Office Hadley Centre, FitzRoy Road, Exeter, EX1 3PB, United Kingdom
- ⁴⁸Environnement Canada, 4905, rue Dufferin, Toronto, Canada.
- ⁴⁹Department of Physics, University of Toronto, 60 St. George Street, Toronto, Ontario, Canada
- ⁵⁰Swiss Federal Research Institute WSL, Birmensdorf 8059, Switzerland
- ⁵¹State Key Laboratory of Soil Erosion and Dryland Farming on the Loess Plateau, Northwest A&F University, Yangling, Shaanxi 712100, China

Correspondance to: Marielle Saunois (marielle.saunois@lsce.ipsl.fr)

Abstract. The global methane (CH₄) budget is becoming an increasingly important component for managing realistic pathways to mitigate climate change. This relevance, due to a shorter atmospheric lifetime and a stronger warming potential than carbon dioxide, is challenged by the still unexplained changes of atmospheric CH₄ over the past decade. Emissions and concentrations of CH₄ are continuing to increase making CH₄ the second most important human-induced greenhouse gas after carbon dioxide. Two major difficulties in reducing uncertainties come from the large variety of diffusive CH₄ sources that overlap geographically, and from the destruction of CH₄ by the very short-lived hydroxyl radical (OH). To address these difficulties, we have established a consortium of multi-disciplinary scientists under the umbrella of the Global Carbon Project to synthesize and stimulate research on the methane cycle, and producing regular (~biennial) updates of the global methane



budget. This consortium includes atmospheric physicists and chemists, biogeochemists of surface and marine emissions, and socio-economists who study anthropogenic emissions. Following Kirschke et al. (2013), we propose here the first version of a living review paper that integrates results of top-down studies (T-D, exploiting atmospheric observations within an atmospheric inverse-modelling framework) and bottom-up models, inventories, and data-driven approaches (B-U, including process-based models for estimating land surface emissions and atmospheric chemistry, and inventories for anthropogenic emissions, data-driven extrapolations).

For the 2003-2012 decade, global methane emissions are estimated by T-D inversions at 558 Tg CH₄ yr⁻¹ (range [540-568]). About 60% of global emissions are anthropogenic (range [50-65%]). B-U approaches suggest larger global emissions (736 Tg CH₄ yr⁻¹ [596-884]) mostly because of larger natural emissions from individual sources such as inland waters, natural wetlands and geological sources. Considering the atmospheric constraints on the T-D budget, it is likely that some of the individual emissions reported by the B-U approaches are overestimated, leading to too large global emissions. Latitudinal data from T-D emissions indicate a predominance of tropical emissions (~64% of the global budget, <30°N) as compared to mid (~32%, 30°N-60°N) and high northern latitudes (~4%, 60°N-90°N). T-D inversions consistently infer lower emissions in China (~58 Tg CH₄ yr⁻¹ [51-72], -14%) and higher emissions in Africa (86 Tg CH₄ yr⁻¹ [73-108], +19%) than B-U values used as prior estimates. Overall, uncertainties for anthropogenic emissions appear smaller than those from natural sources, and the uncertainties on source categories appear larger for T-D inversions than for B-U inventories and models.

The most important source of uncertainty on the methane budget is attributable to emissions from wetland and other inland waters. We show that the wetland extent could contribute for 30-40% on the estimated range for wetland emissions. Other priorities for improving the methane budget include: i) the development of process-based models for inland-water emissions, ii) the intensification of methane observations at local scale (flux measurements) to constrain B-U land surface models, and at regional scale (surface networks and satellites) to constrain T-D inversions, iii) improvements in the estimation of atmospheric loss by OH, and iv) improvements of the transport models integrated in T-D inversions. The data presented here can be downloaded from the Carbon Dioxide Information Analysis Center (doi:10.3334/CDIAC/Global_Methane_Budget_2016).

1 Introduction

The surface dry air mole fraction of atmospheric methane (CH₄) reached 1810 ppb in 2012 (Fig. 1). This level, 2.5 times larger than in 1750, results from human activities related to agriculture (livestock, rice cultivation), fossil fuel usage and waste sectors, and from climate and CO₂ changes affecting natural emissions (Ciais et al., 2013). Atmospheric CH₄ is the second most impactful anthropogenic greenhouse gas after carbon dioxide (CO₂) in terms of radiative forcing. Although its global emissions, estimated at around 550 Tg CH₄ yr⁻¹ (Kirschke et al., 2013), are only 4% of the global CO₂ anthropogenic emissions in units of carbon mass flux, atmospheric CH₄ contributes 20% (~0.48 W.m⁻²) of the additional radiative forcing accumulated in the lower atmosphere since 1750 (Ciais et al., 2013). This is because of the larger warming potential of



methane compared to CO₂, about 28 times on a 100-year horizon as re-evaluated by the IPCC 5th Assessment Report (AR5) (when using Global Warming Potential metric, Myhre et al. (2013)). Also changes in other chemical compounds (such as NO_x or CO) influence the forcing of methane through changes in its lifetime. From an emission point of view, the radiative impact attributed to CH₄ emissions is about 0.97 W m⁻². This is because emission of CH₄ leads to production of ozone, of stratospheric water vapour, and of CO₂, and importantly affects its own lifetime (Myhre et al., 2013; Shindell et al., 2012). CH₄ has a short lifetime in the atmosphere (~about 9 years for the modern inventory (Prather et al., 2012) and a stabilization or reduction of CH₄ emissions leads rapidly to a stabilization or reduction of methane radiative forcing. Reduction in CH₄ emissions is therefore an effective option for climate change mitigation. Moreover, CH₄ is both a greenhouse gas and an air pollutant, and as such covered by two international conventions: the United Nations Framework Convention on Climate Change (UNFCCC) and the Convention on Long Range Transport of Air Pollution (CLRTAP).

Changes in the magnitude and timing (annual to inter-annual) of individual methane sources and sinks over the past decades are uncertain (Kirschke et al., 2013) with relative uncertainties (hereafter reported as min-max ranges) of 20-30% for inventories of anthropogenic emissions in each sector (agriculture, waste, fossil fuels) and for biomass burning, 50% for natural wetland emissions and reaching 100% or more for other natural sources (e.g. inland waters, geological). The uncertainty in the global methane chemical loss by OH, the predominant sink, is estimated between 10% (Prather et al., 2012) and 20% (Kirschke et al., 2013), implying a similar uncertainty in global methane emissions as other sinks are much smaller and the atmospheric growth rate is well-defined (Dlugokencky et al., 2009). Globally, the contribution of natural emissions to the total emissions is reasonably well quantified by combining lifetime estimates with reconstructed preindustrial atmospheric methane concentrations from ice cores (e.g. Ehhalt et al. (2001)). Uncertainties in emissions reach 40-60% at regional scale (e.g. for South America, Africa, China and India). Beyond the intrinsic value of characterizing the biogeochemical cycle of methane, understanding the evolution of the methane budget has strong implications for future climate emission scenarios. Worryingly, the current emission trajectory is tracking the warmest of all IPCC scenarios, the RCP8.5, and is clearly inconsistent with lower temperature scenarios, which show substantial to large reductions of methane emissions (Collins et al., 2013).

Reducing uncertainties in individual methane sources, and thus in the overall methane budget, is not an easy task for, at least, four reasons. First, methane is emitted by a variety of processes that need to be understood and quantified separately, both natural or anthropogenic, point or diffuse sources, and associated with three main emission processes (biogenic, thermogenic, and pyrogenic). Among them, several important anthropogenic CH₄ emission sources are poorly reported. These multiple sources and processes require the integration of data from diverse scientific communities to assess the global budget.

Second, atmospheric methane is removed by chemical reactions in the atmosphere involving radicals (mainly OH), which have very short lifetimes (typically 1 s). Although OH can be measured locally, its spatiotemporal distribution remains uncertain at regional to global scales, which cannot be assessed by direct measurements. Third, only the net methane budget (sources – sinks) is constrained by the precise observations of the atmospheric growth rate (Dlugokencky et al., 2009), leaving the sum of sources and the sum of sinks uncertain. One simplification for CH₄ compared to CO₂ is that the oceanic



contribution to the global methane budget is very small (~1-3%), making source estimation mostly a continental problem (USEPA, 2010). Finally, we lack observations to constrain 1) process models that produce estimates of wetland extent (Stocker et al., 2014; Kleinen et al., 2012) and emissions (Melton et al., 2013; Wania et al., 2013), 2) other inland water sources (Bastviken et al., 2011), 3) inventories of anthropogenic emissions (USEPA, 2010; EDGAR, 2013), and 4) atmospheric inversions, which aim at representing or estimating the different methane emissions from global to regional scales (Houweling et al., 2014; Kirschke et al., 2013; Bohn et al., 2015; Spahni et al., 2011; Tian et al., 2016). Finally, information contained in the ice core methane records has only been used in a few studies to evaluate process models (Zürcher et al., 2013; Singarayer et al., 2011).

The regional constraints brought by atmospheric sampling on atmospheric inversions are significant for northern mid-latitudes thanks to a number of high-precision and high-accuracy surface stations (Dlugokencky et al., 2011). The atmospheric observation density has improved in the tropics with satellite-based column average methane mixing ratios (Buchwitz et al., 2005b; Frankenberg et al., 2005; Butz et al., 2011). However, the optimal usage of satellite data remains limited by systematic errors in satellite retrievals (Bergamaschi et al., 2009; Locatelli et al., 2015). The partition of regional emissions by processes remains very uncertain today, waiting for the development or consolidation of measurements of more specific tracers, such as methane isotopes or ethane, dedicated to constrain the different methane sources or groups of sources (e.g. Simpson et al. (2012); Schaefer et al. (2016), Hausmann et al. (2016)).

The Global Carbon Project (GCP) aims at developing a complete picture of the carbon cycle by establishing a common, consistent scientific knowledge to support policy debate and actions to mitigate the rate of increase of greenhouse gases in the atmosphere (www.globalcarbonproject.org). The objective of this paper is to provide an analysis and synthesis of the current knowledge about the global methane cycle by gathering results of observations and models and by extracting from these the robust features and the uncertainties remaining to be addressed. We combine results from a large ensemble of bottom-up approaches (process-based models for natural wetlands, data-driven approaches for other natural sources, inventories of anthropogenic emissions and biomass burning, and atmospheric chemistry models), and of top-down approaches (methane atmospheric observing networks, atmospheric inversions inferring emissions and sinks from atmospheric observations and models of atmospheric transport and chemistry). This paper is built under the principle of a living review to be published at regular intervals (e.g. every two years) and will synthesize and update new annual data, the introduction of new data products, model development improvements, and new modelling approaches to estimate individual components contributing to the CH₄ budget.

Kirschke et al. (2013), hereafter reported as K13, was the first GCP-like CH₄ budget synthesis. K13 reported decadal mean CH₄ emissions and sinks from 1980 to 2009 based on bottom-up and top-down approaches. Our new analysis, and our approach for the living review budget, will report methane emissions for three targeted time periods: 1) the last calendar decade (2000-2009, for this paper), 2) the last available decade (2003-2012 for this paper), and 3) the last available year (2012, for this paper). Future efforts will also focus in bringing budget data as recent as possible.



Five sections follow this introduction. Section 2 presents the methodology to treat and analyse the data streams. Section 3 presents the current knowledge about methane sources and sinks based on the ensemble of B-U approaches reported here (models, inventories, data-driven approaches). Section 4 reports the atmospheric observations and the T-D inversions gathered for this paper. Section 5, based on Sect. 3 and 4, provides an analysis of the global methane budget (Sect. 5.1), and of the regional methane budget (Sect. 5.2). Finally Sect. 6 discusses future developments, missing components, and the largest remaining uncertainties after this update on the global methane budget.

2 Methodology

Unless specified, the methane budget is presented in teragrams of CH₄ per year ($1\text{Tg CH}_4.\text{yr}^{-1}=10^{12}\text{ gCH}_4.\text{yr}^{-1}$), methane concentrations as dry air mole fractions in parts per billion (ppb) and the methane annual increase, G_{ATM} , in ppb.yr^{-1} . In the different tables, we present mean values and ranges for the last calendar decade (2000-2009, for this paper), the period 2003-2012, together with results for the last available year (2012, for this paper). Results obtained from the previous synthesis are also given (K13, for this paper). Following K13 and considering the relatively small and variable number of studies available, uncertainties are reported as minimum and maximum values in brackets. These minimum and maximum values are those calculated using the boxplot analysis presented below and thus excluding identified outliers when existing.

The CH₄ emission estimates reported in this paper, deriving mainly from statistical calculations, are given with up to three digits to keep closure in the CH₄ budget (in particular in Tables 2 and 4). However, the reader should keep in mind the associated uncertainties and acknowledge a two-digit global methane budget.

2.1 Processing of emission maps

Common data analysis procedures have been applied to the different bottom-up models, inventories and atmospheric inversions whenever gridded products exist. The monthly or yearly fluxes (emissions and sinks) provided by different groups were processed similarly. They were re-gridded on a common grid ($1^\circ\times 1^\circ$) and converted into the same units (Tg CH₄ per grid cell). For coastal pixels of land fluxes, to avoid allocating land emissions into oceanic areas when re-gridding the model output, all emissions were re-allocated to the neighbouring land pixel. The opposite was done for ocean fluxes. Monthly, annual and decadal means were computed from the gridded 1° by 1° maps.

2.2 Definition of the boxplots

Most budgets are presented as boxplots, which have been created using routines in IDL language, provided with the standard version of the IDL software. The values presented in the following are calculated using the classical conventions of boxplots including quartiles (25%, median, 75%), outliers, and minimum and maximum values (without the outliers). Outliers are determined as values below the first quartile minus three times the inter-quartile range or values above third quartile plus



three times the inter-quartile range. Identified outliers (when existing) are plotted as stars on the different figures proposed. The mean values are reported in the tables and represented as “+” symbols in the figures.

2.3 Definition of regions and source categories

Geographically, emissions are reported for the global scale, for three latitudinal bands (<30°N, 30-60°N, 60-90°N, only
5 for gridded products) and for 15 regions (oceans and 14 continental regions, see Sect. 5 and Fig. 7 for region map). As anthropogenic emissions are reported at country level, we chose to define the regions based on a country list (supplementary Table S1). This approach is compatible with all T-D and B-U approaches providing gridded products as well. The number of regions was chosen to be close to the widely used TransCom inter-comparison map (Gurney et al., 2004), but with subdivisions to isolate important countries for the methane cycle (China, India, USA, and Russia). Therefore, the new region
10 map defined here is different from the TransCom map but more adapted to the methane cycle. One caveat is that the regional totals are not directly comparable with other studies reporting methane emissions on the TransCom map, although the name of some regions being the same.

Bottom-up estimates of methane emissions rely on models for individual processes (e.g. wetlands) or on inventories representing different source types (e.g. gas emissions). Chemistry-transport models generally represent methane sinks
15 individually in their chemical schemes (Williams et al., 2012). Therefore, it is possible to represent the bottom-up global methane budget for all individual sources. However, by construction, the total methane emissions derived from a combination of independent bottom-up estimates is not constrained.

For atmospheric inversions (T-D), the situation is different. Atmospheric observations provide a constraint on the global source, given a fairly strong constraint on the global sink derived using a proxy tracer such as methyl chloroform (Montzka et al., 2011b). The inversions reported in this work solve either for a total methane flux (Pison et al., 2013) or for a limited
20 number of flux categories (Bergamaschi et al., 2013). Indeed, the assimilation of CH₄ observations alone, as reported in this synthesis, cannot fully separate individual sources, although sources with different locations or temporal variations could be resolved by the assimilated atmospheric observations. Therefore, following K13, we have defined five broad categories for which top-down estimates of emissions are given: natural wetlands, agriculture and waste emissions, fossil fuel emissions,
25 biomass and biofuel burning emissions, and other natural emissions (other inland waters, wild animals, wildfires, termites, land geological sources, oceanic sources (geological and biogenic), and terrestrial permafrost). Global and regional methane emissions per source category were obtained directly from the gridded optimized fluxes if an inversion solved for the GCP categories. Alternatively, if the inversion solved for total emissions (or for different categories embedding GCP categories), then the prior contribution of each source category at the spatial resolution of the inversion was scaled by the ratio of the total
30 (or embedding category) optimized flux divided by the total (or embedding category) prior flux (K13). Also, the soil uptake was provided separately in order to report the total surface emissions and not net emissions (sources minus soil uptake). For B-U, some individual sources can be found gridded in the literature (anthropogenic emissions, natural wetlands) but some



others are not gridded yet (e.g. inland waters, geological, oceanic sources). The regional B-U methane budget per source category is therefore presented only for gridded categories (all but the “other natural” category).

In summary, bottom-up models and inventories are presented for all individual sources and for the five broad categories defined above at global scale, and only for four broad categories at regional scale. Top-down inversions are reported globally and regionally for the five broad categories of emissions.

3 Methane sources and sinks

Here we provide a complete review of all methane sources and sinks based on an ensemble of B-U approaches from multiple sources: process-based models, inventories, and data-driven methods. For each source, a description of the involved emitting process(es) is given, together with a brief description of the original data sets (measurements, models) and the related methodology. Then, the estimate for the global source and its range is given and analysed. Detailed descriptions of the data sets can be found elsewhere (see references of each component in the different subsections and tables).

Methane is emitted by a variety of sources in the atmosphere. These can be sorted by emitting process (thermogenic, biogenic or pyrogenic) or by anthropogenic versus natural origin. Biogenic methane is the final product of the decomposition of organic matter by *Archaea* in anaerobic environments, such as water-saturated soils, swamps, rice paddies, marine sediments, landfills, waste water facilities, or inside animal intestines. Thermogenic methane is formed on geological time scales by the breakdown of buried organic matter due to heat and pressure deep in the Earth’s crust. Thermogenic methane reaches the atmosphere through marine and land geologic gas seeps and during the exploitation and distribution of fossil fuels (coal mining, natural gas production, gas transmission and distribution, oil production and refinery). Finally, pyrogenic methane is produced by the incomplete combustion of biomass. Peat fires, biomass burning in deforested or degraded areas, and biofuel usage are the largest sources of pyrogenic methane. Methane hydrates, ice-like cages of methane trapped in continental shelves and below sub-sea and land permafrost, can be of biogenic or thermogenic origin. Each of the three process categories has both anthropogenic and natural components. In the following, we choose to present the different methane sources depending on their anthropogenic or natural origin, which seems more relevant for planning climate mitigation activities.

3.1 Anthropogenic methane sources

Various human activities lead to the emissions of methane to the atmosphere. Agricultural processes under anaerobic conditions such as wetland rice cultivation and livestock (enteric fermentation in animals, and the decomposition of animal wastes) emit biogenic CH₄, as does the decomposition of municipal solid wastes. Methane is also emitted during the production and distribution of natural gas and petroleum, and is released as a by-product of coal mining and incomplete fossil fuel and biomass combustion (USEPA, 2016).



Emission inventories were developed to generate bottom-up estimates of sector-specific emissions by compiling data on human activity levels and combining them with the associated emission factors.

An ensemble of individual inventories was gathered here to estimate anthropogenic methane emissions. We also refer to the extensive *AMAP Assessment Report on CH₄ as Arctic climate forcer* (Höglund-Isaksson et al., 2015), which provides a detailed presentation and description of methane inventories and global scale estimates for the year 2005 (see their chapter 5 and in particular their tables 5.1 to 5.5).

3.1.1 Reported global inventories

The main three bottom-up global inventories covering all anthropogenic emissions are from the United States Environmental Protection Agency, USEPA (2012, 2006), the Greenhouse gas and Air pollutant Interactions and Synergies (GAINS) model developed by the International Institute for Applied Systems Analysis (IIASA) (Höglund-Isaksson, 2012) and the Emissions Database for Global Atmospheric Research (EDGAR, 2010, 2013). The latter is an inventory compiled by the European Commission Joint Research Centre (EC-JRC) and Netherland's Environmental Assessment Agency (PBL). These inventories report the major sources of anthropogenic methane emissions: fossil fuel production, transmission and distribution; livestock (enteric fermentation and manure management); rice cultivation; solid waste and wastewater. However, the level of detail provided by country and by sector varies between inventories, as these inventories do not consider the same number of geographical regions and source sectors (Höglund-Isaksson et al., 2015), see their Table 5.2). In these inventories, methane emissions for a given region/country and a given sector are usually calculated as the product of an activity level, an emission factor for this activity and an abatement coefficient to account for regulations implemented to control emissions if existing (see equation 5.1 of Höglund-Isaksson et al. (2015), IPCC (2006)). The integrated emission models USEPA and the GAINS provide estimates every five or ten years for both past and future periods, while EDGAR provides annual estimates only for past emissions. There are major differences between these three inventories. While the USEPA inventory adopts the emissions reported by the countries to the UNFCCC, EDGAR and the GAINS model produced their own estimates using a consistent approach for all countries. As a result, the latter two approaches need large country-specific information or, if not available, they adopt IPCC default factors or emission factors reported to UNFCCC (Olivier et al., 2012; Höglund-Isaksson, 2012). Here, we also integrate the Food and Agriculture Organization (FAO) dataset, which provides estimates of methane emissions at country level but only for agriculture (enteric fermentation, manure management, rice cultivation, energy usage, burning of crop residues and of savannahs) and for biomass burning (Tubiello et al., 2013). It will hereafter be referred as FAO-CH₄. FAO-CH₄ uses activity data from the FAOSTAT database as reported by countries to National Agriculture Statistical Offices (FAO, 2012) and mostly the Tier 1 IPCC methodology for emissions factors (IPCC, 2006), which depend on geographic location and development status of the country. For manure, the necessary country-scale temperature was obtained from the FAO global agro-ecological zone database (GAEZv3.0, 2012).

We use the following versions of these inventories: version EDGARv42FT2010 that provides yearly gridded emissions by sectors from 2000 to 2010 (Olivier and Janssens-Maenhout, 2012; EDGAR, 2013), version 5a of the GAINS model



(Höglund-Isaksson, 2012) that assumes current legislation for air pollution for the future, the revised estimates of 2012 from the USEPA (2012), and finally, for the FAO emission database accessed in April 2016. Further details of the inventories used in this study are provided in Table 1. Overall, only EDGARv4.2FT2010 and GAINS provide gridded emission maps by sectors, and only EDGAR provides gridded maps on a yearly basis, which explains why this inventory is the most used in
 5 inverse modelling. These inventories are not all regularly updated. For the purpose of this study, the estimates from USEPA and GAINS have been linearly interpolated to provide yearly values, as provided by the EDGAR inventory. We also use the EDGARv4.2 FT2012 data, which is an update of the time series of the country total emissions until 2012 (Rogelj et al., 2014; EDGAR, 2014). This update has been developed based on EDGARv4.2FT2010 and uses IEA energy balance statistics (2013) and NIR/CRF of UNFCCC (2013), as described in part III of IEA's CO₂ book by Olivier and Janssens-Maenhout (2014).

10 For this study, engaged before the update of EDGARv4.2 inventory up to 2012, we built our own update from 2008 up to 2012 using FAO emissions to quantify CH₄ emissions from enteric fermentation, manure management and rice cultivation (described above) and BP statistical review of fossil fuel production and consumption (<http://www.bp.com/>) to update CH₄ emissions from coal, oil and gas sectors. In this inventory, called EDGARv4.2EXT, methane emissions after 2008 are set up equal to the FAO emissions (or BP statistics) of year t times the ratio between the mean EDGAR CH₄ emissions ($E_{EDGARv4.2}$)
 15 over 2006-2008 and the mean value of FAO emissions (V_{FAO} in the following equation) (or BP statistics) over 2006-2008. For each emission sector, the country-specific emissions ($E_{EDGARv4.2ext}$) in year (t) are estimated following Eq. (1):

$$E_{EDGARv4.2EXT} = V_{FAO}(t) \times \frac{1}{3} \sum_{i=2006}^{2008} (E_{EDGARv4.2}(i) / V_{FAO}(i)) \quad (1)$$

Other sources than those aforementioned are kept constant at the 2008 level. This extrapolation approach is necessary, and often performed by T-D inversions to define prior emissions, because, up to now, global inventories such as sector-specific
 20 emissions in EDGAR database are not updated on a regular basis. JRC released, however, their update up to 2012 (EDGARv4.2FT2012) containing country total emissions, which allows evaluation of our extrapolation approach. The extrapolated global totals calculated for this study are within 1% of EDGARv4.2FT2012.

3.1.2 Total anthropogenic methane emissions

Based on the ensemble of inventories detailed above, anthropogenic emissions are ~352 [340-360] Tg CH₄ yr⁻¹ for the
 25 decade 2003-2012 (Table 2, including biomass and biofuel burning). For the 2000-2009 period, anthropogenic emissions are estimated at ~338 [329-342] Tg CH₄ yr⁻¹. This estimate is consistent, albeit larger and with a smaller uncertainty range than K13 for the 2000-2009 decade (331 Tg CH₄ yr⁻¹ [304-368]). Such differences are due to the different sets of inventories gathered. The range of our estimate (~5%) is smaller than the range reported in the AMAP assessment report (~20%) both because the latter was reporting more versions of the different inventories and projections, and because it was for the
 30 particular year 2005 and not for a decade as here.

Figure 2 presents the global methane emissions of anthropogenic sources (excluding biomass and biofuel burning) estimated and projected by the different inventories between 2000 and 2020. The inventories consistently estimate that about



300 Tg of methane were released into the atmosphere in 2000 by anthropogenic activities. The main discrepancy between the inventories is observed in their trend after 2005 with the lowest emissions projected by USEPA and the largest emissions estimated by EDGARv4.2FT2012. The increase in CH₄ emissions is mainly determined from coal mining, which activity has increased considerably in China since 2002 (see Sect. 3.1.3).

5 Despite relatively good agreement between the inventories on total emissions from year 2000 onwards, large differences can be found at the sector and country levels (IPCC, 2014). Some of these discrepancies are detailed in the following sections.

For the fifth IPCC Assessment Report, four Representative Concentration Pathways (RCPs) were defined RCP8.5, RCP6, RCP4.5, and RCP2.6 (the latter is also referred to as RCP3PD, where 'PD' stands for Peak and Decline). The numbers refer to the radiative forcing by the year 2100. These four independent pathways developed by four individual modelling groups start from the identical base year 2000 (Lamarque et al., 2010). An interesting feature is the fact that global emission inventories track closer to methane emissions in the most carbon intensive scenario (RCP8.5) and that all other RCPs scenarios remain below the inventories. This suggests the tremendous challenge of climate mitigation that lies ahead, particularly if current trajectories need to change to be consistent with pathways leading to lower levels of global warming (Fig. 2).

3.1.3 Methane emissions from fossil fuel production and use

15 Most of the methane anthropogenic emissions related to fossil fuels come from the exploitation, transportation, and usage of coal, oil, and natural gas. This geological and fossil type of emission (see natural source section) is driven by human activity. Additional emissions reported in this category include small industrial contributions such as production of chemicals and metals, and fossil fuel fires. Some studies based on atmospheric ethane have suggested that methane emissions from fossil fuel extraction and distribution decreased by 10 to 30 Tg CH₄ yr⁻¹ between the 1980s and 2000s, with much of this decrease occurring before 2000 (Aydin et al., 2011; Simpson et al., 2012). However, this decrease is not fully consistent with ¹³C signals in the atmosphere as reported by Levin et al. (2012). More recently, Hausmann et al. (2016) used ethane column observations to infer a significant contribution of fossil fuel to the increase in methane's growth rate since 2007, in contrast to findings from Schaefer et al. (2016) who suggest a biogenic cause based on methane isotope measurements. Spatial distribution of methane emissions from fossil fuel is presented in Fig. 3 based on the mean gridded maps provided by EDGARv4.2FT2010 and GAINS over the 2003-2012 decade.

Global emissions of methane from fossil fuels and other industries are estimated from three global inventories in the range of [114-133] Tg CH₄ yr⁻¹ for the 2003-2012 decade with an average of 121 Tg CH₄ yr⁻¹ (Table 2), but with a large difference in the rate of change depending on inventories. It represents on average 34 % (range 32-39%) of the total global anthropogenic emissions.

30

Coal mining. During mining, methane is emitted from ventilation shafts, where large volumes of air are pumped into the mine to keep methane at a rate below 0.5% to avoid accidental inflammation. To prevent the diffusion of methane in the mining working atmosphere, boreholes are made in order to evacuate methane. In countries of the Organization for Economic



Co-operation and Development (OECD), methane recuperated from ventilation shafts is used as fuel, but in many countries it is still emitted into the atmosphere or flared, despite efforts for coalmine recovery under the UNFCCC Clean Development Mechanisms (<http://cdm.unfccc.int>). Methane emissions also occur during post-mining handling, processing, and transportation. Some CH₄ is released from coal waste piles and abandoned mines. Emissions from these sources are believed to be low because much of the CH₄ would likely be emitted within the mine (IPCC, 2000).

Almost 40% (IEA, 2012) of the world's electricity is produced from coal. This contribution grew in the 2000s at the rate of several per cent per year, driven by Asian production where large reserves exist, but has stalled from 2011 to 2012. In 2012, the top ten largest coal producing nations accounted for 88% of total world emissions for coal mining. Among them, the top three producers (China, USA and India) produced two thirds of the total (CIA, 2016).

Global estimates of methane emissions from coal mining show a large variation, in part due to the lack of comprehensive data from all major producing countries. The range of coal mining emissions is estimated at 18-46 Tg of methane for the year 2005, the highest value being from EDGARv4.2FT2010 and the lower from USEPA.

As announced in Sect. 3.1.2, coal mining is the main source explaining the differences observed between inventories at global scale (Fig. 2). Indeed, such differences are explained mainly by the different CH₄ emission factors used for calculating the fugitive emissions of the coal mining in China. Coal mining emission factors depend strongly on the type of coal extraction (underground mining emitting up to 10 times more than surface mining), the geological underground structure (very region-specific) and the quality of the coal (brown coal emitting more than hard coal). The EDGARv4.2FT2012 seems to have overestimated by a factor of 2 the emission factor for the coal mining in China and allocated this to very few coal mine locations (hotspot emissions). A recent county-based inventory of Chinese methane emissions also confirms the overestimate of about +38% with total anthropogenic emissions estimated at 43±6 Tg CH₄ yr⁻¹ (Peng et al., 2016). EDGARv4.2 follows the IPCC guidelines 2006, which recommends region-specific data. However, the EDGARv4.2 inventory compilation used the European averaged emission factor for CH₄ from coal mine production in substitution for missing data, which seems to be twice too high in China. The upcoming new version of EDGARv4.3 will revise this down and distribute the fugitive CH₄ from coal mining to more than 80 times more coal mining locations in China.

For the 2003-2012 decade, methane emissions from coal mining are estimated at 34% of total fossil fuel related emissions of methane (41 Tg CH₄ yr⁻¹, range of [26-50]), consistent with the AMAP report when considering the evolution since 2005. An additional very small source corresponds to fossil fuel fires (mostly underground coal fires, ~0.1 Tg yr⁻¹, EDGARv4.2).

Oil and natural gas systems. Natural gas is comprised primarily of methane, so any leaks during drilling of the wells, extraction, transportation, storage, gas distribution, and incomplete combustion of gas flares contribute to methane emissions (Lamb et al., 2015; Shorter et al., 1996). Fugitive permanent emissions (e.g. due to leaky valves and compressors) should be distinguished from intermittent emissions due to maintenance (e.g. purging and draining of pipes). During transportation, leakage can occur in gas transmission pipelines, due to corrosion, manufacturing, welding, etc. According to Lelieveld et al. (2005), the CH₄ leakage from gas pipelines should be relatively low, however distribution networks in older cities have



increased leakage, especially those with cast-iron and unprotected steel pipelines. Recent measurement campaigns in different cities in the USA and Europe also revealed that significant leaks occur in specific locations (e.g. storage facilities, city gates, well and pipeline pressurization/depressurization points) along the distribution networks to the end-users (Jackson et al., 2014a; McKain et al., 2015). However, methane emissions can vary a lot from one city to another depending in part on the
5 age of city infrastructure (i.e., older cities on average have higher emissions). Ground movements (landslides, earthquakes, tectonic movements) can also release methane. Finally, additional methane emissions from the oil industry (e.g. refining) and production of charcoal are estimated to be a few Tg CH₄ yr⁻¹ only (EDGAR, 2012). In many facilities, such as gas and oil fields, refineries and offshore platforms, venting of natural gas is now replaced by flaring with a partial conversion into CO₂; these two processes are usually considered together in inventories of oil and gas industries.

10 Methane emissions from oil and natural gas systems also vary greatly in different global inventories (46 to 98 Tg yr⁻¹ in 2005, Höglund-Isaksson et al. (2015)). The inventories rely on the same sources and magnitudes regarding the activity data, thus the derived differences result from different methodologies and parameters used, including both emission and activity factors. Those factors are country- or even site-specific and the few field measurements available often combine oil and gas activities (Brandt et al., 2014) and remain largely unknown for most major oil- and gas-producing countries. Depending on
15 the country, the emission factors reported may vary by two orders of magnitude for oil production and by one order of magnitude for gas production (Table 5.5 of Höglund-Isaksson et al. (2015)). The GAINS estimate of methane emissions from oil production is four times higher than EDGARDv42FT2010 and USEPA. For natural gas, the uncertainty is also large (factor of two), albeit smaller than for oil production. The difference in these estimates comes from the methodology used. Indeed, during oil extraction, the gas generated can be either recovered (re-injected or utilized as an energy source) or not
20 recovered (flared or vented to the atmosphere). The recovery rates vary from one country to another (being much higher in the USA, Europe and Canada than elsewhere), and, accounting for country-specific rates of generation and recovery of associated gas, might lead to an amount of gas released into the atmosphere four times higher during oil production than when using default values (Höglund-Isaksson, 2012). This difference in methodology explains, in part, why GAINS estimates are higher than EDGAR and USEPA. Another challenge lies in determining the amount of flared or vented unrecovered gas, with
25 venting emitting CH₄ whereas flaring converts all or most methane (often >99%) to CO₂. The balance of flaring and venting also depends on the type of oil: flaring is less common for heavy oil wells than conventional ones (Höglund-Isaksson et al., 2015). Satellite images can detect flaring (Elvidge et al., 2009; 2016) and may be used to verify the country estimates, but such satellites can not currently be used to estimate the efficiency of CH₄ conversion to CO₂.

For the 2003-2012 decade, methane emissions from upstream and downstream natural oil and gas sectors are estimated to
30 represent about 65% of total fossil CH₄ emissions (79 Tg CH₄ yr⁻¹, range of [69-88], Table 2), with a lower uncertainty range than for coal emissions for most countries.

Shale gas. Production of natural gas from the exploitation of hitherto unproductive rock formations, especially shale, began in the 1980s in the US on an experimental or small-scale basis, then, from early 2000s, exploitations started at large



commercial scale. Two techniques developed and often applied together are horizontal drilling and hydraulic fracturing. The shale gas contribution to total natural gas production in the United States reached 40% in 2012, growing rapidly from only small volumes produced before 2005 (EIA, 2015). Indeed, the practice of high volume hydraulic fracturing (fracking) for oil and gas extraction is a growing sector of methane and other hydrocarbon production, especially in the U.S. Most recent studies (Miller et al., 2013; Moore et al., 2014; Olivier and Janssens-Maenhout, 2014; Jackson et al., 2014b; Howarth et al., 2011; Pétron et al., 2014; Karion et al., 2013) albeit not all (Allen et al., 2013; Cathles et al., 2012; Peischl et al., 2015), suggest that methane emissions are underestimated by inventories and agencies, including the USEPA. For instance, emissions in the Barnett Shale region of Texas from both bottom-up and top-down measurements showed that methane emissions from upstream oil and gas infrastructure were 90% larger than estimates based on the US EPA's Greenhouse Gas Inventory and corresponded to 1.5% of natural gas production (Zavala-Araiza et al., 2015). Field measurements suggest that emission factors for unconventional gas are higher than for conventional gas, though the uncertainty, largely site-dependent, is large, ranging from small leakage rate of 1-2% (Peischl et al., 2015) to, widely spread rates of 3-17% (Caulton et al., 2014; Schneising et al., 2014). For current technology, the GAINS model has adopted an emission factor of 4.3% for shale-gas mining, still awaiting for more consensus across studies.

3.1.4 Agriculture and waste

This category includes methane emissions related to livestock (enteric fermentation and manure), rice cultivation, landfills, and wastewater handling. Of all types of emission, livestock is by far the largest emitter of CH₄, followed by waste handling and rice cultivation. Field burning of agricultural residues was a minor source of CH₄ reported in emission inventories. The spatial distribution of methane emissions from agriculture and waste handling is presented in Fig. 3 based on the mean gridded maps provided by EDGARv42FT2010 and GAINS over the 2003-2012 decade.

Global emissions for agriculture and waste are estimated at 195 Tg CH₄ yr⁻¹ (range [178-206], Table 2), representing 57% of total anthropogenic emissions.

Livestock: enteric fermentation and manure management. Domestic livestock such as cattle, buffalo, sheep, goats, and camels produce large amount of methane by anaerobic microbial activity in their digestive systems (Johnson et al., 2002). A very stable temperature (39°C), a stable pH (6.5-6.8) in their rumen, and constant flow of plants (cattle graze many hours per day) induce a production of metabolic hydrogen, used by methanogenic *Archaea* together with CO₂ to produce methane. The methane and carbon dioxide are released from the rumen mainly through the mouth of multi-stomached ruminants (eructation, ~87% of emissions) or absorbed in the blood system. The methane produced in the intestines and partially transmitted through the rectum is only ~13 %. There are about 1.4 billion cattle globally, 1 billion sheep, and nearly as many goats. The total number of animals is growing steadily (<http://faostat3.fao.org>), although the number is not linearly related to the CH₄ emissions they produce; emissions are strongly influenced by the total weight of the animals and their diet. Cattle, due to their



large population, large size, and particular digestive characteristics, account for the majority of enteric fermentation CH_4 emissions from livestock, particularly, in the United States (USEPA, 2016).

In addition, when livestock or poultry manure are stored or treated in systems that promote anaerobic conditions (e.g., as a liquid/slurry in lagoons, ponds, tanks, or pits), the decomposition of the volatile solids component in the manure tends to produce CH_4 . When manure is handled as a solid (e.g., in stacks or drylots) or deposited on pasture, range, or paddock lands, it tends to decompose aerobically and produce little or no CH_4 . Ambient temperature, moisture, and manure storage or residency time affect the amount of CH_4 produced because they influence the growth of the bacteria responsible for CH_4 formation. For non-liquid-based manure systems, moist conditions (which are a function of rainfall and humidity) can promote CH_4 production. Manure composition, which varies with animal diet, growth rate, and type, including the animal's digestive system, also affects the amount of CH_4 produced. In general, the greater the energy contents of the feed, the greater the potential for CH_4 emissions. However, some higher-energy feeds also are more digestible than lower quality forages, which can result in less overall waste excreted from the animal (USEPA, 2006).

In 2005, global methane emissions from enteric fermentation and manure are estimated in the range of [96-114] Tg CH_4 yr^{-1} in the GAINS family models (ECLIPSE) and USEPA inventory, respectively, and in the range of [98-105] Tg CH_4 yr^{-1} suggested by K13. They are consistent with the FAO- CH_4 estimate of 105 Tg CH_4 yr^{-1} (Tubiello et al., 2013).

Here, for the 2003-2012 decade, we infer a range of [97-111] Tg CH_4 yr^{-1} for the combination of enteric fermentation and manure with a mean value of 106 Tg CH_4 yr^{-1} (Table 2), about one third of total global anthropogenic emissions.

Waste management. This sector includes emissions from managed and non-managed landfills (solid waste disposal on land), and wastewater handling, where all kinds of waste are deposited, which can emit significant amounts of methane by anaerobic decomposition of organic material by microorganisms. Methane production from waste depends on pH, moisture and temperature. The optimum pH for methane emission is between 6.8 and 7.4 (Thorneloe et al., 2000). The development of carboxylic acids leads to low pH, which limits methane emissions. Food or organic waste, leaves, grass clippings ferment quite easily, while wood and lignin generally ferment slowly, and cellulose and lignin even more slowly (USEPA, 2010).

Waste management is responsible for about 11% of total global anthropogenic methane emissions in 2000 at global scale (K13). A recent assessment of methane emissions in the U.S. accounts landfills for almost 26% of total U.S. anthropogenic methane emissions in 2014, the largest contribution of any CH_4 source in the United States (USEPA, 2016). In Europe, gas control is mandatory on all landfills from 2009 onwards, following the ambitious objective raised in the EU Landfill Directive (1999) to reduce the landfilling of biodegradable waste by 65% below the 1990 level by 2016. This is attempted through source separation and treatment of separated biodegradable waste in composts, bio-digesters, and paper recycling. This approach is assumed more efficient in terms of reducing methane emissions than the more usual gas collection and capture. Collected biogas is either burned by flaring, or used as fuel if it is pure enough (i.e. the content of methane is > 30%). Many managed landfills have the practice to apply cover material (e.g. soil, clay, sand) over the waste being disposed of in the landfill to prevent odour, reduce risk to public health, but also promote microbial communities of methanotrophic organisms



(Bogner et al., 2007; RTI, 2011). In developing countries, very large open landfills still exist, with important health and environmental issues in addition to methane emissions (André et al., 2014).

Wastewater from domestic (municipal sewage) and industrial sources is treated in municipal sewage treatment facilities and private effluent treatment plants. The principal factor in determining the CH₄ generation potential of wastewater is the amount of degradable organic material in the wastewater. Wastewater with high organic content is treated anaerobically and that leads to increased emissions (André et al., 2014).

The inventories give robust emission estimates from solid waste in the range of [28-44] Tg CH₄ yr⁻¹ in the year 2005, and wastewater in the range 9-30 Tg CH₄ yr⁻¹ given by GAINS (ECLIPSE) models and EDGAR inventory.

In this study, global emissions of methane from landfills and waste are estimated in the range of [52-63] Tg CH₄ yr⁻¹ for the 2003-2012 period with a mean value of 59 Tg CH₄ yr⁻¹, about 18% of total global anthropogenic emissions.

Rice cultivation. Most of the world's rice is grown on flooded fields (Baicich, 2013). Under these shallow-flooded conditions, aerobic decomposition of organic matter gradually depletes most of the oxygen in the soil, resulting in anaerobic conditions under which methanogenic *Archaea* decompose organic matter and produce methane. Most of this methane is oxidized in the underlying soil, while some is dissolved in the floodwater and leached away. The remaining methane is released to the atmosphere, primarily by diffusive transport through the rice plants, but also methane escapes from the soil via diffusion and bubbling through floodwaters (USEPA, 2016; Bridgham et al., 2013).

The water management systems used to cultivate rice are one of the most important factors influencing CH₄ emissions and is one of the most promising approach to mitigate the CH₄ emissions from rice cultivation (e.g. periodical drainage and aeration not only causes existing soil CH₄ to oxidize, but also inhibits further CH₄ production in soils (Simpson et al., 1995; USEPA, 2016; Zhang, 2016, submitted). Upland rice fields are not flooded, and therefore are not believed to produce much CH₄. Other factors that influence CH₄ emissions from flooded rice fields include fertilization practices (i.e. the use of urea and organic fertilizers), soil temperature, soil type (texture and aggregated size), rice variety and cultivation practices (e.g., tillage, seeding, and weeding practices) (USEPA, 2011, 2016; Kai et al., 2011; Yan et al., 2009; Conrad et al., 2000). For instance, methane emissions from rice paddies increase with organic amendments (Cai et al., 1997) but can be mitigated by applying other types of fertilizers (mineral, composts, biogas residues, wet seeding) (Wassmann et al., 2000). Some studies have suggested that decreases in microbial emissions, particularly due to changes in the practice of rice cultivation, could be responsible for a ~15 Tg CH₄ yr⁻¹ decrease over the period from 1980s to 2000s (Kai et al., 2011).

The geographical distribution of the emissions is assessed by global ((USEPA, 2006, 2012; EDGAR, 2012)) and regional (Peng et al., 2016; Chen et al., 2013; Chen and Prinn, 2006; Yan et al., 2009; Castelán-Ortega et al., 2014; Zhang et al., 2014) inventories or by land surface models (Spahni et al., 2011; Zhang and Chen, 2014; Ren et al., 2011; Tian et al., 2010; Tian et al., 2011; Li et al., 2005; Pathak et al., 2005). The emissions show a seasonal cycle, peaking in the summer months in the extra-tropics associated with the monsoon and land management. Similar to emissions from livestock, emissions from rice



paddies are influenced not only by extent of rice field area (equivalent to the number of livestock), but also by changes in the productivity of plants as these alter the CH₄ emission factor used in inventories.

The largest emissions are found in Asia (Hayashida et al., 2013), with China (5-11 Tg CH₄ yr⁻¹, Chen et al. (2013), Zhang (2016, submitted)) and India (~3-5 Tg CH₄ yr⁻¹, Bhatia et al. (2013)) accounting for 30 to 50% of global emissions (Fig. 3).

- 5 Furthermore, recent studies revealed that together, high carbon dioxide concentrations and warmer temperatures predicted for the end of the twenty-first century will about double the amount of methane emitted per kilo of rice produced (van Groenigen et al., 2013).

Based on global inventories only, global methane emissions from rice paddies are estimated in the range [24-36] Tg CH₄ yr⁻¹ for the 2003-2012 decade, with a mean value of 30 Tg CH₄ yr⁻¹ (Table 2), about 9% of total global anthropogenic
10 emissions. The lower estimate (24 Tg CH₄ yr⁻¹) is provided by FAO-CH₄ inventory (Tubiello et al., 2013), which is based on a mix of FAO statistics for crop production and IPCC guidelines.

3.1.5 Biomass and biofuel burning

This category includes all the combustion processes: biomass (forests, savannahs, grasslands, peats, agricultural residues), biofuels in the residential sector (stoves, boilers, fireplaces). Biomass and biofuel burning emits methane under incomplete
15 combustion conditions, when oxygen availability is insufficient such as charcoal manufacture and smouldering fires. The amount of methane that is emitted during the burning of biomass depends primarily on the amount of biomass, the burning conditions, and the material being burned. At the global scale, biomass and biofuel burning lead to methane emissions of [27-35] Tg CH₄ yr⁻¹ with an average of 30 Tg CH₄ yr⁻¹ (2003-2012 decade, Table 2), of which 30-50 % is biofuel burning (K13).

In this study, we use the large-scale biomass burning (forest, savannah, grassland and peat fires) from specific biomass
20 burning inventories and the biofuel burning contribution for the inventories (USEPA, GAINS and EDGAR).

The spatial distribution of methane emissions from biomass burning over the 2003-2012 decade is presented in Fig. 3 and is based on the mean gridded maps provided by EDGARv42FT2010 and GAINS for the biofuel burning, and based on the mean gridded maps provided by the biomass burning inventories presented thereafter.

- 25 **Biomass burning.** Fire is the most important disturbance event in terrestrial ecosystems at the global scale (van der Werf et al., 2010), and can be of either natural (typically ~10%, ignited by lightning strikes or started accidentally) or anthropogenic origin (~90%, deliberately initiated fires) (USEPA (2010) chp 9.1). Anthropogenic fires are concentrated in the tropics and subtropics, where forests and savannahs are burned to clear the land for agricultural purposes or to maintained pasturelands. In addition there are small fires associated with agricultural activity, such as field burning and agricultural waste
30 burning, which are often undetected by commonly used remote sensing products.

Usually the biomass burning emissions are estimated using following Eq. (2) (or similar):

$$E(x, t) = A(x, t) * B(x) * FB * EF \quad (2)$$



where $A(x,t)$ is the area burned, $B(x)$ the biomass loading (depending on the biomes) at the location, FB the fraction of the area burned (or the efficiency of the fire depending of the vegetation type and the fire type) and EF the emissions factor (mass of the considered species / mass of biomass burned). Depending on the approach, these parameters are derived using satellite data and/or biogeochemical model, or more simple equations.

- 5 The Global Fire Emission Database (GFED) is the most widely used global biomass burning emission dataset and provides estimates since 1997. In this review, we use both GFED3, (van der Werf et al., 2010) and GFED4s (Giglio et al., 2013; Randerson et al., 2012). GFED is based on the Carnegie-Ames-Stanford-Approach (CASA) biogeochemical model and satellite derived estimates of burned area, fire activity and plant productivity. From November 2000 onwards, these three parameters are inferred from the MODerate resolution Imaging Spectroradiometer (MODIS) sensor. For the period prior to
- 10 MODIS, burned area maps were derived from the Tropical Rainfall Measuring Mission (TRMM) Visible and Infrared Scanner (VIRS) and Along-Track Scanning Radiometer (ATSR) active fire data and estimates of plant productivity derived from Advanced Very High Resolution Radiometer (AVHRR) observations during the same period. GFED3 has provided biomass burning emission estimates from 1997 to 2011 at a 0.5° resolution on a monthly basis. The last versions of GFED
- 15 (GFED4 (without small fires) and GFED4s (with small fires)) are available at a higher resolution (0.25°) and on a daily basis from 2000 to 2014. Compared to GFED3, the main difference comes from the use of additional maps of the burned area product (MCD64A1) leading to a full coverage of land surface in GFED4 (Giglio et al., 2013). The particularity of GFED4s burned area is that small fires are accounted for (Randerson et al., 2012). Indeed small fires occur in several biomes (croplands, wooded savannahs, tropical forests) but are below the detection limit of the global burned area products. Yet the thermal anomalies they generate can be detected by MODIS for instance. Randerson et al. (2012) have shown that small fires
- 20 increase burned area by approximately 35% on the global scale leading to a 35% increase of biomass burning carbon emissions when small fires were included in GFED3. Also it is worth noting that between GFED3 and GFED4, the fuel consumption was lowered to better match observations (van Leeuwen et al., 2014) and that emission factor changes are substantial for some species and some biomes. Indeed global methane emissions are 25% lower in GFED4 than in GFED3 mainly because of the new emission factors updated with Akagi et al. (2011).
- 25 The Fire Inventory from NCAR (FINN, Wiedinmyer et al. (2011)) provides daily, 1km resolution estimates of gas and particle emissions from open burning of biomass (including wildfire, agricultural fires and prescribed burning) over the globe for the period 2003-2014. FINNv1 uses MODIS satellite observations for active fires, land cover and vegetation density. The emission factors are from Akagi et al. (2011), the estimated fuel loading are assigned using model results from Hoelzemann et al. (2004), and the fraction of biomass burned is assigned as a function of tree cover (Wiedinmyer et al., 2006).
- 30 The Global Fire Assimilation System (GFAS, Kaiser et al. (2012)) calculates biomass burning emissions by assimilating Fire Radiative Power (FRP) observations from MODIS at a daily frequency and 0.5° resolution and is available for the time period 2000-2013. After correcting the FRP observations for diurnal cycle, gaps etc., it is linked to dry matter combustion rate using Wooster et al. (2005) and CH_4 emission factors from Andreae and Merlet (2001).



For FAO-CH₄, yearly biomass burning emissions are based on burned area data from the Global Fire Emission Database v.4 (GFED4; Giglio et al. (2013)). For forest, the GFED4 burned forest area is an aggregate of burned area in the following MODIS land cover classes (MCD12Q1, Hansen et al. (2000)): Evergreen Needle-leaf, Evergreen Broadleaf, Deciduous Needle-leaf, Deciduous Broadleaf, and Mixed Forest. For "Humid Tropical Forest," burned area is obtained by overlapping
5 GFED4 Burned Forest area data with the relevant FAO-FRA Global Ecological Zones (GAEZv3.0, 2012). For "Other Forest," it is obtained by difference between other categories. FAO-CH₄ biomass burning emissions are available from 1990 to 2014 (Table 1).

The differences in the biomass burning emission estimates arise from various difficulties among them the ability to represent and know the geographical and meteorological conditions and the fuel composition that highly impact the
10 combustion completeness and the emission factors. Also methane emission factors vary greatly according to fire type, ranging from 2.2 g CH₄ kg⁻¹ dry matter burned for savannah and grassland fires up to 21 g CH₄ kg⁻¹ dry matter burned for peat fires (van der Werf et al., 2010).

During the remarkably strong El Niño of 1997-1998, anomalously high biomass burning emissions, especially from Indonesia and boreal regions, contributed to a higher than normal growth CH₄ rate for this period, though wetland emissions
15 also had a strong impact (Dlugokencky et al., 2001; Langenfelds et al., 2002; van der Werf et al., 2004; Simpson et al., 2006). Apart from strong El Niño periods, biomass burning plays a much smaller role than wetlands in the year-to-year changes in methane emissions. Since 2003, biomass methane emissions seem to have experienced a decreasing trend of -0.7 Tg CH₄ yr⁻¹ (van der Werf et al., 2010).

Tian et al. (2016) estimated that CH₄ emissions from biomass burning during the 2000s are (TD, 17±8 Tg C yr⁻¹; BU,
20 15±5 Tg C yr⁻¹).

In this study, biomass burning emissions are estimated at 18 Tg CH₄ yr⁻¹ [15-21] for the decade 2003-2012, about 5% of total global anthropogenic emissions.

Biofuel burning. Biomass that is used to produce energy for domestic, industrial, commercial, or transportation purposes
25 is hereafter called biofuel burning. A largely dominant fraction of methane emissions from biofuels comes from domestic cooking or heating in stoves, boilers and fireplaces, mostly in open cooking fires where wood, charcoal, agricultural residues, or animal dung are burnt. More than two billion people, mostly in developing and emerging countries, use solid biofuels to cook and heat their homes on a daily basis (André et al., 2014). Other much smaller contributors include agricultural burning (~1-2 Tg yr⁻¹) and road transportation (< 1 Tg yr⁻¹). Biofuel burning estimates are gathered from USEPA, GAINS and
30 EDGAR inventories.

In this study, biofuel burning is estimated to contribute 12 Tg CH₄ yr⁻¹ [10-14] to the global methane budget, about 3% of total global anthropogenic emissions.



3.2 Natural methane sources

Natural methane sources include wetland emissions as well as emissions from other land water systems (lakes, ponds, rivers, estuaries), land geological sources (seeps, microseepage, mud volcanoes, geothermal zones, and volcanoes, marine seepages), wild animals, wildfires, termites, terrestrial permafrost and oceanic sources (geological and biogenic). Many sources have been recognized but their magnitude and variability remain uncertain (USEPA (2010); K13).

3.2.1 Wetlands

Wetlands are generally defined as ecosystems in which water saturation or inundation (permanent or not) dominates the soil development and determines the ecosystem composition (USEPA, 2010). Such a broad definition needs to be refined when it comes to methane emissions. In this work, we define wetlands as ecosystems with inundated or saturated soils where anaerobic conditions lead to methane production (USEPA, 2010; Matthews and Fung, 1987). This includes peatlands (bogs and fens), mineral wetlands (swamps and marshes), and seasonal or permanent floodplains. It excludes exposed water surfaces without emergent macrophytes, such as lakes, rivers, estuaries, ponds, and dams (addressed in the next section), as well as rice agriculture (see Sect. 3.1.4.3). Even with this definition, one can consider that part of the wetlands could be considered as anthropogenic systems, being affected by human-driven land-use changes (Woodward et al., 2012). In the following we keep the generic denomination wetlands for natural and human-influenced wetlands.

A key feature of wetland systems producing methane is anaerobic soils, where high water table or flooded conditions limit oxygen availability and create conditions for methanogenesis. In anoxic conditions, organic matter can be degraded by methanogens that produce CH_4 . The three most important factors influencing methane production in wetlands are the level of anoxia (linked to water table), temperature and substrate availability (Wania et al., 2010; Valentine et al., 1994; Whalen, 2005). Once produced, methane can reach the atmosphere through a combination of three processes: molecular diffusion, plant-mediated transport, and ebullition. On its way to the atmosphere, methane can be partly or completely oxidized by a group of bacteria, called methanotrophs, which use methane as their only source of energy and carbon (USEPA, 2010). Concurrently, methane from the atmosphere can diffuse into the soil column and be oxidized (See Sect. 3.3.4).

Land surface models estimate CH_4 emissions through a series of processes, including CH_4 production, CH_4 oxidation and transportation and are further regulated by the changing environmental factors (Tian et al., 2010; Xu et al., 2010; Melton et al., 2013). In these models, methane emissions from wetlands to the atmosphere are computed as the product of an emission density (which can be negative; mass per unit area and unit time) multiplied by a wetland extent (see the model inter-comparison studies by Melton et al. (2013) and Bohn et al. (2015)). The CH_4 emission density is represented in land surface models with varying levels of complexity. Many models link CH_4 emission to NPP through production of exudates or litter and soil carbon to yield heterotrophic respiration estimates. A proportion of the heterotrophic respiration estimate is then taken to be CH_4 production (Melton et al., 2013). The oxidation of produced (and becoming atmospheric) methane in the soil



column is then either represented explicitly (e.g., Riley et al. (2011), Grant and Roulet (2002)), or just fixed proportionally to the production (Wania et al., 2013).

In land surface models, wetland extent is either prescribed (from inventories or remote sensing data) or computed (using hydrological models accounting for the fraction of grid cell with flat topography prone to high water table (e.g., Stocker et al. (2014), Kleinen et al. (2012)), or from data assimilation against remote-sensed observations (Riley et al., 2011). Mixed approaches can also be implemented with tropical extent prescribed from remote sensing and northern peatland extent explicitly computed (Melton et al., 2013). Wetland extent appears to be a large contributor to uncertainties in methane emissions from wetlands (Bohn et al., 2015). For instance, the maximum wetland extent on a yearly basis appeared to be very different among land surface models in Melton et al. (2013), ranging from 7 to 27 Mkm². Passive and active remote sensing data in the micro-wave domain have been used to retrieve inundated areas, as with the Global Inundation Extent from Multi-Satellites product (GIEMS, Prigent et al. (2007), Papa et al. (2010)). These remote-sensed data do not exactly correspond to wetlands, as all flooded areas are not wetlands (in methane emission sense) and some wetlands (e.g. northern bogs) are not always flooded. Inundated areas also include inland water bodies (lakes, ponds, estuaries) and rice paddies, which have to be filtered out to compute wetland emissions. Overall, current remote sensing of wetlands tends to underestimate wetland extent partly because of signal deterioration over dense vegetation and partly because microwave signals only detect water above or at the soil surface and therefore do not detect non-inundated emitting peatlands (Prigent et al., 2007). For example, the Global Lakes and Wetlands Dataset (GLWD) (Lehner and Döll, 2004), estimates between 8.2 and 10.1 Mkm² of wetlands globally, while remote sensing inundation area is smaller, i.e., ~6 Mkm² (Prigent et al., 2007). Some ancillary data used in the GIEMS processing are not available after 2007 and prevented so far the extension of the data set after 2007.

Integrated at the global scale, wetlands are the largest and most uncertain source of methane to the atmosphere (K13). An ensemble of land surface models estimated the range of methane emissions of natural wetlands at [141-264] Tg CH₄ yr⁻¹ for the 1993-2004 period, with a mean and 1-sigma value of 190±39 Tg CH₄ yr⁻¹ (Melton et al., 2013). K13 assessed a consistently large emission range of [142-287] Tg CH₄ yr⁻¹, using the Melton et al. land surface models and atmospheric inversions. These emissions represent about 30% of the total methane source. The large range in the estimates of wetland emissions results from difficulties in defining wetland CH₄ producing areas as well as in parameterizing terrestrial anaerobic sources and oxidative sinks (Melton et al., 2013; Wania et al., 2013).

In this work, following Melton et al. (2013), eleven land surface models (Table 1) computing net CH₄ emissions have been run under a common protocol with a 30-year spin-up (1901-1930) followed by a simulation until the end of 2012 forced by CRU-NCEP v4.0 reconstructed climate fields. Atmospheric CO₂ influencing NPP was also prescribed in the models, allowing the models to separately estimate carbon availability for methanogenesis. In all models, the same wetland extent (SWAMPS-GLWD) has been prescribed. The SWAMPS-GLWD is a monthly global wetland area dataset, which has been developed to overcome the aforementioned issues and combines remote sensing data from Schroeder et al. (2015) and GLWD inventory in order to develop a monthly global wetland area dataset (Poulter et al., 2016, submitted). Briefly, GLWD was used to set the annual mean wetland area, to which a seasonal cycle of fractional surface water was added using data from the



Surface Water Microwave Product Series Version 2.0 (SWAMPS) (Schroeder et al., 2015). The combined GLWD-SWAMPS product leads to a maximum annual wetland area of 10.5 Mkm² (8.7 Mkm² on average, about 5.5% of than global land surface). The largest wetland areas in the SWAMPS-GLWD are in Amazonia, the Congo Basin, and the Western Siberian Lowlands, which in previous studies have appeared to be strongly underestimated by several inventories (Bohn et al., 5 2015). However, wetlands above 70°N appear under-represented in GLWD as compared to Sheng et al. (2004) and Peregon et al. (2008). Indeed, approximately half of the global natural wetland area lies in the boreal zone between 50°N and 70°N, while 35% can be found in the Tropics, between 20°N and 30°S (Matthews and Fung, 1987; Aselmann and Crutzen, 1989). Despite the lower area extent, the higher per-unit area methane emissions of tropical wetlands results in a larger wetland source from the tropics than from the boreal zone (Melton et al., 2013).

10 The average emission map from wetlands for 2003-2012 built from the 11 models is plotted in Fig. 3. The zones with the largest emissions reflect the GLWD database: the Amazon basin, equatorial Africa and Asia, Canada, western Siberia, eastern India, and Bangladesh. Regions where methane emissions are robustly inferred (i.e., regions where mean flux is larger than the standard deviation of the models) represent 80% of the total methane flux due to natural wetlands. Main primary emission zones are consistent between models, which is clearly favoured by the common wetland extend prescribed. But still, the 15 different sensitivity of the models to temperature can generate substantial different patterns, such as in India. Some secondary (in magnitude) emission zones are also consistently inferred between models: Scandinavia, Continental Europe, Eastern Siberia, Central USA, and tropical Africa. Using improved regional methane emission data sets (such as studies over North America, Africa, China, and Amazon) can enhance the accuracy of the global budget assessment (Tian et al., 2011; Xu and Tian, 2012; Ringeval et al., 2014; Valentini et al., 2014).

20 The resulting global flux range for natural wetland emissions is 153-227 Tg CH₄ yr⁻¹ for the 2003-2012 decade, with an average and 1-sigma of 185±21 Tg CH₄ yr⁻¹ (Table 2).

3.2.2 Other inland water systems (lakes, ponds, rivers, estuaries)

This category includes methane emissions from freshwater systems (lakes, ponds, rivers) and from brackish waters of estuaries. Methane emissions from freshwaters and estuaries occur through a number of pathways including (1) continuous or 25 episodic diffusive flux across water surfaces; (2) ebullition flux from sediments; (3) flux mediated through the *aerenchyma* of emergent aquatic macrophytes (plant transport) in littoral environments, and also for reservoirs; (4) degassing of CH₄ in the turbines; and (5) elevated diffusive emissions in rivers downstream of the turbines especially if water through the turbines is supplied from anoxic CH₄-rich water layers in the reservoir (Bastviken et al., 2004; Guérin et al., 2006; 2015). It is very rare that complete emission budgets are including all these types of fluxes. For methodological reasons many past and present flux 30 measurements only account for the diffusive flux based on short-term flux chamber measurements where non-linear fluxes were often discarded. At the same time, diffusive flux is now recognized as a relatively small flux component in many lakes, especially deeper lakes compared to ebullition and plant fluxes (in lakes with substantial emergent macrophyte communities). The two latter fluxes are very challenging to measure, both typically being associated with shallow near-shore waters and



having high spatiotemporal variability. Ebullition can also occur more frequently in areas with high sediment organic matter load, and is by nature episodic with very high fluxes occurring over time frames of seconds followed by long periods without ebullition.

Freshwater contributions from lakes were first estimated to emit 1-20 Tg CH₄ yr⁻¹ based on measurements in two systems (Great Fresh Creek, Maryland and Lake Erie; Ehhalt (1974)). A subsequent global emission estimate was 11-55 Tg CH₄ yr⁻¹ based on measurements from three arctic lakes and a few temperate and tropical systems (Smith and Lewis, 1992), and 8-48 Tg CH₄ yr⁻¹ using extended data from all of the lake rich biomes (73 lakes; Bastviken et al. (2011)). K13 reported a range of 8-73 Tg CH₄ yr⁻¹. Gradually, methane emissions from reservoirs and rivers have been also included in the most recent global estimate from freshwaters of 103 Tg CH₄ yr⁻¹, including emissions from non-saline lakes, reservoirs, ponds and rivers, respectively (data from 473 systems; Bastviken et al. (2011)). Improved stream and river emission estimates of 27 Tg CH₄ yr⁻¹ was recently suggested (Stanley et al., 2016). Importantly, the previous estimates of this flux are not independent. Instead they represent updates from increasing data quantity and quality. Therefore issues regarding spatiotemporal variability are not considered in consistent ways at present (Wik et al., 2016a; Natchimuthu et al., 2015).

Present data do not allow for separating inland water fluxes over the different time periods investigated in this paper. The global estimates provided are therefore assumed to be constant for this study. Here we combine the latest estimates of global freshwater CH₄ emissions (Bastviken et al., 2011) with a more recent regional estimate for latitudes above 50° North present (Wik et al., 2016b) and new extrapolations for tropical river emissions (Borges et al., 2015; Sawakuchi et al., 2014) and streams (Stanley et al., 2016). High latitude lakes include both post-glacial lakes and thermokarst lakes (water bodies formed by thermokarst), the latter having larger emissions densities but smaller regional emissions than the former because of smaller areal extent (Wik et al., 2016b). Water body depth, sediment type, and eco-climatic region are the key factors explaining variation in methane fluxes from lakes (Wik et al., 2016b).

Altogether, these studies consider data from more than 900 systems, of which ~750 are located north of 50°N. In this context we only consider fluxes from open waters assuming that plant-mediated fluxes are included in the wetland emission term. The average total estimated open water emission including the recent estimates from smaller streams is 122 Tg CH₄ yr⁻¹. The uncertainty is high with a coefficient of variation ranging from 50 to >100% for various flux components and biomes (Bastviken et al., 2011) resulting in a minimum uncertainty range of [60-180] Tg CH₄ yr⁻¹. The present data indicate that lakes or natural ponds, reservoirs, and streams/rivers account for 62, 16 and 22% of the average fluxes, respectively (given the large uncertainty the percentages should be seen as approximate relative magnitudes only).

Potentially, the emissions from reservoirs should be allocated to anthropogenic emissions (not done here). Regarding lakes and reservoirs, tropical (<30° latitude) and temperate (30°-50° latitude) emissions represent 49 and 33% of the flux, respectively, with 18% left for regions above 50° latitude. For comparison, approximately 40% of the surface area is found above 50° latitude in the Northern Hemisphere and 34% of the area is situated between 20°S and 20°N (Verpoorter et al., 2014). Ebullition typically accounted for 50 to more than 90% of the flux from the water bodies, while contributions from ebullition appear lower from rivers, although this is currently debated (e.g. Crawford et al. (2014)). Several aspects will need



consideration to reduce remaining uncertainty in the freshwater fluxes and future updates of a global lake inventory database (e.g. GLOWAB, Verpoorter et al. (2014)) should make it possible, in the coming years, to build a high-resolution global map for freshwater emissions.

3.2.3 Onshore and offshore geological sources

5 Significant amounts of methane, produced within the Earth's crust, naturally migrate to the atmosphere through tectonic faults and fractured rocks. Major emissions are related to hydrocarbon production in sedimentary basins (microbial and thermogenic methane), through continuous exhalation and eruptions from onshore and shallow marine gas/oil seeps and through diffuse soil microseepage (after Etiope (2015)). Specifically, six source categories have been considered. Five are onshore sources: mud volcanoes (sedimentary volcanism), gas and oil seeps (independent of mud volcanism), microseepage
10 (diffuse exhalation from soil in petroleum basins), geothermal (non-volcanic) manifestations and volcanoes. One source is offshore: submarine seepage (several types of gas manifestation at the seabed). Figure 4a shows the areas and locations potentially emitting geological methane, showing diffuse potential micro-seepage regions, macro-seeps locations (oil-gas seeps, mud volcanoes) and geothermal/volcanic areas (built from Etiope (2015)), which represent more than 1000 emitting spots.

15 Studies since 2000 have shown that the natural release to the Earth's surface of methane of geological origin is an important global greenhouse gas source (Etiope and Klusman, 2002; Kvenvolden and Rogers, 2005; Etiope et al., 2008; USEPA, 2010; Etiope, 2012, 2015). Indeed, the geological source is in the top-three natural methane source after wetlands (and with freshwater systems) and about 10% of total methane emissions, of the same magnitude or exceeding other sources or sinks, such as biomass burning, termites and soil uptake, considered in recent IPCC assessment reports (Ciais et al., 2013).

20 In this study, the following provided estimates were derived by bottom-up approaches based on (a) the acquisition of thousands of land-based flux measurements for various seepage types in many countries, and (b) the application of the same procedures typically used for natural and anthropogenic gas sources, following up-scaling methods based on the concepts of "point sources", "area sources", "activity" and "emission factors", as recommended by the air pollutant emission guidebook of the European Environment Agency (EMEP/EEA, 2009). Our estimate is consistent with a top-down global verification,
25 based on observations of radiocarbon-free (fossil) methane in the atmosphere (Etiope et al., 2008; Lassey et al., 2007b), with a range of [33-75] Tg CH₄ yr⁻¹.

As a result, in this study, the global geological methane emission is estimated in the range of [35-76] Tg CH₄ yr⁻¹ (mean of 52 Tg CH₄ yr⁻¹), with 40 Tg CH₄ yr⁻¹ [30-56] for onshore emissions ([10-20] Tg CH₄ yr⁻¹ for mud volcanoes, [3-4] Tg yr⁻¹ for gas-oil seeps, [10-25] Tg yr⁻¹ for microseepage, [2-7] Tg CH₄ yr⁻¹ for geothermal/volcanic manifestations) and 12 Tg CH₄ yr⁻¹
30 [5-20] for offshore emissions through marine seepage ((Rhee et al., 2009; Berchet et al., 2016; Etiope, 2012); see Sect. 3.2.6 for offshore contribution explanations).



3.2.4 Termites

Termites are important decomposer organisms, which play a very relevant role in the cycling of nutrients in tropical and subtropical ecosystems (Sanderson, 1996). The degradation of organic matter in their gut, by symbiotic anaerobic microorganisms, leads to the production of CH₄ and CO₂ (Sanderson, 1996). The up-scaling approaches which have been used to quantify the contribution of termites to global CH₄ emissions (Sanderson, 1996; Sugimoto et al., 1998; Bignell et al., 1997) are affected by large uncertainties, mainly related to the effect of soil and mound environments on net CH₄ emissions; the quantification of termite biomass for each ecosystem type and the impact of land use change on termite biomass. For all these factors, uncertainty mainly comes from the relatively small number of studies compared to other CH₄ sources. In K13 (see their supplementary material), a re-analysis of CH₄ emissions from termites at the global scale was proposed and CH₄ emissions per unit of surface were estimated as the product of termite biomass, termite CH₄ emissions per unit of termite mass and a scalar factor expressing the effect of land use/cover change. The latter two terms were estimated from published literature re-analysis (K13, supplementary). A climate zoning (following the Koppen-Geiger classification) was applied to updated climate datasets by Santini and Di Paola (2015) was adopted to take into account different combinations of termite biomass per unit area and CH₄ emission factor per unit of termite biomass. In case of tropical climate, first termites' biomass was estimated by a simple regression model representing its dependence on gross primary productivity (K13, supplementary), whereas termites biomass for forest and grassland ecosystems of the warm temperate climate and for shrub lands of the Mediterranean sub-climate were estimated from data reported by Sanderson et al. (1996). CH₄ emission factor per unit of termite biomass was derived from published literature and was estimates equal to 2.8 mg CH₄ g⁻¹ termite h⁻¹ for tropical ecosystems and Mediterranean shrublands (K13) and 1.7 mg CH₄ g⁻¹ termite h⁻¹ for temperate forests and grasslands (Fraser et al., 1986). Emissions were scaled-up in GIS environment and annual CH₄ fluxes computed for the three periods 1982-1989, 1990-1999 and 2000-2007 representative of the 1980s', 1990s' and 2000s', respectively. CH₄ emissions showed only little inter-annual and inter-decadal variability (0.1 Tg of CH₄ yr⁻¹) and strong regional variability with tropical South America and Africa being the main sources (36 and 30% of the global total emissions, respectively) due to the extent of their natural forest and savannah ecosystems (Fig. 4b). For the 2000s, a global total of 8.7±3.1 Tg CH₄ yr⁻¹ (range [3-15] Tg CH₄ yr⁻¹) was obtained. This value is close to the average estimate derived from previous up-scaling studies which report values spanning from 2 to 22 Tg CH₄ yr⁻¹ (Ciais et al. (2013).

In this study, we adopt a value of 9 Tg CH₄ yr⁻¹ (range [3-15] Tg CH₄ yr⁻¹, Table 2).

3.2.5 Wild animals

As for domestic ruminants, wild ruminants eruct or exhale methane through the microbial fermentation process occurring in their rumen (USEPA, 2010). Global emissions of CH₄ from wild animals range from 2-6 Tg CH₄ yr⁻¹ (Leng, 1993) to 15 Tg CH₄ yr⁻¹ (Houweling et al., 2000). The global distribution of CH₄ emissions from wild ruminants is generally estimated as a function of the percentage and type of vegetation consumed by the animals (Bouwman et al., 1997).



The range adopted in this study is [2-15] Tg CH₄ yr⁻¹ with a mean value of 10 Tg CH₄ yr⁻¹ (Table 2).

3.2.6 Oceanic sources

Possible sources of oceanic CH₄ include: (1) leaks from geological marine seepage (see also Sect. 3.2.3); (2) production from sediments or thawing sub-sea permafrost; (3) emission from the destabilisation of marine hydrates; (4) in situ production in the water column, especially in the coastal ocean because of submarine groundwater discharge (USEPA, 2010). Once at seabed, methane can be transported through the water column by diffusion in a dissolved form (especially in the upwelling zones), or by ebullition (gas bubbles, e.g. from geological marine seeps), for instance, in shallow waters of continental shelves. Among these different origins of oceanic methane, hydrates have attracted a lot of attention. Methane hydrates (or sometimes called clathrates) are ice-like crystals formed under specific temperature and pressure conditions (Milkov, 2005). The stability zone for methane hydrates (high pressure, ambient temperatures) can be found in the shallow lithosphere (i.e. <2,000 m depth), either in the continental sedimentary rocks of polar regions, or in the oceanic sediments at water depths greater than 300 m (continental shelves, sediment-water interface) (Kvenvolden and Rogers, 2005; Milkov, 2005). Methane hydrates can be either of biogenic origin (formed in situ at depth in the sediment by microbial activity) or of thermogenic origin (non-biogenic gas migrated from deeper sediments and trapped due to pressure/temperature conditions or due to some capping geological structure such as marine permafrost). The total stock of marine methane hydrates is large but uncertain, with global estimates ranging from hundreds to thousands of Pg CH₄ (Klauda and Sandler, 2005; Wallmann et al., 2012).

If the production of methane at seabed can be of importance, for instance, marine seepages emit up to 65 Tg CH₄ yr⁻¹ globally at seabed level (USEPA, 2010); more uncertain is the flux of oceanic methane reaching the atmosphere. A large part of the seabed CH₄ production and emission is oxidised in the water column and does not reach the atmosphere (James et al., 2016). There are several barriers preventing methane to be expelled to the atmosphere. From the bottom to the top, gas hydrates and permafrost serve as a barrier to fluid and gas migration towards the seafloor (James et al., 2016). First, on centennial to millennium timescales, trapped gases may be released when permafrost is perturbed and cracks or through Pingo-like features. At present, microbial processes are the most important control on methane emissions from marine environments. Aerobic oxidation in the water column is a very efficient sink, which allows very little methane even from established and vigorous gas seep areas or even gas well blowouts such as the Deepwater Horizon from reaching the atmosphere. Anaerobic methane oxidation, first described by Reeburgh and Heggie (1977), coupled to sulfate reduction controls methane losses from sediments to the overlying water (Reeburgh, 2007). Methane only escapes marine sediments in significant amounts from rapidly accumulating sedimentary environments or *via* advective processes such as ebullition or groundwater flow in shallow shelf regions. Anaerobic methane oxidation was recently demonstrated to be able to keep up with the thaw front of thawing permafrost in a region that had been inundated within the past 1000 years (Overduin et al., 2015). Second, the oceanic pycnocline is a physical barrier limiting the transport of methane (and other species) towards the surface. Third, another important mechanism stopping methane from reaching the ocean surface is the dissolution of bubbles into the ocean water. Although bubbling is the most efficient way to transfer methane from the seabed to the atmosphere, the



fraction of bubbles actually reaching the atmosphere is very uncertain and critically depends on emission depths (< 100-200m, McGinnis et al. (2015)) and on the size of the bubbles (>5-8 mm, James et al. (2016)). Finally, surface oceans are aerobic and contribute to the oxidation of dissolved methane (USEPA, 2010). However, surface waters can be more supersaturated than the underlying deeper waters, leading to a methane paradox (Sasakawa et al., 2008). Possible explanation
5 involve, upwelling in areas with surface mixed layers covered by sea-ice (Damm et al., 2015), or methane produced within the anoxic centre of sinking particles (Sasakawa et al., 2008), but more work is needed to correct such apparent paradox.

All published estimates agree that contemporary global methane emissions from oceanic sources are only a small contributor to the global methane budget, but the range of estimates is relatively large from 1 to 35 Tg CH₄ yr⁻¹ when
10 summing geological and other emissions (e.g., Rhee et al. (2009), Etiope (2015), USEPA (2010)). For geological emissions, the most used value is 20 Tg yr⁻¹, relying on expert knowledge and literature synthesis proposed in a workshop reported in Kvenvolden et al. (2001), the author of this study recognising that this first estimation needs to be revised. Since then, oceanographic campaigns have been organized, especially to sample bubbling areas. For instance, Shakhova et al. (2010;2014) infer 8-17 Tg CH₄ yr⁻¹ emissions just for the Eastern Siberian Arctic Shelf (ESAS), based on the extrapolation of
15 numerous but local measurements, and possibly related to melting seabed permafrost (Shakhova et al., 2015). Because of the highly heterogeneous distribution of dissolved CH₄ in coastal regions, where bubbles can reach the atmosphere, extrapolation of in situ local measurements to the global scale can be hazardous and lead to biased global estimates. Indeed, using very precise and accurate continuous atmospheric methane observations in the Arctic region, Berchet et al. (2016) showed that Shakhova's estimates are 4-8 times too large to be compatible with atmospheric signals. This recent result suggests that the
20 current estimate of 20 Tg yr⁻¹ for the global emissions due to geological seeps emissions to the atmosphere in coastal oceans is too large and needs revision. Applying crudely the Berchet et al. abatement factor leads to emissions as low as less than 5 Tg CH₄ yr⁻¹.

More studies are needed to sort out this discrepancy and we choose to report here the full range of [5-20] Tg CH₄ yr⁻¹ for marine geological emissions, with a mean value of 12 Tg CH₄ yr⁻¹.

25

Concerning non-geological ocean emissions (biogenic, hydrates), the most common value found in the literature is 10 Tg CH₄ yr⁻¹ (Rhee et al., 2009). It appears that most studies rely on the work of Ehhalt (1974), where the value was estimated on the basis of the measurements done by Swinnerton and co-workers (Lamontagne et al., 1973; Swinnerton and Linnenbom, 1967) for the open ocean, combined with purely speculated emissions from the continental shelf. Based on basin-wide
30 observations using updated methodologies, three studies found estimates ranging from 0.2 to 3 Tg CH₄ yr⁻¹ (Conrad and Seiler, 1988; Bates et al., 1996; Rhee et al., 2009), associated with super-saturations of surface waters that are an order of magnitude smaller than previously estimated, both for the open ocean (saturation anomaly ~0.04, see Rhee et al. (2009), equation 4) and for continental shelf (saturation anomaly ~0.2). In their synthesis indirectly referring to the original observations from Lambert and Schmidt (1993), Wuebbles and Hayhoe (2002) use a value of 5 Tg CH₄ yr⁻¹. Proposed



explanations for discrepancies regarding sea-to air methane emissions in the open ocean rely on experimental biases in the former studies of Swinnerton et al. (Rhee et al., 2009). This may explain why the Bange et al. (1994) compilation cites a global source of [11-18] Tg CH₄ yr⁻¹ with a dominant contribution of coastal regions. Here, we report a range of [0-5] Tg CH₄ yr⁻¹, with a mean value of 2 Tg CH₄ yr⁻¹.

5

Concerning more specifically atmospheric emissions from marine hydrates, Etiope (2015) points that current estimates of methane air-sea flux from hydrates ([2-10] Tg CH₄ yr⁻¹ in e.g. Ciais et al. (2013) or K13) originate from the hypothetical values of Cicerone and Oremland (1988). No experimental data or estimation procedures have been explicitly described along the chain of references since then (Lelieveld et al., 1998; Denman et al., 2007; Kirschke et al., 2013; IPCC, 2001). It was recently estimated that ~473 Tg CH₄ have been released in the water column over 100 years (Kretschmer et al., 2015). Those few Tg per year become negligible once consumption in the water column has been accounted for. While events such as submarine slumps may trigger local releases of considerable amounts of methane from hydrates that may reach the atmosphere (Etiope, 2015; Paull et al., 2002), on a global scale, present-day atmospheric methane emissions from hydrates do not appear to be a significant source to the atmosphere.

15

Overall, these elements suggest the necessity to revise to a lower value the current total oceanic methane source to the atmosphere. Summing biogenic, geological and hydrate emissions from oceans leads to a total oceanic methane emission of 14 Tg CH₄ yr⁻¹ (range [5-25]). Refining this estimate requires to perform more in situ measurements of atmospheric and surface water methane concentrations and of bubbling areas, and would require the development of process-based models for oceanic methane linking sediment production and oxidation, transport and transformation in the water column and atmospheric exchange (James et al., 2016).

20

3.2.7 Terrestrial permafrost and hydrates

Permafrost is defined as frozen soil, sediment, or rock having temperatures at or below 0°C for at least two consecutive years (ACIA, 2005; Arctic-Research-Commission, 2003). The total extent of permafrost zones of the Northern Hemisphere is about 15 % of the land surface, with values around 15 million km² (Slater and Lawrence, 2013; Levavasseur et al., 2011; Zhang et al., 1999). Where soil temperatures have passed the 0°C mark, thawing of the permafrost at its margins occurs, accompanied by a deepening of the active layer (Anisimov and Reneva, 2006) and possible formation of thermokarst lakes (Christensen et al., 2015). A total of 1035 ± 150 Pg of carbon can be found in the upper 3 meters of permafrost regions, or ~1300 Pg of carbon (1100 to 1500) Pg C for all permafrost (Hugelius et al., 2014; Tarnocai et al., 2009).

25

The thawing permafrost can generate direct and indirect methane emissions. Direct methane emissions rely on the release of the methane contained in the thawing permafrost. This flux to the atmosphere is small and estimated to be at maximum 1 Tg CH₄ yr⁻¹ at present (USEPA, 2010). Indirect methane emissions are probably more important. They rely on: 1) methanogenesis induced when the organic matter contained in thawing permafrost is released; 2) the associated changes in

30



land surface hydrology possibly enhancing methane production (McCalley et al., 2014); and 3) the formation of more thermokarst lakes from erosion and soil collapsing. Such methane production is probably already significant today and could be more important in the future associated with a strong positive feedback to climate change. However, indirect methane emissions from permafrost thawing are difficult to estimate at present, with no data yet to refer to, and in any case largely overlap with wetland and freshwater emissions occurring above or around thawing areas.

Here, we choose to report here only the direct emission range of 0-1 Tg CH₄ yr⁻¹, keeping in mind that current wetland, thermokarst lakes and other freshwater methane emissions already likely include a significant indirect contribution originating from thawing permafrost. For the next century, it has been recently estimated that 5-15% of the terrestrial permafrost carbon pool is vulnerable to release in the form of greenhouse gases, corresponding to 130-160 Pg C. The likely progressive release in the atmosphere of such an amount of carbon as carbon dioxide and methane will have a significant impact on climate change trajectory (Schuur et al., 2015). The underlying methane hydrates represent a substantial reservoir of methane, estimated up to 530 000 Tg of CH₄ (Ciais et al., 2013). Present and future emissions related to this reservoir are very difficult to assess at the moment and require more studies.

3.2.8 Vegetation

Over the past decade, a series of studies defined three distinct pathways for the production and emission of methane by living vegetation. First, plants can act as “straws”, transpiring methane produced by microbes from anoxic soils (Rice et al., 2010; Cicerone and Shetter, 1981). Second, plants may produce methane through an unresolved abiotic photochemical process following stress or exposure to UV light (Keppler et al., 2006; Vigano et al., 2008). However, the latter pathway has been criticized (e.g. Dueck et al. (2007); Nisbet et al. (2009)) and its implication for the global methane budget was found small based on additional experiments (e.g. Dueck et al. (2007); Nisbet et al. (2009)) and on atmospheric analyses (Houweling et al., 2008). Third, the wood of living trees also provides an environment suitable for biogenic microbial methanogenesis (Covey et al., 2012; Mukhin and Voronin, 2011; Hietala et al., 2015). Even if methane measured locally in various environments (Terazawa et al., 2007; Pangala et al., 2013; 2015) is “only” transpired by plants, it could still emit a significant amount of methane at global scale (Nisbet et al., 2009). Yet, overlapping of these potential methane emissions with soil uptake or forested wetlands is largely unknown today (Covey et al., 2012). Before potentially integrating such emissions in the global methane budget, further work is needed to resolve the mechanisms, scales, spatio-temporal patterns and magnitudes of these challenging fluxes.

3.3 Methane sinks and lifetime

Methane is the most abundant reactive trace gas in the troposphere and its reactivity is important to both tropospheric and stratospheric chemistry. The main atmospheric sink of methane is its oxidation by the hydroxyl radical (OH), mostly in the troposphere, which contributes about 90% of the total methane sink (Ehhalt, 1974). Other losses are by photochemistry in the stratosphere (reactions with chlorine atoms, Cl, and atomic oxygen, O¹D), by oxidation in soils (Curry, 2007; Dutaur and



Verchot, 2007), and by photochemistry in the marine boundary layer (reaction with Cl; Allan et al. (2007), Thornton et al. (2010)). Uncertainties in the total sink of methane as estimated by atmospheric chemistry models are in the order of 20-40% (K13). It is much less (10-20%) when using atmospheric proxy methods (e.g. methyl chloroform, see below) as in atmospheric inversions (K13). Methane also affects the concentrations of water vapour and ozone in the stratosphere and thus plays a key role in the conversion of reactive chlorine to less reactive HCl. In the present release of the global methane budget, we essentially rely on the former analysis of K13 and IPCC AR5. Following the ACCMIP model intercomparison (Lamarque et al., 2013), the ongoing Climate Chemistry Model Initiative (CCMI) and the upcoming Aerosols Chemistry Modeling Intercomparison Project (AerChemMIP) should allow getting updated estimates on methane chemical sinks and lifetime.

10 3.3.1 OH oxidation

OH radicals are produced following the photolysis of ozone (O_3) in the presence of water vapour. OH is destroyed by reactions with CO, CH_4 , and non-methane volatile organic compounds but since OH exists in photochemical equilibrium with HO_2 , the net effect of CH_4 oxidation on the HO_x budget also depends on the level of NO_x (Lelieveld et al., 2002) and other competitive oxidants. Considering its very short lifetime (a few seconds, Lelieveld et al. (2004)), it is not possible to estimate global OH concentrations directly from observations. Using 16 chemistry-climate models and chemistry-transport models, the Atmospheric Chemistry and Climate Model Intercomparison Project (ACCMIP) proposed a series of experiments aimed at studying the long-term changes in atmospheric composition between 1850 and 2100 (Lamarque et al., 2013). For the year 2000, ACCMIP estimated a global mean (mass-weighted) OH tropospheric concentration of $11.7 \pm 1.0 \times 10^5$ molec./ cm^3 (range [10.3-13.4], Voulgarakis et al. (2013)), consistent with the estimates of Prather et al. (2012) at 11.2 ± 1.3 molec./ cm^3 . The global atmospheric methane burden is 4813 ± 81 Tg CH_4 (range [4678-4980] Tg CH_4 , Naik et al. (2013)).

As with the Mt. Pinatubo eruption in 1991, climate variability can impact the inter-annual variability (IAV) of the chemical destruction of CH_4 by OH radicals (Dlugokencky et al., 1996). OH IAV may also be influenced by the strength of biomass burning (Voulgarakis et al., 2015). Moreover, the recent increase of the oxidizing capacity of the troposphere in South and East Asia, associated with increasing NO_x emissions and decreasing CO emissions (Mijling et al., 2013; Yin et al., 2015) could enhance CH_4 consumption and therefore limit the atmospheric impact of increasing emissions (Dalsøren et al., 2009). Despite such large regional changes, the global mean OH concentration was suggested to have changed only slightly over the past 150 years (Naik et al., 2013). This is due to the concurrent increases of positive influences on OH (water vapour, tropospheric ozone, nitrogen oxides (NO_x) emissions, and UV radiation due to decreasing stratospheric ozone), and of OH sinks (methane burden, carbon monoxide and non-methane volatile organic compound emissions and burden). The sign and integrated magnitude (from 1850 to 2000) of OH changes is uncertain, varying from -13% to +15% among the ACCMIP models (mean of -1%, Naik et al. (2013)). A possible positive OH trend occurred since the 1970s followed by stagnation to



decreasing OH in the 2000s, possibly contributing to recent observed atmospheric methane changes (Dalsøren et al., 2016; Rigby et al., 2008; McNorton et al., 2016).

Accurate methyl chloroform atmospheric observations together with estimates of its emissions (Montzka and Fraser, 2003) allow an estimate of OH changes in the troposphere since the 1980s. Montzka et al. (2011b) inferred small inter-annual OH variability and trends (typical OH changes from year to year of less than 3%), and attributed previously estimated large year-to-year OH variations before 1998 (e.g. Bousquet et al. (2005), Prinn et al. (2001)) to overly large sensitivity of OH concentrations inferred from methyl chloroform measurements to uncertainties in the latter's emissions. However, Prinn et al. (2005) also showed lower post-1998 OH variability that they attributed to the lack of strong post-1998 El Niño's. For the ACCMIP models providing continuous simulations over the past decades, OH inter-annual variability ranged from 0.4% to 0.9%, consistent, although lower, than the value deduced from methyl chloroform measurements. As methyl chloroform has reached very low concentrations in the atmosphere, in compliance with the application of the Montreal Protocol and its amendments, a replacement compound is needed to estimate global OH concentrations. Several HCFCs and HFCs have been tested (Miller et al., 1998; Montzka et al., 2011b; Huang and Prinn, 2002) to infer OH but do not yet provide equivalent results to methyl chloroform. Before 2007, a decrease in methane lifetime in response to the OH increase, because of increasing Asian NO_x emissions, cannot be excluded to explain at least part of the stagnation of atmospheric growth (Dalsøren et al., 2009; Monteil et al., 2011; Dalsøren et al., 2016). Even below 3 %, OH variability in the atmosphere could help explain changes in the methane atmospheric growth rate during the past decades on top of changing emissions, as a 1% change in global OH concentration results in a CH₄ sink change of 5 Tg CH₄.

We report here a climatological range of [454-617] Tg CH₄ yr⁻¹ as in K13 for the total tropospheric loss of methane by OH oxidation in the 2000s.

3.3.2 Stratospheric loss

Approximately 60 Tg CH₄ yr⁻¹ enter the stratosphere by cross-tropopause mixing and the Hadley circulation (Reeburgh, 2007). In the stratosphere, currently approximately 51 [16-84] Tg CH₄ yr⁻¹ (i.e. about 10 [3-16] % of the total chemical loss in the atmosphere) is lost through reactions with excited atomic oxygen O(¹D), atomic chlorine (Cl), atomic fluorine (F), and OH (Voulgarakis et al., 2013; Williams et al., 2012). The fraction of the stratospheric loss due to the different oxidants is uncertain, possibly within 20-35% due to halons, about 25% due to O(¹D), the rest being due to stratospheric OH (Neef et al., 2010). The oxidation of methane in the stratosphere produces significant amounts of water vapour, which has a positive radiative forcing, and stimulates the production of OH through its reaction with atomic oxygen (Forster et al., 2007). Stratospheric methane thus contributes significantly to the observed variability and trend in stratospheric water vapour (Hegglin et al., 2014). Uncertainties in the chemical loss of stratospheric methane are large, due to uncertain inter-annual variability in stratospheric transport as well as through its chemical interactions with stratospheric ozone (Portmann et al., 2012).

We report here a climatological range of [16-84] Tg CH₄ yr⁻¹ as in K13.



3.3.3 Tropospheric reaction with Cl

Halogen atoms can also contribute to the oxidation of methane in the troposphere. Allan et al. (2005) measured mixing ratios of methane and $\delta^{13}\text{C-CH}_4$ at two stations in the southern hemisphere from 1991 to 2003, and found that the apparent kinetic isotope effect of the atmospheric methane sink was significantly larger than that explained by OH alone. A seasonally varying sink due to atomic chlorine (Cl) in the marine boundary layer of between 13 and 37 Tg $\text{CH}_4 \text{ yr}^{-1}$ was proposed as the explaining mechanism (Allan et al., 2007). This sink was estimated to occur mainly over coastal and marine regions, where NaCl from evaporated droplets of seawater react with NO_2 to eventually form Cl_2 , which then UV-dissociates to Cl. However significant production of nitryl chloride (ClNO_2) at continental sites has been recently reported (Riedel et al., 2014) and suggests the broader presence of Cl, which in turn would expand the significance of the Cl sink in the troposphere. More work is needed on this potential re-evaluation of the Cl impact on the methane budget.

We report here a climatological range of [13-37] Tg $\text{CH}_4 \text{ yr}^{-1}$ as in K13.

3.3.4 Soil uptake

Unsaturated oxic soils are sinks of atmospheric methane due to the presence of methanotrophic bacteria, which consume methane as a source of energy. Wetlands with temporally variable saturation, can also act as methane sinks. Dutaur and Verchot (2007) conducted a comprehensive meta-analysis of field measurements of CH_4 uptake spanning a variety of ecosystems. They reported a range of 36 ± 23 Tg $\text{CH}_4 \text{ yr}^{-1}$, but also showed that stratifying the results by climatic zone, ecosystem and soil type led to a narrower range (and lower mean estimate) of 22 ± 12 Tg $\text{CH}_4 \text{ yr}^{-1}$. A modeling study by Ridgwell et al. (1999) simulated the sink to be [20–51] Tg $\text{CH}_4 \text{ yr}^{-1}$. Curry (2007) used a process-based methane consumption scheme coupled to a land surface model (and calibrated to field measurements) to obtain a global estimate of 28 Tg $\text{CH}_4 \text{ yr}^{-1}$, with a range of [9-47] Tg $\text{CH}_4 \text{ yr}^{-1}$, which is the result reported in K13. Tian et al. (2016) further updated the CH_4 uptake from soil, with the estimate of 30 ± 19 Tg $\text{CH}_4 \text{ yr}^{-1}$. In that model, CH_4 uptake was determined by the diffusion rate of methane and oxygen through the uppermost soil layer, which was in turn dependent upon the soil characteristics (e.g. texture, bulk density) and water content (Curry, 2007). Riley et al. (2011) used another process-based model and estimated a global atmospheric CH_4 sink of 31- Tg $\text{CH}_4 \text{ yr}^{-1}$. The methane consumption rate was also dependent on the available soil water, soil temperature, and nutrient availability. Although not addressed in that model, it should be noted that if the soil water content increases enough to inhibit the diffusion of oxygen, the soil could become a methane source (Lohila et al., 2016). This transition can be rapid, thus creating areas that can be either a source or a sink of methane depending on the season.

Following Curry (2007), and consistent with Tian et al. (2015), we report here a climatological range of [9-47] Tg $\text{CH}_4 \text{ yr}^{-1}$ as in K13.



3.3.5 CH₄ lifetime

The methane lifetime due to tropospheric OH, defined as the atmospheric burden divided by the oxidation by OH in the troposphere, is of 9.3 years (range [7.1-10.6], Voulgarakis et al. (2013)); K13). Integrating all other sink processes on the top of tropospheric loss due to OH leads to a total methane lifetime of 8.2 ± 0.8 years (for year 2000, range [6.4-9.2], Voulgarakis et al. (2013)). This is smaller than, although statistically consistent with the value reported in Table 6.8 of the IPCC AR5 of 9.1 ± 0.9 years (which was the observationally constrained estimate of Prather et al. (2012)) most commonly used in the literature (Ciais et al., 2013). The multi-model mean methane lifetime from ACCMIP is simulated to have increased by 2.3% from 1850 to 1980, with a large inter-model difference in magnitude and sign: six models simulated decreases in methane lifetime (maximum -8%) while the rest simulated increases in methane lifetime (maximum +14%). In contrast, from 1980 to 2000, all models simulated a decrease in methane lifetime with a mean lifetime reduction of -4 %. Similarly, by analysing global chemistry-transport modelling against methyl chloroform observations, Holmes et al. (2013) inferred a 2.2 ± 1.8 % decrease in methane lifetime for the 1980–2005 period consistent with Dalsøren et al. (2016), but not with Montzka et al. (2011a). The decrease in methane lifetime reported by Holmes et al. (2013) corroborated studies on the potential impact of recent CO and NO_x emissions towards increasing the atmosphere's oxidizing capacity and decreasing the methane lifetime (Dalsøren et al., 2009; Gupta et al., 1998). At present, such OH changes are only indirectly inferred in atmospheric inversions, through the proxy analysis of methyl chloroform atmospheric changes.

4 Atmospheric observations and top-down inversions

4.1 Atmospheric observations

The first systematic atmospheric CH₄ observations began in 1978 (Blake et al., 1982) with infrequent measurements from discrete air samples collected in the Pacific at a range of latitudes from 67°N to 53°S. Because most of these air samples were from well-mixed oceanic air masses and the measurement technique was precise and accurate, they were sufficient to establish an increasing trend and the first indication of the latitudinal gradient of methane. Spatial and temporal coverage was greatly improved soon after (Blake and Rowland, 1986) with the addition of the NOAA flask network (Steele et al. (1987), Fig. 1), and of AGAGE (Cunnold et al., 2002), CSIRO (Francey et al., 1999), and other networks (e.g. ICOS network in Europe, <https://www.icos-ri.eu/>). The combined datasets provide the longest time series of globally averaged CH₄ abundance. Since the early-2000s, remotely sensed retrievals of CH₄ provide CH₄ atmospheric column averaged mole fractions (Buchwitz et al., 2005a; Frankenberg et al., 2005; Butz et al., 2011; Crevoisier et al., 2009; Wunch et al., 2011). Fourier transform infrared (FTIR) measurements at fixed locations also provide methane column observations (Wunch et al., 2011).



4.1.1 In situ CH₄ observations and atmospheric growth rate at the surface

Four observational networks provide globally averaged CH₄ mole fractions at the Earth's surface: the Earth System Research Laboratory from US National Oceanic and Atmospheric Administration (NOAA/ESRL, Dlugokencky et al. (1994)), the Advanced Global Atmospheric Gases Experiment (AGAGE, Prinn et al. (2000), Cunnold et al. (2002), Rigby et al. (2008)), the Commonwealth Scientific and Industrial Research Organisation (CSIRO, Francey et al. (1999)) and the University of California Irvine (UCI, Simpson et al. (2012)). The data are archived at the World Data Centre for Greenhouse Gases (WDCGG) of the WMO Global Atmospheric Watch (WMO-GAW) program, including measurements from other sites that are not operated as part of the four networks.

The networks differ in their sampling strategies, including the frequency of observations, spatial distribution, and methods of calculating globally averaged CH₄ mole fractions. Details are given in the supplementary material of K13. For the global average values of CH₄ concentrations presented here, all measurements are made using gas chromatography with flame ionization detection (GC/FID), although chromatographic schemes vary among the labs. Because GC/FID is a relative measurement method, the instrument response must be calibrated against standards. NOAA maintains the WMO CH₄ mole fraction scale X2004A; NOAA and CSIRO global means are on this scale. AGAGE uses an independent standard scale (Aoki et al., 1992), but direct comparisons of standards and indirect comparisons of atmospheric measurements show that differences are below 5 ppb (WMO RoundRobin programme). UCI uses another independent scale that was established in 1978 and is traceable to NIST (Simpson et al., 2012), but has not been included in standard exchanges with other networks so differences with the other networks cannot be quantitatively defined. Additional experimental details are presented in the supplementary material from K13 and references therein.

In Fig. 1, (a) globally averaged CH₄ and (b) its growth rate (derivative of the deseasonalized trend curve) through 2012 are plotted for a combination of the four measurement programs using a procedure of signal decomposition described in Thoning et al. (1989). We define the annual increase G_{ATM} as the increase in the growth rate from Jan. 1 in one year to Jan. 1 in the next year. Agreement among the four networks is good for the global growth rate, especially since ~1990. The long-term behaviour of globally averaged atmospheric CH₄ shows a decreasing but positive growth rate (defined as the derivative of the deseasonalized mixing ratio) from the early-1980s through 1998, a near-stabilization of CH₄ concentrations from 1999 to 2006, and a renewed period with positive but stable growth rates since 2007. When a constant atmospheric lifetime is assumed, the decreasing growth rate from 1983 through 2006 implies that atmospheric CH₄ was approaching steady state, with no trend in emissions. The NOAA global mean CH₄ concentration was fitted with a function that describes the approach to a first-order steady state ($_{SS}$ index): $[CH_4](t) = [CH_4]_{SS} - ([CH_4]_{SS} - [CH_4]_0)e^{-t/\tau}$; solving for the lifetime, τ , gives 9.3 years, which is very close to current literature values (e.g., Prather et al. (2012)).

On decadal timescales, the annual increase is on average 2.1 ± 0.3 ppb yr⁻¹ for 2000-2009, 3.5 ± 0.2 ppb yr⁻¹ for 2003-2012 and 5.0 ± 1.0 ppb yr⁻¹ for the year 2012. The two decadal values hide a jump in the growth rate after 2006. Indeed, from 1999 to 2006, the annual increase of atmospheric CH₄ was remarkably small at 0.6 ± 0.1 ppb yr⁻¹. In the last 8 years, the atmospheric



growth rate has recovered to a level similar to that of the mid-1990s ($\sim 5\text{ppb yr}^{-1}$), before the stabilization period of 1999-2006, as stated in K13.

4.1.2 Satellite data of column average CH_4

In the 2000s, two space-borne instruments sensitive to atmospheric methane were put in orbit and have provided atmospheric methane column-averaged dry air mole fraction (XCH_4), using either shortwave Infrared spectrometry (SWIR) or thermal infrared spectrometry (TIR).

Between 2003 and 2012, the Scanning Imaging Absorption spectrometer for Atmospheric Cartography (SCIAMACHY) was operated on board the ESA ENVIRONMENTAL SATellite (ENVISAT), providing nearly 10 years of XCH_4 sensitive to the atmospheric boundary layer (Burrows et al., 1995; Buchwitz et al., 2006; Dils et al., 2006; Frankenberg et al., 2011). These satellite retrievals were the first to be used for global and regional inverse modelling of methane fluxes (Meirink et al., 2008a; Bergamaschi et al., 2007; Bergamaschi et al., 2009). The relative long time record allowed the analysis of the inter-annual methane variability (Bergamaschi et al., 2013). However, the use of SCIAMACHY necessitates important bias correction, especially after 2005 (up to 40 ppb from south to north) (Bergamaschi et al., 2009; Houweling et al., 2014; Alexe et al., 2015).

In January 2009, the JAXA satellite Greenhouse Gases Observing SATellite (GOSAT) was launched containing the TANSO-FTS instrument, which observes in the shortwave infrared (SWIR). Different retrievals of methane based on TANSO-FTS/GOSAT products are made available to the community (Yoshida et al., 2013; Schepers et al., 2012; Parker et al., 2011) based on two retrieval approaches, Proxy and Full Physics. The proxy method retrieves the ratio of methane column (XCH_4) and carbon dioxide column (XCO_2), from which XCH_4 is derived after multiplication with transport model-derived XCO_2 (Chevallier et al., 2010; Peters et al., 2007; Frankenberg et al., 2006). It intends mostly to remove biases due to light scattering on clouds and aerosols, and is highly efficient owing to the small spectral distance between CO_2 and CH_4 sunlight absorption bands ($1.65\mu\text{m}$ for CH_4 and $1.60\mu\text{m}$ for CO_2). Because of this, scattering-induced errors are similar for XCO_2 and XCH_4 and cancel out in the ratio. The second approach is the Full Physics algorithm, which retrieves the aerosol properties (amount, size and height) along with CO_2 and CH_4 columns (e.g. Butz et al. (2011)). Although GOSAT retrievals still show significant unexplained biases (possibly also linked to atmospheric transport modelling (Locatelli et al., 2015)) and limited sampling in cloud covered regions and in the high latitude winter, it represents an important improvement compared to SCIAMACHY both for random and systematic observation errors (see Table S2 of Buchwitz et al. (2016)).

Atmospheric inversions based on SCIAMACHY or GOSAT CH_4 retrievals have been carried out by different research groups (Monteil et al., 2013; Cressot et al., 2014; Alexe et al., 2015; Bergamaschi et al., 2013; Locatelli et al., 2015). For GOSAT, differences between the use of Proxy and Full Physics retrievals have been investigated. In addition, joint CO_2 - CH_4 inversions have been conducted to investigate the use of GOSAT retrieved ratios avoiding a model-derived hard constraint on XCO_2 (Pandey et al., 2015; 2016; Fraser et al., 2013). Results from some of these studies are reported in Sect. 5 of this paper.



4.1.3 Other atmospheric observations not integrated in this study

Other types of methane measurements are available, which are not commonly used to infer fluxes from inverse modelling (yet), but are used to verify its performance (see e.g. Bergamaschi et al. (2013)). Aircraft or balloon-borne in situ measurements can deliver vertical profiles with high vertical resolution. Such observations can also be used to test remote sensing measurement from space or from the surface and bring them on the same scale as the in situ surface measurements. Aircraft measurements have been undertaken in various regions either during campaigns (Wofsy, 2011; Beck et al., 2012; Chang et al., 2014; Paris et al., 2010), or in a recurrent mode using small aircrafts in the PBL (Sweeney et al., 2015; Umezawa et al., 2014; Gatti et al., 2014) and commercial aircrafts (Schuck et al., 2012; Brenninkmeijer et al., 2007; Umezawa et al., 2012; 2014; Machida et al., 2008). Balloons can carry in situ instruments (e.g. Joly et al. (2008); using Accordable Laser Diodes Spectrometry) or air samplers (e.g. aircores, Karion et al. (2010)) up to 30 km height.

In October 2006, the Infrared Atmospheric Sounding Interferometer (IASI) on board the European MetOp-A satellite began to operate. Measuring the thermal radiation from Earth and the atmosphere in the TIR, it provides mid-to-upper troposphere columns of methane (representative of the 5-15 km layer) over the tropics using an infrared sounding interferometer (Crevoisier et al., 2009). Despite its sensitivity being limited to the mid-to-upper troposphere, its use in flux inversions has shown consistent results in the tropics with surface and other satellite-based inversions (Cressot et al., 2014).

The Total Carbon Column Observing Network (TCCON) uses ground-based Fourier transform spectrometers (FTS) to measure atmospheric column abundances of CO₂, CO, CH₄, N₂O and other molecules that absorb sunlight in the near-infrared spectral region (Wunch et al., 2011). As TCCON measurements make use of sunlight, they can be performed throughout the day during clear sky conditions, with the sun typically 10° above the horizon. The TCCON network has been established as reference for the validation of column retrievals, like those from SCIAMACHY and GOSAT. TCCON data can be obtained from the TCCON Data Archive, hosted by the Carbon Dioxide Information Analysis Center (CDIAC, <http://cdiac.ornl.gov/>).

Finally, the isotopic composition of atmospheric methane is measured at a subset of surface stations (Quay et al., 1991; 1999; Lowe et al., 1994; Miller et al., 2002; Morimoto et al., 2006; Tyler et al., 2007). The two main isotopologues of CH₄ are ¹³CH₄ and CH₃D. δ¹³CH₄ measurements are made mainly on flask air samples analysed with gas-chromatograph isotope ratio spectrometry for which an accuracy of 0.05 per mil can be achieved (Rice et al., 2001; Miller et al., 2002). These isotopic measurements based on air flask sampling have relatively low spatial and temporal resolutions. Laser-based absorption spectrometers and isotope ratio mass spectrometry techniques have recently been developed to increase sampling frequency and allow in situ operation (McManus et al., 2010; Santoni et al., 2012). Measurements of ¹³CH₄ can help to partition the different methanogenic processes of methane: biogenic, thermogenic or pyrogenic sources (Quay et al., 1991; Miller et al., 2002; Fisher et al., 2011) or even the methanogenic pathway (McCalley et al., 2014). dD provides valuable information on the oxidation by the OH radicals (Röckmann et al., 2011) and emissions also show substantial differences in dD isotopic signatures (Melton et al., 2012; Quay et al., 1999). Some studies have simulated such observations (Neef et al., 2010; Monteil et al., 2011) or used them as additional constraints to inverse systems (Mikaloff Fletcher et al., 2004; Hein et al., 1997;



Bousquet et al., 2006; Neef et al., 2010). Since 2007, the average annual growth rate amounts to 5.5 ± 0.6 ppb yr^{-1} . Scenarios of increasing fossil and microbial sources have been proposed to explain the sustained increased growth rate since 2007 (Bousquet et al., 2011; Bergamaschi et al., 2013; Nisbet et al., 2014). Whereas the decreasing trend in $\delta^{13}\text{C}$ in CH_4 suggests a significant, if not dominant, contribution from increasing emissions by microbial CH_4 sources (Schaefer et al., 2016; Nisbet et al., 2014), concurrent ethane and methane column measurements suggest a significant role (likely at least 39%) for oil and gas production (Hausmann et al., 2016), which could be consistent when assuming a concomitant decrease in biomass burning emissions (heavy source for ^{13}C), as suggested by the GFED database (Giglio et al., 2013). ^{14}C - CH_4 measurements (Quay et al., 1991; 1999; Lowe et al., 1988) may also help to partition for fossil fuel contribution. For example, Lassey et al. (2007a) used more than 200 measurements of radioactive ^{14}C - CH_4 (with a balanced weight between Northern and Southern hemispheres) to further constrain the fossil fuel contribution to the global methane source emission to $30 \pm 2\%$ for the period 1986-2000. Using pseudo-observations, Rigby et al. (2012) found that Quantum Cascade Laser-based isotopic observations would reduce the uncertainty in four major source categories by about 10% at the global scale (microbial, biomass burning, landfill and fossil fuel) and by up to 50% at the local scale.

4.2 Top-down inversions

4.2.1 Principle of inversions

An atmospheric inversion for methane fluxes (sources and sinks) optimally combines atmospheric observations of methane and associated uncertainties, a prior knowledge of the fluxes including their uncertainties, and a chemistry-transport model to relate fluxes to concentrations (Rodgers, 2000). In this sense, T-D inversions integrate all the components of the methane cycle described previously in this paper. The observations can be surface or upper-air in situ observations, satellite and surface retrievals. Prior emissions generally come from B-U approaches such as process-based models or data-driven extrapolations (natural sources) and inventories (anthropogenic sources). The chemistry-transport model can be Eulerian or Lagrangian, and global or regional, depending on the scale of the flux to be optimized. Atmospheric inversions generally rely on the Bayes theorem, which leads to the minimization of a cost function as Eq (3):

$$J(\mathbf{x}) = \frac{1}{2}(\mathbf{y} - H(\mathbf{x}))^T \mathbf{R}^{-1}(\mathbf{y} - H(\mathbf{x})) + \frac{1}{2}(\mathbf{x} - \mathbf{x}_b)^T \mathbf{B}^{-1}(\mathbf{x} - \mathbf{x}_b) \quad (3)$$

where \mathbf{y} is a vector containing the atmospheric observations, \mathbf{x} is a state vector containing the methane emission and other appropriate variables (like OH concentrations or CH_4 concentrations at the start of the assimilation window) to be estimated, and \mathbf{x}^b is the prior state of \mathbf{x} , H is the observation operator, here the combination of an atmospheric transport and chemistry model and an interpolation procedure sampling the model at the measurement coordinates. \mathbf{R} is the error covariance matrix of the observations and \mathbf{P}_b is the error covariance matrix associated to \mathbf{x}^b . The errors on the modelling of atmospheric transport and chemistry are included in the \mathbf{R} matrix (Tarantola, 1987). The minimization of a linearized version of J leads to the optimized state vector \mathbf{x}^a (Eq. 4):



$$\mathbf{x}_a = \mathbf{x}_b + (\mathbf{H}^T \mathbf{R}^{-1} \mathbf{H} + \mathbf{P}_b^{-1})^{-1} \mathbf{H}^T \mathbf{R}^{-1} (\mathbf{y} - H(\mathbf{x}))$$

(4)

where \mathbf{P}_a is given by Eq. 5 and represents the error covariance matrix associated to \mathbf{x}^a , and \mathbf{H} contains the sensitivities of any observation to any component of state vector \mathbf{x} (linearized version of the observation operator $H(\mathbf{x})$).

$$\mathbf{P}_a = (\mathbf{H}^T \mathbf{R}^{-1} \mathbf{H} + \mathbf{P}_b^{-1})^{-1}$$

(5)

Unfortunately, the size of the inverse problem usually does not allow computing \mathbf{P}^a , which is therefore approximated using the leading eigenvectors of the Hessian of J (Chevallier et al., 2005) or from stochastic ensembles (Chevallier et al., 2007). Therefore, the optimized fluxes \mathbf{x}^a are obtained using classical minimization algorithms (Chevallier et al., 2005; Meirink et al., 2008b). Alternatively, Chen and Prinn (2006) computed monthly emissions by applying a recursive Kalman filter in which \mathbf{P}^a is computed explicitly for each month. Emissions are generally derived at weekly to monthly time scales, and for spatial resolutions ranging from model grid resolution to large aggregated regions. Spatio-temporal aggregation of state vector elements reduces the size of the inverse problem and allows the computation of \mathbf{P}_a . However, such aggregation can also generate aggregation errors inducing possible biases in the inferred emissions and sinks (Kaminski et al., 2001). The estimated \mathbf{x}_a can represent either the net methane flux in a given region or contributions from specific source categories.

Atmospheric inversions use bottom-up models and inventories as prior estimates of the emissions and sinks in their setup, which make B-U and T-D approaches generally not independent.

4.2.2 Reported inversions

A group of nine atmospheric inversion systems using global Eulerian transport models were used in this synthesis. Each inversion system provides from one to ten inversions, including sensitivity tests varying the assimilated observations (surface or satellite) or the inversion setup. This represents a total of 30 inversion runs with different time coverage: generally 2000-2012 for surface-based observations, 2003-2012 for SCIAMACHY-based inversions and 2009-2012 for GOSAT-based inversions (Table 3). When multiple sensitivity tests were performed we use the mean of this ensemble not to overweight one particular inverse model. Bias correction procedures have been developed to assimilate SCIAMACHY (Bergamaschi et al., 2009; 2013; Houweling et al., 2014) and GOSAT data (Cressot et al., 2014; Houweling et al., 2014; Locatelli et al., 2015). These procedures can lead to corrections from several ppb and up to several tens of ppb (Bergamaschi et al., 2009; Locatelli et al., 2015). Although partly due to transport model errors, the large corrections applied to satellite total column CH_4 data questions the comparably low systematic errors reported in satellite validation studies using TCCON (Dils et al., 2014; CCI-Report, 2016). It should also be noticed that some satellite-based inversions are in fact combined satellite and surface inversions as they use either instantaneous in situ data simultaneously (Bergamaschi et al., 2013; Alexe et al., 2015) or annual mean surface observations to correct satellite bias (Locatelli et al., 2015). Nevertheless, these inversions are still referred to as satellite-based inversions.



General characteristics of the inversion systems are provided in Table 3. Further detail can be found in the referenced papers. Each group was asked to provide gridded flux estimates for the period 2000-2012, using either surface or satellite data, but no additional constraints were imposed so that each group could use their preferred inversion setup. This approach is appropriate for our purpose of flux assessment, but not necessarily for model inter-comparison. Each group provided gridded
5 monthly maps of emissions for both their prior and posterior total and for sources per category (see the categories Sect. 2.3). Results are reported in Sect. 5. Atmospheric sinks were not analysed for this budget, which still relies on K13 for B-U budget and on a global mass balance for T-D budget (difference between the global source and the observed atmospheric increase).

The last year of reported inversion results is 2012, which represents a 4 year-lag with the present. Satellite observations are linked to operational data chains and are generally available within days to weeks after the recording of the spectra.
10 Surface observations can lag from months to years because of the time for flask analyses and data checks in (mostly) non-operational chains. With operational networks such as ICOS in Europe, these lags will be reduced in the future. In addition, the final six months of inversions are generally ignored (spin down) because the estimated fluxes are not constrained by as many observations as the previous months. Finally, the long inversion runs and analyses can take up to months to be performed. For the next GCP-CH₄ budget the objective is to represent more recent years by reducing the analysis time and
15 shortening the in situ atmospheric observation release.

5 Methane budget: top-down and bottom-up comparison

5.1 Global methane budget

5.1.1 Global budget of total methane emissions

T-D estimates. At the global scale, the total emissions inferred by the ensemble of 30 inversions is 558 Tg CH₄ yr⁻¹ [540-
20 570] for the 2003-2012 decade (Table 4), with a higher value of 568 Tg CH₄ yr⁻¹ [560-580] for 2012. Global emissions for 2000-2009 (552 Tg CH₄ yr⁻¹) are consistent with K13 and the range of uncertainties for global emissions [535-566] is in line as well with that of K13 [526-569], although eight out of the 30 inversions presented here (~25%) are different. The latitudinal breakdown of emissions inferred from atmospheric inversions reveals a dominance of tropical emissions at 359 Tg CH₄ yr⁻¹ [339-386], representing 64% of the global total. Thirty-two per cent of the emissions are from the mid-latitudes and
25 4% from high latitudes (above 60°N).

B-U estimates. The picture given by the bottom-up approaches is quite different with global emissions of 736 Tg CH₄ yr⁻¹ [596-884] for 2003-2012 (Table 2). This estimate is much larger than T-D estimates. The bottom-up estimate is given by the sum of individual anthropogenic and natural processes, with no constraint on the total. As noticed in K13, such a large global
30 emissions rate is not consistent with atmospheric constraints brought by OH optimization and is very likely overestimated.



This overestimation likely results from errors in the extrapolation of specific sources or in the atmospheric sink terms, and double counting of some natural sources (e.g. wetlands versus inland waters).

5.1.2 Global methane emissions per source category

The global methane budget for five source categories (see Sect. 2.3) for 2003-2012 is presented in Fig. 5 and Table 2. T-D estimates attribute about 60% of the total emissions to anthropogenic activities (range of [50-70]%), and 40% to natural emissions. As natural emissions from B-U models are much larger, the anthropogenic versus natural emission ratio is more balanced for B-U (~50% each). A predominant role of anthropogenic sources of methane emissions is strongly supported by the ice core and atmospheric methane records. The data indicate that atmospheric methane varied around 700 ppb during the last millennium before increasing by a factor of 2.6 to ~1800 ppb. Accounting for the decrease in mean-lifetime over the industrial period, Prather et al. (2012) estimates from these data a total source of 554 ± 56 Tg-CH₄ in 2010 of which about 64% (352 ± 45 Tg-CH₄) are of anthropogenic origin, very consistent estimates with our synthesis.

Wetlands. For 2003-2012, the top-down and bottom-up derived estimates of respectively 167 Tg CH₄ yr⁻¹ (range [127-202]) and 185 Tg CH₄ yr⁻¹ (range [153-227]) are statistically consistent. Mean wetland emissions for the 2000-2009 period appear similar, albeit slightly smaller than found in K13: 166 Tg CH₄ yr⁻¹ in this study versus 175 Tg CH₄ yr⁻¹ in K13 for T-D (-4%) and 183 Tg CH₄ yr⁻¹ in this study versus 217 Tg yr⁻¹ in K13 for B-U (-15%). Note that more inversions (T-D) and more wetland models (B-U) were used in this study. Inversions have difficulty in separating wetlands from other sources, so that uncertainties on T-D wetland emissions remain large. In this study, all BU models were forced with the same wetland extent and climate forcings (Poulter et al., 2016, submitted), with the result that the amplitude of the range of emissions of [151-222] for 2000-2009 has narrowed by a third compared to the previous estimates from Melton et al. (2013) ([141-264]) and from K13 ([177-284]). This suggests that differences in wetland extent explain about a third (30-40%) of the former range of the emission estimates of global natural wetlands. The remaining range is due to differences in model structures and parameters. It is also worth noting that B-U and T-D estimates differ less in this study (~17 Tg yr⁻¹ for the mean) than in K13 (~30 Tg yr⁻¹), although results from many more models are reported here. For TD inversions, natural wetlands represent 30% on average of the total methane emissions but only 25% for B-U models (because of higher total emissions inferred by B-U models).

Other natural emissions. The discrepancy between T-D and B-U budgets is the largest for the natural emission total, which is 384 Tg CH₄ yr⁻¹ [257-524] for B-U and only 231 Tg CH₄ yr⁻¹ [194-296] for T-D over the 2003-2012 decade. Processes other than natural wetlands (Fig. 5), namely freshwater systems, geological sources, termites, oceans, wild animals, wildfires, and permafrost, explain this large discrepancy. For the 2003-2012 decade, T-D inversions infer non-wetland natural emissions of 64 Tg CH₄ yr⁻¹ [21-132] whereas the sum of the individual B-U emissions is 199 Tg CH₄ yr⁻¹ [104-297]. The two main contributors to this large B-U total are freshwaters (~60%) and geological emissions (~20%), both of which have large



uncertainties without spatially explicit representation. Because of the discrepancy, this category represents 10% of total emissions for T-D inversions, but 27% for B-U approaches.

Improved area estimates of freshwater emissions would be beneficial. For example, stream fluxes are difficult to assess because of the high-expected spatial variability and very uncertain areas of headwater streams where methane-rich ground water may be rapidly degassed. There are also uncertainties in the geographical distinction between wetlands, small lakes (e.g. thermokarst lakes), and floodplains that will need more attention to avoid double counting. In addition, major uncertainty is still associated with representation of ebullition. The intrinsic nature of this large but very locally distributed flux highlights the need for cost-efficient high-resolution techniques for resolving the spatio-temporal variations of these fluxes. In this context of observational gaps in space and time, freshwater fluxes are considered underestimated until measurement techniques designed to properly account for ebullition become more common (Wik et al., 2016a). On the contrary, global estimates for freshwater emissions rely on up-scaling of uncertain emission factors and emitting areas, with probable overlapping of wetland emissions (K13), which may also lead to an overestimate. More work is needed, based on both observations and process modelling, to overcome these uncertainties.

For geological emissions, relatively large uncertainties come from the extrapolation of only a subset of direct measurements to estimate the global fluxes. Moreover, marine seepage emissions are still widely debated (Berchet et al., 2016), and particularly diffuse emissions from microseepages are highly uncertain. However, summing up all fossil-CH₄ related sources (including the anthropogenic emissions) leads to a total of 173 Tg CH₄ yr⁻¹ [149-209], which is about 31% [25-35%] of global methane emissions. This result is consistent with ¹⁴C atmospheric isotopic analyses inferring a 30% contribution of fossil-CH₄ to global emissions (Lassey et al., 2007b; Etiope et al., 2008). All non-geological and non-wetland land source categories (wild animals, wildfires, termites, permafrost) have been evaluated at a lower level than in K13 and contribute only 23 Tg CH₄ yr⁻¹ [9-36] to global emissions. From a T-D point of view, the sum of all natural sources is more robust than the partitioning between wetlands and others natural sources. To reconcile T-D inversions and B-U estimates, the estimation and proper partition of methane emissions from wetlands and freshwater systems should receive a high priority.

Anthropogenic emissions. Total anthropogenic emissions are found statistically consistent between T-D (328 Tg CH₄ yr⁻¹, range [259-370]) and B-U approaches (352 Tg CH₄ yr⁻¹, range [340-360]), although T-D average is about 7% smaller than B-U average over 2003-2012. The partition of anthropogenic emissions between agriculture and waste, fossil fuels extraction and use, and biomass and biofuel burning, also shows good consistency between T-D and B-U approaches (Table 2 and Fig. 7). For 2003-2012, agriculture and waste contributed 188 Tg CH₄ yr⁻¹ [115-243] for T-D and 195 Tg CH₄ yr⁻¹ [178-206] for B-U. Fossil fuel emissions contributed 105 Tg CH₄ yr⁻¹ [77-133] for T-D and 121 Tg CH₄ yr⁻¹ [114-133] for B-U. Biomass and biofuel burning contributed 34 Tg CH₄ yr⁻¹ [15-53] for T-D and 30 Tg CH₄ yr⁻¹ [27-35] for B-U. Biofuel methane emissions rely on very few estimates at the moment (Wuebbles and Hayhoe (2002), IIASA). Although biofuel is a small source globally (~12 Tg CH₄ yr⁻¹), more estimates are needed to allow a proper uncertainty assessment. Overall for T-D inversions the global fraction of total emissions for the different source categories is 33% for agriculture and waste, 20% for



fossil fuels, and 6% for biomass and biofuel burnings. With the exception of biofuel emissions, the global uncertainty of anthropogenic emissions appears to be smaller than that of natural sources but with asymmetric uncertainty distribution (mean significantly different than median). In poorly observed regions, T-D inversions rely on the prior estimates and bring little or no additional information to constrain the (often) spatially overlapping emissions (e.g. in India, China). Therefore, the relative agreement between T-D and B-U may indicate the limited capability of the inversion to separate the emissions, and should therefore be treated with caution. Although the uncertainty range of some emissions has been decreased in this study compared to K13 (e.g. oceans, termites, geological), there is no uncertainty reduction in the regional budgets because of the larger range reported for emissions from freshwater systems.

5.2 Regional methane budget

5.2.1 Regional budget of total methane emissions

At regional scale, for the 2003-2012 decade (Table 4 and Fig. 6), total methane emissions are dominated by Africa with 86 Tg CH₄ yr⁻¹ [73-108], tropical South America with a total of 84 Tg CH₄ yr⁻¹ [65-101], and South East Asia with 73 Tg CH₄ yr⁻¹ [55-84]. These three (mainly) tropical regions represent almost 50% of methane emissions worldwide. The other high-emitting source regions are China (58 Tg CH₄ yr⁻¹ [51-72]), Central Eurasia and Japan (46 Tg CH₄ yr⁻¹ [38-54]), contiguous USA (41 Tg CH₄ yr⁻¹ [34-49]), Russia (38 Tg CH₄ yr⁻¹ [31-44]), India (39 Tg CH₄ yr⁻¹ [37-46]) and Europe (28 Tg CH₄ yr⁻¹ [26-29]). The other regions (boreal and central North America, temperate South America, Oceania, oceans) contribute between 7 and 20 Tg CH₄ yr⁻¹. This budget is consistent with K13 within the large ranges around the mean emissions, although larger emissions are found here for South America, South East Asia, and Europe and lower emissions are found for Africa, North America, and China. The regions with the largest changes are usually the least constrained by the surface networks.

The different inversions assimilated either satellite or ground-based observations. It is of interest to determine whether these two types of data provide consistent surface emissions. To do so, we computed global, hemispheric and regional methane emissions using satellite-based inversions and ground-based inversions separately for the 2010-2012 time period, which is the longest time period for which results from both GOSAT satellite-based and surface-based inversions were available. At the global scale, satellite-based inversions infer significantly higher emissions (+12 Tg CH₄ yr⁻¹, p=0.04) than ground-based inversions. At the regional scale, emissions varied between the satellite-based and surface-based inversions, although the difference is not statistically significant due to too few inversions and some outliers making the ensemble not robust enough. Yet the largest differences (satellite-based minus surface based inversions) are observed over the tropical region: tropical South America +11 Tg CH₄ yr⁻¹; southern Africa +6 Tg CH₄ yr⁻¹; India -6 Tg CH₄ yr⁻¹ and over China -7 Tg CH₄ yr⁻¹. Satellite data provide more constraints on fluxes in tropical regions than surface-based inversions, due to a much larger spatial coverage. It is therefore not surprising that most differences between these two types of observations are found in the tropical band. However, such differences could also be due to the larger systematic errors of satellite data as compared



to surface networks (Dils et al., 2014). In this context, the way the stratosphere is treated in the atmospheric models used to produce atmospheric methane columns from remote-sensing measurements (e.g. GOSAT or TCCON) seems important to further investigate (Locatelli et al., 2015; Monteil et al., 2011; Bergamaschi et al., 2009). Recent papers have developed methodologies to extract tropospheric partial column abundances from the TCCON data (Saad et al., 2014; Wang et al., 2014). Such partitioning could help explain the discrepancies between atmospheric models and satellite data.

5.2.2 Regional methane emissions per source category

The analysis of the regional methane budget per source category (Fig. 7) can be performed both for B-U and T-D approaches but with limitations. On the B-U side, some natural emissions are not (yet) available at regional scale (oceans, geological, inland waters). Therefore, the category “others” is not shown for B-U results. On the T-D side, as already noted, the partition of emissions per source category has to be considered with caution. Indeed, using only atmospheric methane observations to constrain methane emissions makes this partition largely dependent on prior emissions. However, differences in spatial patterns and seasonality of emissions can still be constrained by atmospheric methane observations for those inversions solving for different sources categories (see Sect. 2.3).

Wetland emissions largely dominate methane emissions in tropical South America, boreal North America, southern Africa, temperate South America and South East Asia, although agriculture and waste emissions are almost as important for the last two regions. Agriculture and waste emissions dominate in India, China, contiguous USA, central North America, Europe and northern Africa. Fossil fuel emissions dominate in Russia and are close to agriculture and waste emissions in the region named central Eurasia and Japan. In China, fossil fuel emissions are on average close, albeit smaller, than agriculture and waste emissions. Comparison between B-U and T-D approaches show good consistency but one has to consider the generally large error bars, especially for T-D inversions. The largest discrepancy occurs for wetland emissions in boreal North America where B-U models infer larger emissions (32 Tg CH₄ yr⁻¹) than T-D inversions (13 Tg CH₄ yr⁻¹). Indeed, one particular B-U model infers a 61 Tg CH₄.yr⁻¹ emission for this region, largely above estimates from other models, which lay between 15 and 45 Tg CH₄ yr⁻¹. T-D models results are consistent with the climatology proposed by Kaplan (2002), whereas B-U models are more in line, albeit larger, than the climatology of Matthews and Fung (1987) who infer about 30 Tg CH₄ yr⁻¹ for boreal North America. Interestingly, the situation is different for Russia where T-D and B-U approaches show similar mean emissions from natural wetlands (mostly boreal, ~13-14 Tg CH₄ yr⁻¹), consistently with Kaplan (2002) but not with Matthews and Fung (1987), who infer almost 50 Tg CH₄ yr⁻¹ for Russia. Wetland emissions from Russia appear very uncertain, as also found by Bohn et al. (2015) for Western Siberia. Wetland emissions from tropical South America are found more consistent in this work than in K13 where T-D inversions showed two times less emissions than B-U models. The larger number of B-U models (11 against 3) and TD inversions (30 against 8) are plausible causes explaining the improved agreement in this tropical region, poorly constrained by the surface networks (Pison et al., 2013).

Anthropogenic emissions remain close between T-D and B-U approaches for most regions, again with the possibility that part of this agreement is due to the lack of information brought by atmospheric observations to T-D inversions for some



regions. One noticeable exception is the lower emissions for China as compared to the prior, visible also in Fig. 6. A priori anthropogenic emissions for China are mostly provided by the EDGARv4.2 inventory. Starting from prior emissions of 67 Tg CH₄ yr⁻¹ [58-77], the mean of the atmospheric derived estimates for China is 58 Tg CH₄ yr⁻¹ [51-72], corresponding to a -14% difference of the Chinese emissions. A T-test performed for the available estimates suggests that the mean posterior total emission for China is different from the prior emission at the 95% confidence level. Several atmospheric studies have already suggested a possible overestimation of methane emissions from coal in China in the EDGAR4.2 inventory (Bergamaschi et al., 2013; Kirschke et al., 2013; Tohjima et al., 2014; Umezawa et al., 2014). Indeed, comparing the results of T-D inversions to EDGARv42 inventory (maximum of B-U estimates for China on Fig. 7), fossil fuel emissions are reduced by 33% from 30 Tg CH₄ yr⁻¹ to 20 Tg CH₄ yr⁻¹ (range [9-30]) and agriculture and waster emissions are reduced by 27% from 37 Tg CH₄ yr⁻¹ to 27 Tg CH₄ yr⁻¹ (range [16-37]. This result is consistent with a new inventory for methane emissions from China based on county-scale data (43±6 Tg yr⁻¹), indicating that coal-related methane emissions are 37% (-7 Tg yr⁻¹) lower than reported in the EDGARv4.2 inventory (Peng et al., 2016) (see also Sect. 3.1.2). It demonstrates that inversions are capable of verifying regional emissions when biases in the inventories are substantial, as in the case of China.

In contrast to the Chinese estimates, emissions inferred for Africa and especially southern Africa are significantly larger than in the prior estimates (Fig. 6). For example, for southern Africa, the mean of the inversion ensemble is 44 Tg CH₄ yr⁻¹ [37-53], starting a mean prior of 36 Tg CH₄ yr⁻¹ [27-35]. This is a 25% increase compared to mean prior estimates for southern Africa. A T-test performed for the available estimates suggests that the mean posterior for southern Africa is different from the prior at the 98% confidence level. An increase of northern African emissions is also inferred from the ensemble of inversions but is less significant.

For all other regions, emission changes compared to prior values remain within the first and third quartiles of the distributions. In particular, contiguous USA (without Alaska) is found to emit 41 Tg CH₄ yr⁻¹ [34-49], which is close to the prior estimates. T-D and B-U estimates are consistent for anthropogenic sources in this region. Only natural wetlands are lower as estimated by T-D models (9 Tg CH₄ yr⁻¹ [6-13]) than by B-U models (13 Tg CH₄ yr⁻¹ [6-23]). In addition, no clear trend is observed between 2000-2009 and 2003-2012, which is inconsistent with the large trend over the US recently reported by Turner et al. (2016). More, none of the 30 inversions show a significant trend for USA for the 2000-2012 time period.

6 Future developments, missing elements, and remaining uncertainties

K13 identified four main shortcomings in the assessment of regional to global CH₄ budgets, which we revisit now.

Annual to decadal CH₄ emissions from natural wetlands and fresh water systems are highly uncertain. The work by Poulter et al. (2016, submitted), following Melton et al. (2013) allows partitioning the uncertainty (expressed as the range in the estimates) of methane emissions from natural wetlands between wetland extent and other components, based on the use of a common and newly-developed database for wetland extent. This approach confirms that wetland extent dominates the



uncertainty of modelled methane emissions from wetlands (30–40% of the uncertainty). The rest of the uncertainty lies in the model parametrisations of the flux density, which remains poorly constrained due to very few methane flux measurements available for different ecosystems over time. In addition, the footprint of flux measurements are largely on too small scales (e.g. chamber measurements) to be compared with the lower resolution that land surface models operate. Although more and

5 more flux sites now integrate measurements of methane fluxes by eddy-covariance, such technique can reveal unexpected issues (e.g. Baldocchi et al. (2012)). There is a need for integration of methane flux measurements on the model of the FLUXNET activity (<http://fluxnet.ornl.gov>). This would allow further refinement of the model parametrisations (Turetsky et al., 2014; Glagolev et al., 2011). A comparison of the model ensemble estimates against bottom-up inventory for West Siberia by Glagolev et al. (2011) made by Bohn et al. (2015) showed that there still is a sizable disagreement between their results.

10 A more complete analysis of the literature for fresh water emissions has led to a 50% increase of the reported range compared to K13. Emitting pathways such as ebullition remain poorly understood and quantified. There is a need for systematic measurements from a suite of sites reflecting the diversity of lake morphologies to better understand the short-term biological control on ebullition variability (Wik et al., 2014). Further efforts are needed: 1) extending the monitoring of the methane emissions from the different aquatic systems (wetlands and freshwaters) complemented with key environmental variables to

15 allow proper interpretation (e.g. soil temperature and moisture, vegetation types, water temperature, acidity, nutrient concentrations, NPP, soil carbon density); 2) developing process-based modelling approaches to estimate inland emissions instead of data-driven extrapolations of unevenly-distributed and local flux observations; and 3) creating a global flux product for all inland water emissions at high resolution allowing to avoid double counting between wetlands and freshwater systems.

20 *The partitioning of CH₄ emissions and sinks by region and process is not sufficiently constrained by atmospheric observations in top-down models.* In this work, we report inversions assimilating satellite data from GOSAT (and one inversion using SCIAMACHY), which bring more constraints, especially over tropical continents. The extension of the CH₄ surface networks to poorly observed regions (e.g. Tropics, China, India, high latitudes) is still critical to complement satellite data which do not observe well in cloudy regions and at high latitudes, but also to evaluate and correct satellite biases. Such

25 data now exist for China (Fang et al., 2015), India (Tiwari and Kumar, 2012; Lin et al., 2015) and Siberia (Sasakawa et al., 2010; Winderlich et al., 2010) and can be assimilated in inversions in the upcoming years. Observations from other tracers could help partitioning the different methane emitting processes. Carbon monoxide (Fortems-Cheiney et al., 2011) can provide constraints for biomass burning for instance. However, additional tracers can also bring contradictory trends in emissions such as the ones suggested since 2007 by ¹³C (Schaefer et al., 2016), and ethane (Hausmann et al., 2016). Such

30 discrepancies have to be understood and solved to be able to properly use additional tracers to constrain methane emissions. An update of OH fields is expected in 2016 with an ensemble of Chemistry Transport Models (CTM) and Climate Chemistry Models (CCM) simulations in the framework of CCMI (Chemistry-Climate Model Initiative) spanning the past three decades (<http://www.met.reading.ac.uk/ccmi/>). The outcome of this experiment will contribute to an improved representation of the methane sink (Lamarque et al., 2013). The development of regional components of the global methane budget is also a way to



improve global totals by developing regional T-D and B-U approaches. Such efforts are underway for South and East Asia Asia (Patra et al., 2013; Lin et al., 2015) and for the Arctic (Bruhwiler et al., 2015), where seasonality (e.g. Zona et al. (2016) for tundra) and magnitude (e.g. Berchet et al. (2016) for continental shelves) of methane emissions remain poorly understood.

5 *The ability to allocate observed atmospheric changes to changes of a given source is limited.* Most inverse groups use EDGARv4.2 inventory as a prior, being the only annual gridded anthropogenic inventory to date. An updated version of the EDGAR4.2 inventory has been recently released (EDGARv4.2FT2012), which is very close at a global scale to the extrapolation performed in this paper based on statistics from BP (<http://www.bp.com/>) and on agriculture emissions from
10 FAO (<http://faostat3.fao.org>). However, the significant changes in emissions in China (decrease) and Africa (increase) found in this synthesis, strongly suggest the necessity to further revise the EDGAR inventory, in particular for coal-related emissions (China). Such an update is an on-going effort in the EDGAR group. More extensive comparisons and exchange between the different inventory teams would also favour a path towards more consistency.

15 *Uncertainties in the modelling of atmospheric transport and chemistry limit the optimal assimilation of atmospheric observations and increase the uncertainties of the inversion-derived flux estimates.* In this work, we gathered more inversion models than in K13, leading to small to significant regional differences in the methane budget for 2000-2009. For the next release, it is important to stabilize the core group of participating inversions in order not to create artificial changes in the reporting of uncertainties. More, the recent results of Locatelli et al. (2015) who studied the sensitivity of inversion results to the representation of atmospheric transport suggest that regional changes in the balance of methane emissions between
20 inversions may be due to different characteristics of the transport models used here as compared to K13. Indeed, the TRANSCOM experiment synthesized in Patra et al. (2011) showed a large sensitivity of the representation of atmospheric transport on methane concentrations in the atmosphere. As an illustration, in their study, the modelled CH₄ budget appeared to depend strongly on the troposphere-stratosphere exchange rate and thus on the model vertical grid structure and circulation in the lower stratosphere. These results put pressure to continue to improve atmospheric transport models, especially on the
25 vertical.

7 Conclusions

We have built a global methane budget by gathering and synthesizing a large ensemble of published results using a consistent methodology, including atmospheric observations and inversions (T-D inversions), process-based models for land surface emissions and atmospheric chemistry, and inventories of anthropogenic emissions (B-U models and inventories). For
30 the 2003-2012 decade, global methane emissions are 558 Tg CH₄ yr⁻¹ (range of [540-568]), as estimated by T-D inversions. About 60% of global emissions are anthropogenic (range of [50-70]%). B-U models and inventories suggest much larger global emissions (736 Tg CH₄ yr⁻¹ [596-884]) mostly because of larger and more uncertain natural emissions from inland



water systems, natural wetlands and geological leaks. Considering the atmospheric constraints on the T-D budget, it is likely that some of the individual emissions reported by the B-U approaches are overestimated, leading to too large global emissions from a B-U perspective.

The latitudinal breakdown inferred from T-D approaches reveals a domination of tropical emissions (~64%) as compared to mid (~32%) and high (~4%) northern latitudes (above 60°N). The three largest emitting regions (South America, Africa, South East Asia) account for almost 50% of the global budget. T-D inversions consistently infer lower emissions in China (~58 Tg CH₄ yr⁻¹ [51-72]) compared with the EDGAR4.2 inventories (>70 Tg CH₄ yr⁻¹) but more consistent with the USEPA and IIASA inventories and with a recent regional inventory (~45 Tg yr⁻¹). On the other hand, B-U methane emissions from Africa are lower than inferred from T-D inversions. These differences between T-D inversions and inventories call for a revisit of the emission factors and activity numbers used by the latter, at least for China and Africa.

Our results, including an extended set of inversions, are compared with the former synthesis of K13, showing good consistency overall when comparing the same decade (2000-2009) at the global scale. Significant differences occur at the regional scale when comparing the 2000-2009 decadal emissions. This important result indicates that using different transport models and inversion setups can significantly change the partition of emissions at the regional scale, making it less robust. It also means that we need to gather a stable, and as complete as possible, core of transport models in the next release of the budget in order to integrate this uncertainty within the budget.

Among the different uncertainties raised in K13, the present work estimated that 30-40% of the large range associated with modelled wetland emissions in K13 was due to the estimation of wetland extent. The magnitudes and uncertainties of all other natural sources have been revised and update which has led to decreased the emission estimates for oceans, termites, wild animals and wildfires, and to increased emission estimates and range for freshwater systems. Although the risk of double counting emissions between natural and anthropogenic gas leaks exists, total fossil-related reported emissions are found consistent with atmospheric ¹⁴C. This places a clear priority on reducing uncertainties in emissions from inland water systems by better quantifying the emission factors of each contributor (streams, rivers, lakes, ponds) and eliminating the (plausible) double counting with wetland emissions. The development of process-based models for inland water emissions, constrained by observations, is a priority to overcome the present uncertainties on inland water emissions. Also important, although not addressed here, is to revise and update the magnitude, regional- distribution, inter-annual variability and decadal trends in the OH radicals in the troposphere and stratosphere. This should be possible soon by the release of the CCMI on-going multi-model inter-comparison (<http://www.jgacproject.org/CCMI>). Our work also suggests the need for more interactions among groups developing the emission inventories in order to resolve discrepancies on the magnitude of emissions and trends in key regions such as China or Africa. Particularly, the budget assessment of these regions should strongly benefit from the on-going effort to develop a network of in situ atmospheric measurement stations. Finally, additional tracers (methane isotopes, ethane, CO) have potential to bring more constraint on the global methane cycle if their information content relative to methane emission trends is consistent with each other, which is not fully the case at present (Schaefer et al., 2016; Hausmann et al., 2016). Building on the improvement of the points above, our aim is to update this synthesis as a living review paper on



a regular basis (~every two years). Each update will produce a more recent decadal CH₄ budget, highlight changes in emissions and trends, show the availability and inclusion of new data, and model improvements.

Acknowledgements

5 F. J. and R.S. acknowledge support by the Swiss National Science Foundation. H-S.K. and S.M. acknowledge use of the GOSAT Research Computation Facility. D.B. acknowledge support from the Swedish Research Council VR. D.R.B. and I.J.S. (UCI) acknowledge funding support from NASA. JGC thanks the support from the Australian Climate Change Science Program. M.S. and P.Bou. acknowledge the Global Carbon Project for the scientific advises, the computing power of LSCE for data analyses. P. Ber. and M.A. acknowledge the support by the European Commission Seventh Framework Programme
10 (FP7/2007–2013) project MACC-II under grant agreement 283576, by the European Commission Horizon2020 Programme project MACC-III under grant agreement 633080, and by the ESA Climate Change Initiative Greenhouse Gases Phase 2 project. W.J.R. and X.X. acknowledge support by the US Department of Energy, BER, under contract #DE-AC02-05CH11231. The FAOSTAT database is supported by regular programme funding from all FAO member countries. P.K.P. is supported by the Environment Research and Technology Development Fund (2-1502) of the Ministry of the Environment,
15 Japan. D.J.B. acknowledges support from an ERC Advanced grant (CDREG, 322998) and NERC (NE/J00748X/1). D.B. and P.C. acknowledge support from the Swedish Research Council VR. G.P. acknowledges the support of the Research Council of Norway project 244074. H.T. and B.Z. acknowledge funding support from NASA (NNX14AF93G; NNX14AO73G) and NSF (1243232; 1243220). C. Peng acknowledges the support by National Science and Engineering Research Council of Canada (NSERC) discovery grant and China's QianRen Program. The CSIRO and the Australian Government Bureau of
20 Meteorology are thanked for their ongoing long-term support of the Cape Grim station and the Cape Grim science program. The CSIRO flask network is supported by CSIRO Australia, Australian Bureau of Meteorology, Australian Institute of Marine Science, Australian Antarctic Division, NOAA USA, and the Meteorological Service of Canada. The operation of the AGAGE instruments at Mace Head, Trinidad Head, Cape Matatula, Ragged Point, and Cape Grim is supported by the National Aeronautic and Space Administration (NASA) (grants NAG5-12669, NNX07AE89G, and NNX11AF17G to MIT
25 and grants NNX07AE87G, NNX07AF09G, NNX11AF15G, and NNX11AF16G to SIO), the Department of Energy and Climate Change (DECC, UK) contract GA01081 to the University of Bristol, and the Commonwealth Scientific and Industrial Research Organization (CSIRO Australia) and Bureau of Meteorology (Australia). N.G. and A.W. acknowledge support by the Joint DECC/Defra Met Office Hadley Centre Climate Programme (GA01101).

M. S. and P. Bous. acknowledge Lyla Taylor (Univ. Sheffield/UK), Chris Jones (Met office/UK), and Charlie Koven
30 (Lawrence Berkeley National Laboratory/USA) for their participation to land surface modelling of wetland emissions. M.S. and P. Bous. acknowledge Theodore J. Bohn (ASU/USA), Kristofer Covey (Yale/USA), Jens Greinhert (Geomar/the Netherlands), Charles Miller (JPL/USA), Tonatiuh Guillermo Nunez Ramirez (MPI Jena/Germany) for their useful comments and suggestions on the manuscript. M. S. and P. Bou. acknowledge Martin Herold (WU/the Netherlands), Mario Herrero (CSIRO/Australia), Paul Palmer (University of Edinburgh/UK), Matthew Rigby (university of Bristol /UK), Taku Umezawa



(NIES/Japan), Ray Wang (GIT/USA), Jim White (INSTAAR/USA), Tatsuya Yokota (NIES/Japan), Ayyoob Sharifi and Yoshiaki Yamagata (NIES/GCP/Japan), Lingxi Zhou (CMA/China), for their interest and discussions on the Global Carbon project methane.

5

References

- ACIA: Arctic Climate Impact Assessment, Cambridge University Press, available at <http://www.acia.uaf.edu>, 1042, 2005.
- 10 Akagi, S. K., Yokelson, R. J., Wiedinmyer, C., Alvarado, M. J., Reid, J. S., Karl, T., Crounse, J. D., and Wennberg, P. O.: Emission factors for open and domestic biomass burning for use in atmospheric models, *Atmos. Chem. Phys.*, 11, 4039-4072, doi:10.5194/acp-11-4039-2011, 2011.
- Alexe, M., Bergamaschi, P., Segers, A., Detmers, R., Butz, A., Hasekamp, O., Guerlet, S., Parker, R., Boesch, H., Frankenberg, C., Scheepmaker, R. A., Dlugokencky, E., Sweeney, C., Wofsy, S. C., and Kort, E. A.: Inverse modelling of CH₄ emissions for 2010–2011 using different satellite retrieval products from GOSAT and SCIAMACHY, *Atmos. Chem. Phys.*, 15, 113-133, doi:10.5194/acp-15-113-2015, 2015.
- 15 Allan, W., Lowe, D. C., Gomez, A. J., Struthers, H., and Brailsford, G. W.: Interannual variation of ¹³C in tropospheric methane: Implications for a possible atomic chlorine sink in the marine boundary layer, *Journal of Geophysical Research-Atmospheres*, 110, doi:10.1029/2004JD005650, 2005.
- Allan, W., Struthers, H., and Lowe, D. C.: Methane carbon isotope effects caused by atomic chlorine in the marine boundary layer: Global model results compared with Southern Hemisphere measurements, *Journal of Geophysical Research-Atmospheres*, 112, D04306, doi:10.1029/2006jd007369, 2007.
- 20 Allen, D. T., Torres, V. M., Thomas, J., Sullivan, D. W., Harrison, M., Hendler, A., Herndon, S. C., Kolb, C. E., Fraser, M. P., Hill, A. D., Lamb, B. K., Miskimins, J., Sawyer, R. F., and Seinfeld, J. H.: Measurements of methane emissions at natural gas production sites in the United States, *Proc. Natl. Acad. Sci. USA* 110, 17,768-71,773, doi:10.1073/pnas.1304880110, 2013.
- 25 André, J.-C., Boucher, O., Bousquet, P., Chanin, M.-L., Chappellaz, J., and Tardieu, B.: Le méthane : d'où vient-il et quel est son impact sur le climat ?, EDP Sciences, Académie des Sciences et Technologies, Paris, 170 pp., 2014.
- Andreae, M. O., and Merlet, P.: Emission of trace gases and aerosols from biomass burning, *Global Biogeochemical Cycles*, 15, 955–966, 2001.
- 30 Anisimov, O., and Reneva, S.: Permafrost and changing climate: the Russian perspective, *Ambio*, 35, 169-175, 2006.
- Aoki, S., Nakazawa, T., Murayama, S., and Kawaguchi, S.: Measurements of atmospheric methane at the Japanese Antarctic Station. Syowa., *Tellus* 44B, 273-281, doi:10.1034/j.1600-0889.1992.t01-3-00005.x., 1992.
- Arctic-Research-Commission: U.S. Arctic Research Commission Permafrost Task Force. Climate Change, Permafrost, and Impacts on Civil Infrastructure, Arlington, Virginia, 2003.
- 35 Aselmann, I., and Crutzen, P. J.: Global distribution of natural freshwater wetlands and rice paddies, their net primary productivity, seasonality and possible methane emissions, *Journal of Atmospheric Chemistry*, 8, 307-358, doi:10.1007/bf00052709, 1989.
- Aydin, M., Verhulst, K. R., Saltzman, E. S., Battle, M. O., Montzka, S. A., Blake, D. R., Tang, Q., and Prather, M. J.: Recent decreases in fossil-fuel emissions of ethane and methane derived from firm air, *Nature*, 476, 198-201, doi:10.1038/nature10352, 2011.
- 40 Baicich, P.: The Birds and Rice Connection, *Bird Watcher's Digest*. Available online at http://www.greatbirdingprojects.com/images/BWD_J-A_13_BIRDS_N_RICE.pdf, 2013.
- Baldocchi, D., Detto, M., Sonnentag, O., Verfaillie, J., Teh, Y. A., Silver, W., and Kelly, N. M.: The challenges of measuring methane fluxes and concentrations over a peatland pasture, *Agricultural and Forest Meteorology*, 153, 177-187, doi:10.1016/j.agrformet.2011.04.013, 2012.
- 45



- Bange, H. W., Bartell, U. H., Rapsomanikis, S., and Andreae, M. O.: Methane in the Baltic and North Seas and a reassessment of the marine emissions of methane, *Global Biogeochemical Cycles*, 8, 465-480, doi:10.1029/94gb02181, 1994.
- Bastviken, D., Cole, J., Pace, M., and Tranvik, L.: Methane emissions from lakes: Dependence of lake characteristics, two regional assessments, and a global estimate, *Global Biogeochem. Cycles*, 18, GB4009, doi:10.1029/2004gb002238, 2004.
- 5 Bastviken, D., Tranvik, L. J., Downing, J. A., Crill, P. M., and Enrich-Prast, A.: Freshwater Methane Emissions Offset the Continental Carbon Sink, *Science*, 331, 50, doi:10.1126/science.1196808, 2011.
- Bates, T. S., Kelly, K. C., Johnson, J. E., and Gammon, R. H.: A reevaluation of the open ocean source of methane to the atmosphere, *Journal of Geophysical Research: Atmospheres*, 101, 6953-6961, doi:10.1029/95jd03348, 1996.
- 10 Beck, V., Chen, H., Gerbig, C., Bergamaschi, P., Bruhwiler, L., Houweling, S., Röckmann, T., Kolle, O., Steinbach, J., Koch, T., Sapart, C. J., van der Veen, C., Frankenberg, C., Andreae, M. O., Artaxo, P., Longo, K. M., and Wofsy, S. C.: Methane airborne measurements and comparison to global models during BARCA, *Journal of Geophysical Research: Atmospheres*, 117, D15310, doi:10.1029/2011jd017345, 2012.
- Berchet, A., Bousquet, P., Pison, I., Locatelli, R., Chevallier, F., Paris, J. D., Dlugokencky, E. J., Laurila, T., Hatakka, J., Viisanen, Y., Worthy, D. E. J., Nisbet, E. G., Fisher, R. E., France, J. L., Lowry, D., and Ivakhov, V.: Atmospheric constraints on the methane emissions from the East Siberian Shelf, *Atmospheric Chemistry and Physics* 16, 4147–4157, doi:10.5194/acp-16-4147-2016, 2016.
- 15 Bergamaschi, P., Frankenberg, C., Meirink, J. F., Krol, M., Dentener, F., Wagner, T., Platt, U., Kaplan, J. O., Koerner, S., Heimann, M., Dlugokencky, E. J., and Goede, A.: Satellite cartography of atmospheric methane from SCIAMACHY on board ENVISAT: 2. Evaluation based on inverse model simulations, *Journal of Geophysical Research-Atmospheres*, 112, doi:10.1029/2006jd007268, 2007.
- Bergamaschi, P., Frankenberg, C., Meirink, J. F., Krol, M., Villani, M. G., Houweling, S., Dentener, F., Dlugokencky, E. J., Miller, J. B., Gatti, L. V., Engel, A., and Levin, I.: Inverse modeling of global and regional CH₄ emissions using SCIAMACHY satellite retrievals, *Journal of Geophysical Research-Atmospheres*, 114, doi:10.1029/2009jd012287, 2009.
- 25 Bergamaschi, P., Houweling, S., Segers, A., Krol, M., Frankenberg, C., Scheepmaker, R. A., Dlugokencky, E., Wofsy, S. C., Kort, E. A., Sweeney, C., Schuck, T., Brenninkmeijer, C., Chen, H., Beck, V., and Gerbig, C.: Atmospheric CH₄ in the first decade of the 21st century: Inverse modeling analysis using SCIAMACHY satellite retrievals and NOAA surface measurements, *Journal of Geophysical Research: Atmospheres*, 118, 7350-7369, doi:10.1002/jgrd.50480, 2013.
- Bhatia, A., Jain, N., and Pathak, H.: Methane and nitrous oxide emissions from Indian rice paddies, agricultural soils and crop residue burning, *Greenhouse Gases: Science and Technology*, 3, 196-211, doi:10.1002/ghg.1339, 2013.
- 30 Bignell, D. E., Eggleton, P., Nunes, L., and Thomas, K. L.: Termites as mediators of forest carbon fluxes in tropical forests: budgets for carbon dioxide and methane emissions, in: *Forests and Insects*, edited by: Watt, A. D., Stork, N. E., and Hunter, M. D., Chapman and Hall, London, 109-134, 1997.
- Blake, D. R., Mayer, E. W., Tyler, S. C., Makide, Y., Montague, D. C., and Rowland, F. S.: Global Increase in Atmospheric Methane Concentrations between 1978 and 1980, *Geophysical Research Letters*, 9, 477-480, 1982.
- 35 Blake, D. R., and Rowland, F. S.: World-wide increase in tropospheric methane, 1978–1983, *Journal of Atmospheric Chemistry*, 4, 43-62, 1986.
- Bogner, J., Abdelrafie Ahmed, M., Diaz, C., Faaij, A., Gao, Q., Hashimoto, S., Mareckova, K., Pipatti, R., and Zhang, T.: Waste Management, in: *In Climate Change (2007), Mitigation. Contribution of Working Group III to the Fourth Assessment Report of the Intergovernmental Panel on Climate Change*, edited by: Metz, B., Davidson, O. R., Bosch, P. R., Dave, R., and Meyer, L. A., Cambridge University Press, Cambridge, United Kingdom and New York, NY, USA, 2007.
- 40 Bohn, T. J., Melton, J. R., Ito, A., Kleinen, T., Spahni, R., Stocker, B. D., Zhang, B., Zhu, X., Schroeder, R., Glagolev, M. V., Maksyutov, S., Brovkin, V., Chen, G., Denisov, S. N., Eliseev, A. V., Gallego-Sala, A., McDonald, K. C., Rawlins, M. A., Riley, W. J., Subin, Z. M., Tian, H., Zhuang, Q., and Kaplan, J. O.: WETCHIMP-WSL: Intercomparison of wetland methane emissions models over West Siberia, *Biogeosciences*, 12, 3321-3349, doi:10.5194/bg-12-3321-2015, 2015.
- 45 Borges, A. V., Darchambeau, F., Teodoru, C. R., Marwick, T. R., Tamooh, F., Geeraert, N., Omengo, F. O., Guerin, F., Lambert, T., Morana, C., Okuku, E., and Bouillon, S.: Globally significant greenhouse-gas emissions from African inland waters, *Nature Geosci*, 8, 637-642, doi:10.1038/ngeo2486, 2015.



- Bousquet, P., Hauglustaine, D. A., Peylin, P., Carouge, C., and Ciais, P.: Two decades of OH variability as inferred by an inversion of atmospheric transport and chemistry of methyl chloroform, *Atmospheric Chemistry and Physics*, 5, 2635-2656, 2005.
- 5 Bousquet, P., Ciais, P., Miller, J. B., Dlugokencky, E. J., Hauglustaine, D. A., Prigent, C., Van der Werf, G. R., Peylin, P., Brunke, E. G., Carouge, C., Langenfelds, R. L., Lathiere, J., Papa, F., Ramonet, M., Schmidt, M., Steele, L. P., Tyler, S. C., and White, J.: Contribution of anthropogenic and natural sources to atmospheric methane variability, *Nature*, 443, 439-443, 2006.
- 10 Bousquet, P., Ringeval, B., Pison, I., Dlugokencky, E. J., Brunke, E. G., Carouge, C., Chevallier, F., Fortems-Cheiney, A., Frankenberg, C., Hauglustaine, D. A., Krummel, P. B., Langenfelds, R. L., Ramonet, M., Schmidt, M., Steele, L. P., Szopa, S., Yver, C., Viovy, N., and Ciais, P.: Source attribution of the changes in atmospheric methane for 2006-2008, *Atmospheric Chemistry and Physics*, 11, 3689-3700, 2011.
- Bouwman, A. F., Lee, D. S., Asman, W. A. H., Dentener, F. J., Van Der Hoek, K. W., and Olivier, J. G. J.: A global high-resolution emission inventory for ammonia, *Global Biogeochemical Cycles*, 11, 561-587, doi:10.1029/97gb02266, 1997.
- 15 Brandt, A. R., Heath, G. A., Kort, E. A., O'Sullivan, F., Pétron, G., Jordaan, S. M., Tans, P., Wilcox, J., Gopstein, A. M., Arent, D., Wofsy, S., Brown, N. J., Bradley, R., Stucky, G. D., Eardley, D., and Harriss, R.: Methane Leaks from North American Natural Gas Systems, *Science*, 343, 733-735, doi:10.1126/science.1247045, 2014.
- Brenninkmeijer, C. A. M., Crutzen, P., Boumard, F., Dauer, T., Dix, B., Ebinghaus, R., Filippi, D., Fischer, H., Franke, H., Frieß, U., Heintzenberg, J., Helleis, F., Hermann, M., Kock, H. H., Koepfel, C., Lelieveld, J., Leuenberger, M., Martinsson, B. G., Miemczyk, S., Moret, H. P., Nguyen, H. N., Nyfeler, P., Oram, D., O'Sullivan, D., Penkett, S., Platt, U., Pucek, M., Ramonet, M., Randa, B., Reichelt, M., Rhee, T. S., Rohwer, J., Rosenfeld, K., Scharffe, D., Schlager, H., Schumann, U., Slemr, F., Sprung, D., Stock, P., Thaler, R., Valentino, F., van Velthoven, P., Waibel, A., Wandel, A., Waschitschek, K., Wiedensohler, A., Xueref-Remy, I., Zahn, A., Zech, U., and Ziereis, H.: Civil Aircraft for the regular investigation of the atmosphere based on an instrumented container: The new CARIBIC system., *Atmospheric Chemistry and Physics*, 7, 4953-4976, doi:10.5194/acp-7-4953-2007, 2007.
- 25 Bridgman, S. D., Cadillo-Quiroz, H., Keller, J. K., and Zhuang, Q.: Methane emissions from wetlands: biogeochemical, microbial, and modeling perspectives from local to global scales, *Global Change Biology*, 19, 1325-1346, doi:10.1111/gcb.12131, 2013.
- Bruhwyler, L., Dlugokencky, E., Masarie, K., Ishizawa, M., Andrews, A., Miller, J., Sweeney, C., Tans, P., and Worthy, D.: CarbonTracker-CH₄: an assimilation system for estimating emissions of atmospheric methane, *Atmospheric Chemistry and Physics*, 14, 8269-8293, 2014.
- 30 Bruhwiler, L., Bousquet, P., Houweling, S., and Melton, J.: Modeling of atmospheric methane using inverse (and forward) approaches, Chapter 7 in *AMAP Assessment 2015: Methane as an Arctic Climate Forcer*, p. 77-89, available at <http://www.amap.no/documents/doc/AMAP-Assessment-2015-Methane-as-an-Arctic-climate-forcer/1285>, 2015.
- 35 Buchwitz, M., de Beek, R., Burrows, J. P., Bovensmann, H., Warneke, T., Notholt, J., Meirink, J. F., Goede, A. P. H., Bergamaschi, P., Korner, S., Heimann, M., and Schulz, A.: Atmospheric methane and carbon dioxide from SCIAMACHY satellite data: initial comparison with chemistry and transport models, *Atmospheric Chemistry and Physics*, 5, 941-962, 2005a.
- Buchwitz, M., de Beek, R., Noel, S., Burrows, J. P., Bovensmann, H., Bremer, H., Bergamaschi, P., Korner, S., and Heimann, M.: Carbon monoxide, methane and carbon dioxide columns retrieved from SCIAMACHY by WFM-DOAS: year 2003 initial data set, *Atmospheric Chemistry and Physics*, 5, 3313-3329, 2005b.
- 40 Buchwitz, M., de Beek, R., Noel, S., Burrows, J. P., Bovensmann, H., Schneising, O., Khlystova, I., Bruns, M., Bremer, H., Bergamaschi, P., Korner, S., and Heimann, M.: Atmospheric carbon gases retrieved from SCIAMACHY by WFM-DOAS: version 0.5 CO and CH₄ and impact of calibration improvements on CO₂ retrieval, *Atmospheric Chemistry and Physics*, 6, 2727-2751, 2006.
- 45 Buchwitz, M., Dils, B., Boesch, H., Crevoisier, C., Detmers, R., Frankenberg, C., Hasekamp, O., Hewson, W., Laeng, A., Noel, S., Nothold, J., Parker, R., Reuter, M., and Schneising, O.: Product Validation and Intercomparison Report (PVIR) for the Essential Climate Variable (ECV) Greenhouse Gases (GHG), ESA Climate Change Initiative (CCI), report version 4, Feb 2016, http://www.esa-ghg-cci.org/?q=webfm_send/300, 2016.
- 50 Burrows, J. P., Hölzle, B., Goede, A. P. H., Visser, H., and Fricke, W.: SCIAMACHY - Scanning Imaging Absorption Spectrometer for Atmospheric Chartography, *Acta Astr.*, 35, 445-451, 1995.



- Butz, A., Guerlet, S., Hasekamp, O., Schepers, D., Galli, A., Aben, I., Frankenberg, C., Hartmann, J. M., Tran, H., Kuze, A., Keppel-Aleks, G., Toon, G., Wunch, D., Wennberg, P., Deutscher, N., Griffith, D., Macatangay, R., Messerschmidt, J., Notholt, J., and Warneke, T.: Toward accurate CO₂ and CH₄ observations from GOSAT, *Geophysical Research Letters*, 38, L14812, doi:10.1029/2011gl047888, 2011.
- 5 Cai, Z. C., Xing, G., Yan, X., Xu, H., Tsuruta, H., Yagi, K., and Minami, K.: Methane and nitrous oxide emissions from rice paddy fields as affected by nitrous fertilizers and water management, *Plant and Soil*, 196, 7-14, 1997.
- Cao, M., Marshall, S., and Gregson, K.: Global carbon exchange and methane emissions from natural wetlands: Application of a process-based model, *Journal of Geophysical Research: Atmospheres*, 101, 14399-14414, doi:10.1029/96jd00219, 1996.
- 10 Castelan-Ortega, O. A., Carlos Ku-Vera, J., and Estrada-Flores, J. G.: Modeling methane emissions and methane inventories for cattle production systems in Mexico, *Atmósfera*, 27, 185-191, doi:10.1016/S0187-6236(14)71109-9, 2014.
- Cathles, L., Brown, L., Taam, M., and Hunter, A.: A commentary on “The greenhouse-gas footprint of natural gas in shale formations” by R.W. Howarth, R. Santoro, and Anthony Ingraffea, *Climatic Change*, 113, 525-535, doi:10.1007/s10584-011-0333-0, 2012.
- 15 Cautlon, D., Shepson, P. B., Santoro, R. L., Sparks, J. P., Howarth, R. W., R., A., Ingraffea, A. R., Cambaliza, M. O. L., Sweeney, C., Karion, A., Davis, K. J., Stirm, B. H., Montzka, S. A., and Miller, B. R.: Toward a better understanding and quantification of methane emissions from shale gas development, *Proceedings of the National Academy of Sciences USA*, 111, 6237-6242, doi:10.1073/pnas.1316546111, 2014.
- CCI-Report: Comprehensive Error Characterisation Report: University of Leicester full physics XCH₄ retrieval algorithm for CRDP3 – OCFPv1.0 for the Essential Climate Variable (ECV): Greenhouse Gases (GHG), 2016.
- 20 Chang, R. Y.-W., Miller, C. E., Dinardo, S. J., Karion, A., Sweeney, C., Daube, B. C., Henderson, J. M., Mountain, M. E., Eluszkiewicz, J., Miller, J. B., Bruhwiler, L. M. P., and Wofsy, S. C.: Methane emissions from Alaska in 2012 from CARVE airborne observations, *Proceedings of the National Academy of Sciences*, 111, 16694-16699, doi:10.1073/pnas.1412953111, 2014.
- 25 Chen, H., Zhu, Q. a., Peng, C., Wu, N., Wang, Y., Fang, X., Jiang, H., Xiang, W., Chang, J., Deng, X., and Yu, G.: Methane emissions from rice paddies natural wetlands, lakes in China: Synthesis new estimate, *Global Change Biology*, 19, 19-32, doi:10.1111/gcb.12034, 2013.
- Chen, Y. H., and Prinn, R. G.: Estimation of atmospheric methane emissions between 1996 and 2001 using a three-dimensional global chemical transport model, *Journal of Geophysical Research-Atmospheres*, 111, doi:10.1029/2005JD006058, 2006.
- 30 Chevallier, F., Fisher, M., Peylin, P., Serrar, S., Bousquet, P., Breon, F. M., Chedin, A., and Ciais, P.: Inferring CO₂ sources and sinks from satellite observations: Method and application to TOVS data, *Journal of Geophysical Research-Atmospheres*, 110, doi:10.1029/2005jd006390, 2005.
- Chevallier, F., Bréon, F. M., and Rayner, P. J.: Contribution of the Orbiting Carbon Observatory to the estimation of CO₂ sources and sinks: Theoretical study in a variational data assimilation framework, *J Geophys Res-Atmos*, 112, D09307, doi:10.1029/2006jd007375, 2007.
- 35 Chevallier, F., Ciais, P., Conway, T. J., Aalto, T., Anderson, B. E., Bousquet, P., Brunke, E. G., Ciattaglia, L., Esaki, Y., Frohlich, M., Gomez, A., Gomez-Pelaez, A. J., Haszpra, L., Krummel, P. B., Langenfelds, R. L., Leuenberger, M., Machida, T., Maignan, F., Matsueda, H., Morgui, J. A., Mukai, H., Nakazawa, T., Peylin, P., Ramonet, M., Rivier, L., Sawa, Y., Schmidt, M., Steele, L. P., Vay, S. A., Vermeulen, A. T., Wofsy, S., and Worthy, D.: CO₂ surface fluxes at grid point scale estimated from a global 21 year reanalysis of atmospheric measurements, *J Geophys Res-Atmos*, 115, 2010.
- 40 Christensen, T. R., van Huissteden, K., and Sachs, T.: Natural terrestrial methane sources in the Arctic, Chapter 3 in *AMAP Assessment 2015: Methane as an Arctic Climate Forcer*, p. 15-25, available at <http://www.amap.no/documents/doc/AMAP-Assessment-2015-Methane-as-an-Arctic-climate-forcer/1285>, 2015.
- 45 CIA: The World Factbook. Natural gas - production. Available at <https://www.cia.gov/library/publications/the-world-factbook/rankorder/2249rank.html>, 2016.
- Ciais, P., Sabine, C., Bala, G., Bopp, L., Brovkin, V., Canadell, J., Chhabra, A., DeFries, R., Galloway, J., M., H., Jones, C., Le Quéré, C., Myneni, R. B., Piao, S., and Thornton, P.: Carbon and Other Biogeochemical Cycles, in: *In Climate Change 2013: The Physical Science Basis. Contribution of Working Group I to the Fifth Assessment Report of IPCC*, edited by:



- Stocker, T. F., Qin, D., Plattner, G.-K., Tignor, M., Allen, S. K., Boschung, J., Nauels, A., Xia, Y., Bex, V., and Midgley, P. M., Cambridge University Press, Cambridge, 2013.
- Cicerone, R. J., and Shetter, J. D.: Sources of atmospheric methane: Measurements in rice paddies and a discussion, *Journal of Geophysical Research*, 86, 7203-7209, 1981.
- 5 Cicerone, R. J., and Oremland, R. S.: Biogeochemical aspects of atmospheric methane, *Global Biogeochemical Cycles*, 2, 299-327, 1988.
- Collins, M., Knutti, R., Arblaster, J., Dufresne, J.-L., Fichetef, T., Friedlingstein, P., Gao, X., Gutowski, W. J., Johns, T., Krinner, G., Shongwe, M., Tebaldi, C., Weaver, A. J., and Wehner, M.: Long-term Climate Change: Projections, Commitments and Irreversibility., in: *Climate Change 2013: The Physical Science Basis. Contribution of Working Group I to the Fifth Assessment Report of the Intergovernmental Panel on Climate Change.*, edited by: Stocker, T. F., Qin, D., Plattner, G.-K., Tignor, M., Allen, S. K., Boschung, J., Nauels, A., Xia, Y., Bex, V., and Midgley, P. M., Cambridge University Press, Cambridge, United Kingdom and New York, NY, USA, 2013.
- Conrad, R., and Seiler, W.: Influence of the surface microlayer on the flux of nonconservative trace gases (CO, H₂, CH₄, N₂O) across the ocean-atmosphere interface, *Journal of Atmospheric Chemistry*, 6, 83-94, 1988.
- 15 Conrad, R., Klose, M., and Claus, P.: Phosphate Inhibits Acetotrophic Methanogenesis on Rice Roots, *Applied and Environmental Microbiology*, 66, 828-831, 2000.
- Covey, K. R., Wood, S. A., Warren, R. J., Lee, X., and Bradford, M. A.: Elevated methane concentrations in trees of an upland forest, *Geophysical Research Letters*, 39, doi:10.1029/2012gl052361, 2012.
- Crawford, J. T., Stanley, E. H., Spawn, S. A., Finlay, J. C., Loken, L. C., and Striegl, R. G.: Ebullitive methane emissions from oxygenated wetland streams, *Global Change Biology*, 20, 3408-3422 doi:10.1111/gcb.12614, 2014.
- 20 Cressot, C., Chevallier, F., Bousquet, P., Crevoisier, C., Dlugokencky, E. J., Fortems-Cheiney, A., Frankenberg, C., Parker, R., Pison, I., Scheepmaker, R. A., Montzka, S. A., Krummel, P. B., Steele, L. P., and Langenfelds, R. L.: On the consistency between global and regional methane emissions inferred from SCIAMACHY, TANSO-FTS, IASI and surface measurements, *Atmospheric Chemistry and Physics*, 14, 577-592, doi:10.5194/acp-14-577-2014, 2014.
- 25 Crevoisier, C., Nobileau, D., Fiore, A. M., Armante, R., Chedin, A., and Scott, N. A.: Tropospheric methane in the tropics - first year from IASI hyperspectral infrared observations, *Atmospheric Chemistry and Physics*, 9, 6337-6350, 2009.
- Cunnold, D. M., Steele, L. P., Fraser, P. J., Simmonds, P. G., Prinn, R. G., Weiss, R. F., Porter, L. W., O'Doherty, S., Langenfelds, R. L., Krummel, P. B., Wang, H. J., Emmons, L., Tie, X. X., and Dlugokencky, E. J.: In situ measurements of atmospheric methane at GAGE/AGAGE sites during 1985-2000 and resulting source inferences, *J Geophys Res-Atmos*, 107, doi:10.1029/2001jd001226, 2002.
- 30 Curry, C. L.: Modeling the soil consumption of atmospheric methane at the global scale, *Global Biogeochemical Cycles*, 21, GB4012, doi:10.1029/2006gb002818, 2007.
- Dalsøren, S. B., Isaksen, I. S. A., Li, L., and Richter, A.: Effect of emission changes in Southeast Asia on global hydroxyl and methane lifetime, *Tellus B*, 61, 588-601, doi:10.1111/j.1600-0889.2009.00429.x, 2009.
- 35 Dalsøren, S. B., Myhre, C. L., Myhre, G., Gomez-Pelaez, A. J., Søvdde, O. A., Isaksen, I. S. A., Weiss, R. F., and Harth, C. M.: Atmospheric methane evolution the last 40 years, *Atmospheric Chemistry and Physics*, 16, 3099-3126, doi:10.5194/acp-16-3099-2016, 2016.
- Damm, E., Rudels, B., Schauer, U., Mau, S., and Dieckmann, G.: Methane excess in Arctic surface water- triggered by sea ice formation and melting, *Scientific Reports*, 5, 16179, doi:10.1038/srep16179, 2015.
- 40 Denman, K. L., G. Brasseur, A. Chidthaisong, P. Ciais, P.M. Cox, R.E. Dickinson, D. Hauglustaine, C. Heinze, E. Holland, D. Jacob, U. Lohmann, S Ramachandran, P.L. da Silva Dias, Wofsy, S. C., and X. Zhang: *Couplings Between Changes in the Climate System and Biogeochemistry*, Cambridge University Press, Cambridge, United Kingdom and New York, NY, USA., 2007.
- Dils, B., De Mazière, M., Müller, J. F., Blumenstock, T., Buchwitz, M., de Beek, R., Demoulin, P., Duchatelet, P., Fast, H., Frankenberg, C., Gloudemans, A., Griffith, D., Jones, N., Kerzenmacher, T., Kramer, I., Mahieu, E., Mellqvist, J., Mittermeier, R. L., Notholt, J., Rinsland, C. P., Schrijver, H., Smale, D., Strandberg, A., Straume, A. G., Stremme, W., Strong, K., Sussmann, R., Taylor, J., van den Broek, M., Velasco, V., Wagner, T., Warneke, T., Wiacek, A., and Wood, S.: Comparisons between SCIAMACHY and ground-based FTIR data for total columns of CO, CH₄, CO₂ and N₂O, *Atmospheric Chemistry and Physics*, 6, 1953-1976, doi:10.5194/acp-6-1953-2006, 2006.



- Dils, B., Buchwitz, M., Reuter, M., Schneising, O., Boesch, H., Parker, R., Guerlet, S., Aben, I., Blumenstock, T., Burrows, J. P., Butz, A., Deutscher, N. M., Frankenberg, C., Hase, F., Hasekamp, O. P., Heymann, J., De Mazière, M., Notholt, J., Sussmann, R., Warneke, T., Griffith, D., Sherlock, V., and Wunch, D.: The Greenhouse Gas Climate Change Initiative (GHG-CCI): Comparative validation of GHG-CCI SCIAMACHY/ENVISAT and TANSO-FTS/GOSAT CO₂ and CH₄ retrieval algorithm products with measurements from the TCCON, *Atmospheric Measurement Technologies*, 7, 1723-1744, doi:10.5194/amt-7-1723-2014, 2014.
- 5 Dlugokencky, E. J., Steele, L. P., Lang, P. M., and Masarie, K. A.: The Growth-Rate and Distribution of Atmospheric Methane, *Journal of Geophysical Research-Atmospheres*, 99, 17,021-017,043, 1994.
- Dlugokencky, E. J., Dutton, E. G., Novelli, P. C., Tans, P. P., Masarie, K. A., Lantz, K. O., and Madronich, S.: Changes in CH₄ and CO growth rates after the eruption of Mt Pinatubo and their link with changes in tropical tropospheric UV flux, *Geophysical Research Letters*, 23, 2761-2764, 1996.
- 10 Dlugokencky, E. J., Walter, B. P., Masarie, K. A., Lang, P. M., and Kasischke, E. S.: Measurements of an anomalous global methane increase during 1998, *Geophysical Research Letters*, 28, 499-502, 2001.
- Dlugokencky, E. J., Bruhwiler, L., White, J. W. C., Emmons, L. K., Novelli, P. C., Montzka, S. A., Masarie, K. A., Lang, P. M., Crotwell, A. M., Miller, J. B., and Gatti, L. V.: Observational constraints on recent increases in the atmospheric CH burden, *Geophysical Research Letters*, 36, L18803, 10.1029/2009GL039780, 2009.
- 15 Dlugokencky, E. J., Nisbet, E. G., Fisher, R., and Lowry, D.: Global atmospheric methane: budget, changes and dangers, *Philos T R Soc A*, 369, 2058-2072, 2011.
- Dueck, T. A., de Visser, R., Poorter, H., Persijn, S., A. Gorissen, A., W. de Visser, W., Schapendonk, A., Verhagen, J., Snel, J., Harren, F. J. M., Ngai, A. K. Y., Verstappen, F., Bouwmeester, H., Voesenek, L. A. C. J., and van der Werf, A.: No evidence for substantial aerobic methane emission by terrestrial plants: a ¹³C-labelling approach, *New Phytologist*, doi:10.1111/j.1469-8137.2007.02103.x, 2007.
- Dutaur, L., and Verchot, L. V.: A global inventory of the soil CH₄ sink, *Global Biogeochem Cycles* 21, GB4012, doi:10.1029/2006GB002734, 2007.
- 25 EDGAR: European Commission, Joint Research Centre (JRC)/Netherlands Environmental Assessment Agency (PBL). Emission Database for Global Atmospheric Research (EDGAR), release version 4.1. <http://edgar.jrc.ec.europa.eu>, 2010.
- EDGAR: European Commission, Joint Research Centre (JRC)/Netherlands Environmental Assessment Agency (PBL). Emission Database for Global Atmospheric Research (EDGAR), release version 4.2. <http://edgar.jrc.ec.europa.eu>, 2012.
- EDGAR: European Commission, Joint Research Centre (JRC)/Netherlands Environmental Assessment Agency (PBL). Emission Database for Global Atmospheric Research (EDGAR), release EDGARv4.2 FT2010, <http://edgar.jrc.ec.europa.eu>, 2013.
- 30 EDGAR: European Commission, Joint Research Centre (JRC)/Netherlands Environmental Assessment Agency (PBL). Emission Database for Global Atmospheric Research (EDGAR), release EDGARv4.2 FT2012, <http://edgar.jrc.ec.europa.eu>, 2014.
- Ehhalt, D., Prather, M., Dentener, F., Derwent, R., Dlugokencky, E., Holland, E., Isaksen, I., Katima, J., Kirchhoff, V., Matson, P., Midgley, P., and Wang, M.: Atmospheric chemistry and greenhouse gases. In: *Climate Change 2001: The Scientific Basis. Contribution of Working Group I to the Third Assessment Report of the Intergovernmental Panel on Climate Change*. [Houghton, J.T., et al. (eds.)]. Cambridge University Press, Cambridge, United Kingdom and New York, NY, USA, pp. 239-287, 2001.
- 35 Ehhalt, D. H.: The atmospheric cycle of methane, *Tellus*, 26, 58-70, doi:10.1111/j.2153-3490.1974.tb01952.x, 1974.
- EIA: The Annual Energy Outlook with projections to 2014, DOE/EIA-0383, 2015.
- Elvidge, C., Ziskin, D., Baugh, K., Tuttle, B., Ghosh, T., Pack, D., Erwin, E., and Zhizhin, M.: A Fifteen Year Record of Global Natural Gas Flaring Derived from Satellite Data, *Energies*, 2, 595, 2009.
- Elvidge, C. D., Zhizhin, M., Baugh, K., Hsu, F.-C., and Ghosh, T.: Methods for Global Survey of Natural Gas Flaring from Visible Infrared Imaging Radiometer Suite Data, *Energies*, 9 (1), doi:10.3390/en9010014, 2016.
- 45 EMEP/EEA: European Monitoring and Evaluation Programme/EEA). EMEP/EEA air pollutant emission inventory guidebook—2009. Technical guidance to prepare national emission inventories, EEA technical report no 6/2009. Available online at www.eea.europa.eu/publications, 10.2800/23924, 2009.
- Etiopie, G., and Klusman, R. W.: Geologic emissions of methane to the atmosphere, *Chemosphere*, 49, 777-789, 2002.



- Etiopie, G., Lassey, K. R., Klusman, R. W., and Boschi, E.: Reappraisal of the fossil methane budget and related emission from geologic sources, *Geophysical Research Letters*, 35, L09307, doi:10.1029/2008gl033623, 2008.
- Etiopie, G.: Climate science: Methane uncovered, *Nature Geoscience*, 5, 373-374, doi:10.1038/ngeo1483, 2012.
- Etiopie, G.: Natural Gas Seepage. *The Earth's Hydrocarbon Degassing*, Springer International Publishing, 199 pp., 2015.
- 5 EU-Landfill-Directive: http://ec.europa.eu/environment/waste/landfill_index.htm, 1999.
- Fang, S., Tans, P. P., Dong, F., Zhou, H., and Luan, T.: Characteristics of atmospheric CO₂ and CH₄ at the Shangdianzi regional background station in China, *Atmospheric Environment*, 131, 1-8, doi:10.1016/j.atmosenv.2016.01.044, 2015.
- FAO: FAOSTAT. Food and Agriculture Organization of the United Nations. Statistical Division. Available at: <http://faostat.fao.org>, 2012.
- 10 Fisher, R. E., Sriskantharajah, S., Lowry, D., Lanoiselle, M., Fowler, C. M. R., James, R. H., Hermansen, O., Myhre, C. L., Stohl, A., Greinert, J., Nisbet-Jones, P. B. R., Mienert, J., and Nisbet, E. G.: Arctic methane sources: Isotopic evidence for atmospheric inputs, *Geophysical Research Letters*, 38, L21803, doi:10.1029/2011gl049319, 2011.
- Forster, P., Ramaswamy, V., Artaxo, P., Bernsten, T., Betts, B., Fahey, D. W., Haywood, J., Lean, J., Lowe, D. C., Myhre, G., Nganga, J., Prinn, R., Raga, G., Schulz, M., and Van Dorland, R.: *Changes in Atmospheric Constituents and in Radiative Forcing*, Cambridge University Press, Cambridge, United Kingdom and New York, NY, USA., 2007.
- 15 Fortems-Cheiney, A., Chevallier, F., Pison, I., Bousquet, P., Szopa, S., Deeter, M. N., and Clerbaux, C.: Ten years of CO emissions as seen from Measurements of Pollution in the Troposphere (MOPITT), *Journal of Geophysical Research-Atmospheres*, 116, 2011.
- Francey, R. J., Steele, L. P., Langenfelds, R. L., and Pak, B. C.: High precision long-term monitoring of radiatively active and related trace gases at surface sites and from aircraft in the southern hemisphere atmosphere, *Journal of the Atmospheric Sciences*, 56, 279-285, 1999.
- Frankenberg, C., Meirink, J. F., van Weele, M., Platt, U., and Wagner, T.: Assessing methane emissions from global spaceborne observations, *Science*, 308, 1010-1014, 2005.
- Frankenberg, C., Meirink, J. F., Bergamaschi, P., Goede, A. P. H., Heimann, M., Korner, S., Platt, U., van Weele, M., and Wagner, T.: Satellite cartography of atmospheric methane from SCIAMACHY on board ENVISAT: Analysis of the years 2003 and 2004, *Journal of Geophysical Research-Atmospheres*, 111, D07303, doi: 10.1029/2005JD006235, 2006.
- Frankenberg, C., Aben, I., Bergamaschi, P., Dlugokencky, E. J., van Hees, R., Houweling, S., van der Meer, P., Snel, R., and Tol, P.: Global column-averaged methane mixing ratios from 2003 to 2009 as derived from SCIAMACHY: Trends and variability, *Journal of Geophysical Research-Atmospheres*, 116, D04302, doi:10.1029/2010jd014849, 2011.
- 30 Fraser, A., Palmer, P. I., Feng, L., Boesch, H., Cogan, A., Parker, R., Dlugokencky, E. J., Fraser, P. J., Krummel, P. B., Langenfelds, R. L., O'Doherty, S., Prinn, R. G., Steele, L. P., van der Schoot, M., and Weiss, R. F.: Estimating regional methane surface fluxes: the relative importance of surface and GOSAT mole fraction measurements, *Atmospheric Chemistry and Physics*, 13, 5697-5713, doi:10.5194/acp-13-5697-2013, 2013.
- Fraser, P. J., Rasmussen, R. A., Creffield, J. W., French, J. R., and Khalil, M. A. K.: Termites and global methane – Another assessment, *Journal of Atmospheric Chemistry*, 4, 295-310, 1986.
- 35 GAEZv3.0: Global Agro-Ecological Zones, available at: <http://www.gaez.iiasa.ac.at/>, 2012.
- Gatti, L. V., Gloor, M., Miller, J. B., Doughty, C. E., Malhi, Y., Domingues, L. G., Basso, L. S., Martinewski, A., Correia, C. S. C., Borges, V. F., Freitas, S., Braz, R., Anderson, L. O., Rocha, H., Grace, J., Phillips, O. L., and Lloyd, J.: Drought sensitivity of Amazonian carbon balance revealed by atmospheric measurements, *Nature*, 506, 76-80, doi:10.1038/nature12957, 2014.
- 40 Giglio, L., Randerson, J. T., and van der Werf, G. R.: Analysis of daily, monthly, and annual burned area using the fourth-generation global fire emissions database (GFED4), *Journal of Geophysical Research - Biogeosciences*, 118, 317-328, doi:10.1002/jgrg.20042, 2013.
- Glagolev, M., Kleptsova, I., Filippov, I., Maksyutov, S., and Machida, T.: Regional methane emission from West Siberia mire landscapes, *Environmental Research Letters*, 6, 045214, doi:10.1088/1748-9326/6/4/045214, 2011.
- 45 Grant, R. F., and Roulet, N. T.: Methane efflux from boreal wetlands: Theory and testing of the ecosystem model Ecosys with chamber and tower flux measurements, *Global Biogeochemical Cycles*, 16, 2-1-2-16, 10.1029/2001gb001702, 2002.
- Guérin, F., Abril, G., Richard, S., Burban, B., Reynouard, C., Seyler, P., and Delmas, R.: Methane and carbon dioxide emissions from tropical reservoirs: Significance of downstream rivers, *Geophysical Research Letters*, 33, L21407, 10.1029/2006GL027929, 2006.
- 50



- Guérin, F., Deshmukh, C., Labat, D., Pighini, S., Vongkhamkao, A., Guédant, P., Rode, W., Godon, A., Chanudet, V., Descloux, S., and Serça, D.: Effect of sporadic destratification, seasonal overturn and artificial mixing on CH₄ emissions at the surface of a subtropical hydroelectric reservoir (Nam Theun 2 Reservoir, Lao PDR), *Biogeosciences Discussions*, 2015, 11349-11385, doi:10.5194/bgd-12-11349-2015, 2015.
- 5 Gupta, M. L., Cicerone, R. J., and Elliott, S.: Perturbation to global tropospheric oxidizing capacity due to latitudinal redistribution of surface sources of NO_x, CH₄ and CO, *Geophysical Research Letters*, 25, 3931-3934, doi:10.1029/1998gl900099, 1998.
- Gurney, K. R., Law, R. M., Denning, A. S., Rayner, P. J., Pak, B. C., Baker, D., Bousquet, P., Bruhwiler, L., Chen, Y. H., Ciais, P., Fung, I. Y., Heimann, M., John, J., Maki, T., Maksyutov, S., Peylin, P., Prather, M., and Taguchi, S.: Transcom 3 inversion intercomparison: Model mean results for the estimation of seasonal carbon sources and sinks, *Global Biogeochemical Cycles*, 18, GB2010, doi:10.1029/2003gb002111, 2004.
- 10 Hansen, M. C., DeFries, R. S., Townshend, J. R. G., and Sohlberg, R.: Global land cover classification at the 1km spatial resolution using a classification tree approach, *International Journal of Remote Sensing*, 21, 1331-1364, 2000.
- Hausmann, P., Sussmann, R., and Smale, D.: Contribution of oil and natural gas production to renewed increase in atmospheric methane (2007–2014): top-down estimate from ethane and methane column observations, *Atmospheric Chemistry and Physics*, 16, 3227-3244, doi:10.5194/acp-16-3227-2016, 2016.
- 15 Hayashida, S., Ono, A., Yoshizaki, S., Frankenberg, C., Takeuchi, W., and Yan, X.: Methane concentrations over Monsoon Asia as observed by SCIAMACHY: Signals of methane emission from rice cultivation, *Remote Sensing of Environment*, 139, 246-256, doi:10.1016/j.rse.2013.08.008, 2013.
- 20 Hayman, G. D., O'Connor, F. M., Dalvi, M., Clark, D. B., Gedney, N., Huntingford, C., Prigent, C., Buchwitz, M., Schneising, O., Burrows, J. P., Wilson, C., Richards, N., and Chipperfield, M.: Comparison of the HadGEM2 climate-chemistry model against in situ and SCIAMACHY atmospheric methane data, *Atmospheric Chemistry and Physics*, 14, 13257-13280, doi:10.5194/acp-14-13257-2014, 2014.
- Hegglin, M. I., Plummer, D. A., Shepherd, T. G., Scinocca, J. F., Anderson, J., Froidevaux, L., Funke, B., Hurst, D., Rozanov, A., Urban, J., von Clarmann, T., Walker, K. A., Wang, H. J., Tegtmeier, S., and Weigel, K.: Vertical structure of stratospheric water vapour trends derived from merged satellite data, *Nature Geoscience*, 7, 768-776, doi:10.1038/ngeo2236, 2014.
- 25 Hein, R., Crutzen, P. J., and Heimann, M.: An inverse modeling approach to investigate the global atmospheric methane cycle, *Global Biogeochemical Cycles*, 11, 43-76, 1997.
- 30 Hietala, A., Dörsch, P., Kvaalen, H., and Solheim, H.: Carbon Dioxide and Methane Formation in Norway Spruce Stems Infected by White-Rot Fungi, *Forests*, 6, 3304, 2015.
- Hodson, E. L., Poulter, B., Zimmermann, N. E., Prigent, C., and Kaplan, J. O.: The El Niño Southern Oscillation and wetland methane interannual variability, *Geophysical Research Letters*, 38, L08810, doi:10.1029/2011gl046861, 2011.
- 35 Hoelzemann, J. J., Schultz, M. G., Brasseur, G. P., Granier, C., and Simon, M.: Global Wildland Fire Emission Model (GWEM): Evaluating the use of global area burnt satellite data, *Journal of Geophysical Research*, 109, D14S04, doi:10.1029/2003jd003666, 2004.
- Höglund-Isaksson, L.: Global anthropogenic methane emissions 2005-2030: Technical mitigation potentials and costs, *Atmospheric Chemistry and Physics*, 12, 9079-9096, doi:10.5194/acp-12-9079-2012, 2012.
- 40 Höglund-Isaksson, L., Thomson, A., Kupiainen, K., Rao, S., and Janssens-Maenhout, G.: Anthropogenic methane sources, emissions and future projections, Chapter 5 in AMAP Assessment 2015: Methane as an Arctic Climate Forcer, p. 39-59, available at <http://www.amap.no/documents/doc/AMAP-Assessment-2015-Methane-as-an-Arctic-climate-forcer/1285>, 2015.
- Holmes, C. D., Prather, M. J., Søvde, O. A., and Myhre, G.: Future methane, hydroxyl, and their uncertainties: key climate and emission parameters for future predictions, *Atmospheric Chemistry and Physics*, 13, 285-302, doi:10.5194/acp-13-285-2013, 2013.
- 45 Houweling, S., Dentener, F., and Lelieveld, J.: Simulation of preindustrial atmospheric methane to constrain the global source strength of natural wetlands, *Journal of Geophysical Research-Atmospheres*, 105, 17,243-217,255, doi:10.1029/2000JD900193, 2000.
- 50 Houweling, S., van der Werf, G. R., Goldewijk, K. K., Rockmann, T., and Aben, I.: Early anthropogenic CH₄ emissions and the variation of CH₄ and (CH₄)-¹³C over the last millennium, *Global Biogeochemical Cycles*, 22, 2008.



- Houweling, S., Krol, M., Bergamaschi, P., Frankenberg, C., Dlugokencky, E. J., Morino, I., Notholt, J., Sherlock, V., Wunch, D., Beck, V., Gerbig, C., Chen, H., Kort, E. A., Röckmann, T., and Aben, I.: A multi-year methane inversion using SCIAMACHY, accounting for systematic errors using TCCON measurements, *Atmospheric Chemistry and Physics*, 14, 3991-4012, doi:10.5194/acp-14-3991-2014, 2014.
- 5 Howarth, R., Santoro, R., and Ingraffea, A.: Methane and the greenhouse-gas footprint of natural gas from shale formations, *Climatic Change*, 106, 679-690, doi:10.1007/s10584-011-0061-5, 2011.
- Huang, J., and Prinn, R. G.: Critical evaluation of emissions of potential new gases for OH estimation, *Journal of Geophysical Research*, 107, 4784, doi:10.1029/2002jd002394, 2002.
- Hugelius, G., Strauss, J., Zubrzycki, S., Harden, J. W., Schuur, E. A. G., Ping, C. L., Schirmer, L., Grosse, G., Michaelson, G. J., Koven, C. D., O'Donnell, J. A., Elberling, B., Mishra, U., Camill, P., Yu, Z., Palmtag, J., and Kuhry, P.: Estimated stocks of circumpolar permafrost carbon with quantified uncertainty ranges and identified data gaps, *Biogeosciences*, 11, 6573-6593, doi:10.5194/bg-11-6573-2014, 2014.
- IEA: International Energy Agency. Annual Report. Available at: https://www.iea.org/publications/freepublications/publication/IEA_Annual_Report_publicversion.pdf, 2012.
- 15 IEA: International Energy Agency. Annual Report. Available at: https://www.iea.org/publications/freepublications/publication/2013_AnnualReport.pdf and online data service at www.iea.org, 2013.
- IPCC: Good Practice Guidance and Uncertainty Management in National Greenhouse Gas Inventories. Intergovernmental Panel on Climate Change, National Greenhouse Gas Inventories Programme. Montreal, IPCC-XVI/Doc.10(1.IV.2000), May 2000. ISBN 4-88788-000-6, 2000.
- 20 IPCC: Climate change 2001: The scientific basis. Contribution of working group I to the third assessment report of the Intergovernmental Panel on Climate Change, Cambridge University Press, Cambridge, United Kingdom and New York, NY, USA, 881, 2001.
- IPCC: IPCC Guidelines for National Greenhouse Gas Inventories. The National Greenhouse Gas Inventories Programme, Eggleston H.S., Buendia L., Miwa K., Ngara T. and Tanabe K. (eds). The Intergovernmental Panel on Climate Change, IPCC TSU NGGIP, IGES. Institute for Global Environmental Strategy, Hayama, Kanagawa, Japan. Available online at: http://www.ipcc-nggip.iges.or.jp/support/Primer_2006GLs.pdf, 2006.
- IPCC: Climate Change 2014: Mitigation of Climate Change. Contribution of Working Group III to the Fifth Assessment Report of the Intergovernmental Panel on Climate Change. Edenhofer, O., R. Pichs-Madruga, Y. Sokona, E. Farahani, S. Kadner, K. Seyboth, A. Adler, I. Baum, S. Brunner, P. Eickemeier, B. Kriemann, J. Savolainen, S. Schlömer, C. von Stechow, T. Zwickel and J.C. Minx (eds.). Cambridge University Press, 2014.
- 30 Ishizawa, M., Mabuchi, K., Shirai, T., Inoue, M., Morino, I., Uchino, O., Yoshida, Y., Maksyutov, S., and Belikov, D.: Inter-annual variability of CO₂ exchange in Northern Eurasia inferred from GOSAT XCO₂, *Environmental Research Letters*, 2016, submitted.
- 35 Ito, A., and Inatomi, M.: Use of a process-based model for assessing the methane budgets of global terrestrial ecosystems and evaluation of uncertainty, *Biogeosciences*, 9, 759-773, doi:10.5194/bg-9-759-2012, 2012.
- Jackson, R. B., Down, A., Phillips, N. G., Ackley, R. C., Cook, C. W., Plata, D. L., and Zhao, K.: Natural gas pipeline leaks across Washington, D.C, *Environmental Science and Technology*, 48, 2051-2058, doi:10.1021/es404474x, 2014a.
- Jackson, R. B., Vengosh, A., Carey, J. W., Davies, R. J., Darrah, T. H., O'Sullivan, F., and Pétron, G.: The Environmental Costs and Benefits of Fracking, *Annual Review of Environment and Resources*, 39, 327-362, doi:10.1146/annurev-environ-031113-144051, 2014b.
- 40 James, R. H., Bousquet, P., Bussmann, I., Haeckel, M., Kipfer, R., Leifer, I., Niemann, H., Ostrovsky, I., Piskozub, J., Rehder, G., Treude, T., Vielstädte, L., and Greinert, J.: Effects of climate change on methane emissions from seafloor sediments in the Arctic Ocean: A review, *Limnology and Oceanography*, 61, doi:10.1002/lno.10307, 2016.
- 45 Johnson, D. E., Phetteplace, H. W., and Seidl, A. F.: Methane, nitrous oxide and carbon dioxide emissions from ruminant livestock production systems, GHGs and animal agriculture. Proceedings of the 11th International Conference on GHGs and Animal Agriculture, Obihiro, November 2001, 2002, 77-85,
- Joly, L., Robert, C., Parvite, B., Catoire, V., Durry, G., Richard, G., Nicoulaud, B., and Zéninari, V.: Development of a spectrometer using a cw DFB quantum cascade laser operating at room temperature for the simultaneous analysis of N₂O and CH₄ in the Earth's atmosphere *Applied Optics*, 47, 1206-1214 2008.
- 50



- Kai, F. M., Tyler, S. C., Randerson, J. T., and Blake, D. R.: Reduced methane growth rate explained by decreased Northern Hemisphere microbial sources, *Nature*, 476, 194-197, 2011.
- Kaiser, J. W., Heil, A., Andreae, M. O., Benedetti, A., Chubarova, N., Jones, L., Morcrette, J. J., Razinger, M., Schultz, M. G., Suttie, M., and van der Werf, G. R.: Biomass burning emissions estimated with a global fire assimilation system based on observed fire radiative power, *Biogeosciences*, 9, 527-554, doi:10.5194/bg-9-527-2012, 2012.
- 5 Kaminski, T., Rayner, P. J., Heimann, M., and Enting, I. G.: On aggregation errors in atmospheric transport inversions, *Journal of Geophysical Research-Atmospheres*, 106, 4703-4715, 2001.
- Kaplan, J. O.: Wetlands at the Last Glacial Maximum: Distribution and methane emissions, *Geophysical Research Letters*, 29, 1079, doi:10.1029/2001gl013366, 2002.
- 10 Karion, A., Sweeney, C., Tans, P., and Newberger, T.: AirCore: An Innovative Atmospheric Sampling System, *Journal of Atmospheric and Oceanic Technology* 27, 1839-1853 2010.
- Karion, A., Sweeney, C., Pétron, G., Frost, G., Michael Hardesty, R., Kofler, J., Miller, B. R., Newberger, T., Wolter, S., Banta, R., Brewer, A., Dlugokencky, E., Lang, P., Montzka, S. A., Schnell, R., Tans, P., Trainer, M., Zamora, R., and Conley, S.: Methane emissions estimate from airborne measurements over a western United States natural gas field, *Geophysical Research Letters*, 40, 4393-4397, doi:10.1002/grl.50811, 2013.
- 15 Kepler, F., Hamilton, J. T. G., Brass, M., and Rockmann, T.: Methane emissions from terrestrial plants under aerobic conditions, *Nature*, 439, 187-191, 2006.
- Kim, H.-S., Maksyutov, S., Glagolev, M. V., Machida, T., Patra, P. K., Sudo, K., and Inoue, G.: Evaluation of methane emissions from West Siberian wetlands based on inverse modeling, *Environmental Research Letters*, 6, 2011.
- 20 Kirschke, S., Bousquet, P., Ciais, P., Saunoy, M., Canadell, J. G., Dlugokencky, E. J., Bergamaschi, P., Bergmann, D., Blake, D. R., Bruhwiler, L., Cameron-Smith, P., Castaldi, S., Chevallier, F., Feng, L., Fraser, A., Heimann, M., Hodson, E. L., Houweling, S., Josse, B., Fraser, P. J., Krummel, P. B., Lamarque, J. F., Langenfelds, R. L., Le Quere, C., Naik, V., O'Doherty, S., Palmer, P. I., Pison, I., Plummer, D., Poulter, B., Prinn, R. G., Rigby, M., Ringeval, B., Santini, M., Schmidt, M., Shindell, D. T., Simpson, I. J., Spahni, R., Steele, L. P., Strode, S. A., Sudo, K., Szopa, S., van der Werf, G. R., Voulgarakis, A., van Weele, M., Weiss, R. F., Williams, J. E., and Zeng, G.: Three decades of global methane sources and sinks, *Nature Geoscience*, 6, 813-823, doi:10.1038/ngeo1955, 2013.
- 25 Klauda, J. B., and Sandler, S. I.: Global distribution of methane hydrate in ocean sediment, *Energy and Fuels*, 19, 459-470, 2005.
- Kleinen, T., Brovkin, V., and Schuldt, R. J.: A dynamic model of wetland extent and peat accumulation: results for the Holocene, *Biogeosciences*, 9, 235-248, doi:10.5194/bg-9-235-2012, 2012.
- 30 Klimont, Z., Höglund-Isaksson, L., Heyes, C., Rafaj, P., Schöpp, W., Cofala, J., Borken-Kleefeld, J., Purohit, P., Kupiainen, K., Winiwarter, W., Amann, M., Zhao, B., Wang, S. X., Bertok, I., and Sander, R.: Global scenarios of air pollutants and methane: 1990–2050, (in preparation), 2016.
- Kretschmer, K., Biastoch, A., Rüpke, L., and Burwicz, E.: Modeling the fate of methane hydrates under global warming, *Global Biogeochem Cycles*, 29, 610-625, doi:10.1029/2014GB005011, 2015.
- 35 Kvenvolden, K. A., Reeburgh, W. S., and Lorenson, T. D.: Attention turns to naturally occurring methane seepages, *EOS Transactions, American Geophysical Union*, 82, 457, 2001.
- Kvenvolden, K. A., and Rogers, B. W.: Gaia's breath - global methane exhalations, *Marine and Petroleum Geology*, 22, 579-590, 2005.
- 40 Lamarque, J. F., Bond, T. C., Eyring, V., Granier, C., Heil, A., Klimont, Z., Lee, D., Liousse, C., Mieville, A., Owen, B., Schultz, M. G., Shindell, D., Smith, S. J., Stehfest, E., Van Aardenne, J., Cooper, O. R., Kainuma, M., Mahowald, N., McConnell, J. R., Naik, V., Riahi, K., and van Vuuren, D. P.: Historical (1850–2000) gridded anthropogenic and biomass burning emissions of reactive gases and aerosols: methodology and application, *Atmospheric Chemistry and Physics*, 10, 7017-7039, doi:10.5194/acp-10-7017-2010, 2010.
- 45 Lamarque, J. F., Shindell, D. T., Josse, B., Young, P. J., Cionni, I., Eyring, V., Bergmann, D., Cameron-Smith, P., Collins, W. J., Doherty, R., Dalsoren, S., Faluvegi, G., Folberth, G., Ghan, S. J., Horowitz, L. W., Lee, Y. H., MacKenzie, I. A., Nagashima, T., Naik, V., Plummer, D., Righi, M., Rumbold, S. T., Schulz, M., Skeie, R. B., Stevenson, D. S., Strode, S., Sudo, K., Szopa, S., Voulgarakis, A., and Zeng, G.: The Atmospheric Chemistry and Climate Model Intercomparison Project (ACCMIP): overview and description of models, simulations and climate diagnostics, *Geoscientific Model Development*, 6, 179-206, doi:10.5194/gmd-6-179-2013, 2013.
- 50



- Lamb, B. K., Edburg, S. L., Ferrara, T. W., Howard, T., Harrison, M. R., Kolb, C. E., Townsend-Small, A., Dyck, W., Possolo, A., and Whetstone, J. R.: Direct Measurements Show Decreasing Methane Emissions from Natural Gas Local Distribution Systems in the United States, *Environmental Science & Technology*, 49, 5161-5169, doi:10.1021/es505116p, 2015.
- 5 Lambert, G., and Schmidt, S.: Reevaluation of the oceanic flux of methane: Uncertainties and long term variations, *Chemosphere*, 26, 579-589, doi:10.1016/0045-6535(93)90443-9, 1993.
- Lamontagne, R. A., Swinnerton, J. W., Linnenbom, V. J., and Smith, W. D.: Methane concentrations in various marine environments, *Journal of Geophysical Research*, 78, 5317-5324, doi:10.1029/JC078i024p05317, 1973.
- Langenfelds, R. L., Francey, R. J., Pak, B. C., Steele, L. P., Lloyd, J., Trudinger, C. M., and Allison, C. E.: Interannual growth rate variations of atmospheric CO₂ and its delta ¹³C, H₂, CH₄, and CO between 1992 and 1999 linked to biomass burning, *Global Biogeochemical Cycles*, 16, 1048, doi:10.1029/2001GB001466, 2002.
- 10 Lassey, K. R., Etheridge, D. M., Lowe, D. C., Smith, A. M., and Ferretti, D. F.: Centennial evolution of the atmospheric methane budget: what do the carbon isotopes tell us?, *Atmospheric Chemistry and Physics*, 7, 2119-2139, 2007a.
- Lassey, K. R., Lowe, D. C., and Smith, A. M.: The atmospheric cycling of radiomethane and the "fossil fraction" of the methane source, *Atmospheric Chemistry and Physics*, 7, 2141-2149, 2007b.
- 15 Lehner, B., and Döll, P.: Development and validation of a global database of lakes, reservoirs and wetlands, *Journal of Hydrology*, 296, 1-22, doi:10.1016/j.jhydrol.2004.03.028, 2004.
- Lelieveld, J., Crutzen, P. J., and Dentener, F. J.: Changing concentration, lifetime and climate forcing of atmospheric methane, *Tellus Series B-Chemical and Physical Meteorology*, 50, 128-150, doi:10.1034/j.1600-0889.1998.t01-1-00002.x, 1998.
- 20 Lelieveld, J., Peters, W., Dentener, F. J., and Krol, M. C.: Stability of tropospheric hydroxyl chemistry, *Journal of Geophysical Research-Atmospheres*, 107, 10.1029/2002jd002272, 2002.
- Lelieveld, J., Dentener, F. J., Peters, W., and Krol, M. C.: On the role of hydroxyl radicals in the self-cleansing capacity of the troposphere, *Atmospheric Chemistry and Physics*, 4, 337-2344, 2004.
- 25 Lelieveld, J., Lechtenbohm, S., Assonov, S. S., Brenninkmeijer, C. A. M., Dienst, C., Fishedick, M., and Hanke, T.: Greenhouse gases: Low methane leakage from gas pipelines, *Nature*, 434, 841-842, doi:10.1038/434841a, 2005.
- Leng, R. A.: The impact of livestock development on environmental change, in: *Strategies for Sustainable Animal Agriculture in Developing Countries*, Food and Agriculture Organization of the United Nations. ed., FAO, Rome, 1993.
- Levvasseur, G., Vrac, M., Roche, D. M., Paillard, D., Martin, A., and Vandenberghe, J.: Present and LGM permafrost from climate simulations: contribution of statistical downscaling, *Climate of the Past*, 7, 1225-1246, doi:10.5194/cp-7-1225-2011, 2011.
- 30 Levin, I., Veidt, C., Vaughn, B. H., Brailsford, G., Bromley, T., Heinz, R., Lowe, D., Miller, J. B., Posz, C., and White, J. W. C.: No inter-hemispheric [dgr] ¹³CH₄ trend observed, *Nature*, 486, doi:10.1038/nature11175, 2012.
- Li, C., Frohling, S., Xiao, X., Moore, B., Boles, S., Qiu, J., Huang, Y., Salas, W., and Sass, R.: Modeling impacts of farming management alternatives on CO₂, CH₄, and N₂O emissions: A case study for water management of rice agriculture of China, *Global Biogeochemical Cycles*, 19, doi:10.1029/2004gb002341, 2005.
- 35 Lin, X., Indira, N. K., Ramonet, M., Delmotte, M., Ciais, P., Bhatt, B. C., Reddy, M. V., Angchuk, D., Balakrishnan, S., Jorphaal, S., Dorjai, T., Mahey, T. T., Patnaik, S., Begum, M., Brenninkmeijer, C., Durairaj, S., Kirubakaran, R., Schmidt, M., Swathi, P. S., Vinithkumar, N. V., Yver Kwok, C., and Gaur, V. K.: Long-lived atmospheric trace gases measurements in flask samples from three stations in India, *Atmospheric Chemistry and Physics*, 15, 9819-9849, doi:10.5194/acp-15-9819-2015, 2015.
- 40 Locatelli, R., Bousquet, P., Saunois, M., Chevallier, F., and Cressot, C.: Sensitivity of the recent methane budget to LMDz sub-grid-scale physical parameterizations, *Atmospheric Chemistry and Physics*, 15, 9765-9780, doi:10.5194/acp-15-9765-2015, 2015.
- 45 Lohila, A., Aalto, T., Aurela, M., Hatakka, J., Tuovinen, J.-P., Kilkki, J., Penttilä, T., Vuorenmaa, J., Hänninen, P., Sutinen, R., Viisanen, Y., and Laurila, T.: Large contribution of boreal upland forest soils to a catchment-scale CH₄ balance in a wet year, *Geophysical Research Letters*, 43, 2946-2953, doi:10.1002/2016gl067718, 2016.
- Lowe, D. C., Brenninkmeijer, C. A. M., Manning, M. R., Sparks, R., and Wallace, G.: Radiocarbon determination of atmospheric methane at Baring Head, New Zealand, *Nature*, 332, 522-525, 1988.



- Lowe, D. C., Brenninkmeijer, C. A. M., Brailsford, G. W., Lassey, K. R., Gomez, A. J., and Nisbet, E. G.: Concentration and ^{13}C records of atmospheric methane in New Zealand and Antarctica: Evidence for changes in methane sources, *Journal of Geophysical Research: Atmospheres*, 99, 16913-16925, doi:10.1029/94jd00908, 1994.
- 5 Machida, T., Matsueda, H., Sawa, Y., Nakagawa, Y., Hirofumi, K., Kondo, N., Goto, K., Nakazawa, T., Ishikawa, K., and Ogawa, T.: Worldwide measurements of atmospheric CO_2 and other trace gas species using commercial airlines, *Journal Atmospheric and Oceanic Technology*, 25, 1744-1754, doi:10.1175/2008JTECHA1082.1, 2008.
- Matthews, E., and Fung, I.: Methane emission from natural wetlands: Global distribution, area, and environmental characteristics of sources, *Global Biogeochemical Cycles*, 1, 61-86, doi:10.1029/GB001i001p00061, 1987.
- 10 McCalley, C. K., Woodcroft, B. J., Hodgkins, S. B., Wehr, R. A., Kim, E.-H., Mondav, R., Crill, P. M., Chanton, J. P., Rich, V. I., Tyson, G. W., and Saleska, S. R.: Methane dynamics regulated by microbial community response to permafrost thaw, *Nature*, 514, 478-481, doi:10.1038/nature13798, 2014.
- McGinnis, D. F., Kirillin, G., Tang, K. W., Flury, S., Bodmer, P., Engelhardt, C., Casper, P., and Grossart, H.-P.: Enhancing Surface Methane Fluxes from an Oligotrophic Lake: Exploring the Microbubble Hypothesis, *Environmental Science and Technology*, 49, 873-880, doi:10.1021/es503385d, 2015.
- 15 McKain, K., Down, A., Raciti, S. M., Budney, J., Hutyra, L. R., Floerchinger, C., Herndon, S. C., Nehrkorn, T., Zahniser, M. S., Jackson, R. B., Phillips, N., and Wofsy, S. C.: Methane emissions from natural gas infrastructure and use in the urban region of Boston, Massachusetts, *Proceedings of the National Academy of Sciences*, 112, 1941-1946, doi:10.1073/pnas.1416261112, 2015.
- McManus, J. B., Nelson, D. D., and Zahniser, M. S.: Long-term continuous sampling of $^{12}\text{CO}_2$, $^{13}\text{CO}_2$ and $^{12}\text{C}^{18}\text{O}^{16}\text{O}$ in ambient air with a quantum cascade laser spectrometer, *Isotopes in Environmental and Health Studies*, 46, 49-63, doi:10.1080/10256011003661326, 2010.
- McNorton, J., Chipperfield, M. P., Gloor, M., Wilson, C., Feng, W., Hayman, G. D., Rigby, M., Krummel, P. B., O'Doherty, S., Prinn, R. G., Weiss, R. F., Young, D., Dlugokencky, E., and Montzka, S. A.: Role of OH variability in the stalling of the global atmospheric CH_4 growth rate from 1999 to 2006, *Atmospheric Chemistry and Physics Discussion*, 2016, 1-24, doi:10.5194/acp-2015-1029, 2016.
- 25 Meirink, J. F., Bergamaschi, P., Frankenberg, C., d'Amelio, M. T. S., Dlugokencky, E. J., Gatti, L. V., Houweling, S., Miller, J. B., Rockmann, T., Villani, M. G., and Krol, M. C.: Four-dimensional variational data assimilation for inverse modeling of atmospheric methane emissions: Analysis of SCIAMACHY observations, *Journal of Geophysical Research-Atmospheres*, 113, D17, 2008a.
- 30 Meirink, J. F., Bergamaschi, P., and Krol, M. C.: Four-dimensional variational data assimilation for inverse modelling of atmospheric methane emissions: method and comparison with synthesis inversion, *Atmospheric Chemistry and Physics*, 8, 6341-6353, 2008b.
- Melton, J. R., Schaefer, H., and Whiticar, M. J.: Enrichment in ^{13}C of atmospheric CH_4 during the Younger Dryas termination, *Climate of the Past*, 8, 1177-1197, doi:10.5194/cp-8-1177-2012, 2012.
- 35 Melton, J. R., Wania, R., Hodson, E. L., Poulter, B., Ringeval, B., Spahni, R., Bohn, T., Avis, C. A., Beerling, D. J., Chen, G., Eliseev, A. V., Denisov, S. N., Hopcroft, P. O., Lettenmaier, D. P., Riley, W. J., Singarayer, J. S., Subin, Z. M., Tian, H., Zürcher, S., Brovkin, V., van Bodegom, P. M., Kleinen, T., Yu, Z. C., and Kaplan, J. O.: Present state of global wetland extent and wetland methane modelling: conclusions from a model intercomparison project (WETCHIMP), *Biogeosciences*, 10, 753-788, doi:10.5194/bg-10-753-2013, 2013.
- 40 Melton, J. R., and Arora, V. K.: Competition between plant functional types in the Canadian Terrestrial Ecosystem Model (CTEM) v. 2.0, *Geoscientific Model Development*, 9, 323-361, doi:10.5194/gmd-9-323-2016, 2016.
- Mijling, B., van der A, R. J., and Zhang, Q.: Regional nitrogen oxides emission trends in East Asia observed from space, *Atmospheric Chemistry and Physics*, 13, 12003-12012, doi:10.5194/acp-13-12003-2013, 2013.
- 45 Mikaloff Fletcher, S. E. M., Tans, P. P., Bruhwiler, L. M., Miller, J. B., and Heimann, M.: CH_4 sources estimated from atmospheric observations of CH_4 and its $^{13}\text{C}/^{12}\text{C}$ isotopic ratios: 1. Inverse modeling of source processes, *Global Biogeochemical Cycles*, 18, GB4004, doi:10.1029/2004GB002223, 2004.
- Milkov, A. V.: Molecular and stable isotope compositions of natural gas hydrates: A revised global dataset and basic interpretations in the context of geological settings, *Organic Geochemistry*, 36, 681-702, 2005.
- 50 Miller, J. B., Mack, K. A., Dissly, R., White, J. W. C., Dlugokencky, E. J., and Tans, P. P.: Development of analytical methods and measurements of $^{13}\text{C}/^{12}\text{C}$ in atmospheric CH_4 from the NOAA Climate Monitoring and Diagnostics



- Laboratory Global Air Sampling Network, *Journal of Geophysical Research: Atmospheres*, 107, D13, doi:10.1029/2001jd000630, 2002.
- Miller, L. G., Sasson, C., and Oremland, R. S.: Difluoromethane, a new and improved inhibitor of methanotrophy, *Applied and Environmental Microbiology*, 64, 4357–4362, 1998.
- 5 Miller, S. M., Wofsy, S. C., Michalak, A. M., Kort, E. A., Andrews, A. E., Biraud, S. C., Dlugokencky, E. J., Eluszkiewicz, J., Fischer, M. L., Janssens-Maenhout, G., Miller, B. R., Miller, J. B., Montzka, S. A., Nehrkorn, T., and Sweeney, C.: Anthropogenic emissions of methane in the United States, *Proceedings of the National Academy of Sciences of the United States of America*, 110, 20,018-020,022, doi:10.1073/pnas.1314392110, 2013.
- Monteil, G., Houweling, S., Dlugokencky, E. J., Maenhout, G., Vaughn, B. H., White, J. W. C., and Rockmann, T.: 10 Interpreting methane variations in the past two decades using measurements of CH₄ mixing ratio and isotopic composition, *Atmospheric Chemistry and Physics*, 11, 9141-9153, doi:10.5194/acp-11-9141-2011, 2011.
- Monteil, G., Houweling, S., Butz, A., Guerlet, S., Schepers, D., Hasekamp, O., Frankenberg, C., Scheepmaker, R., Aben, I., and Röckmann, T.: Comparison of CH₄ inversions based on 15 months of GOSAT and SCIAMACHY observations, *J Geophys Res-Atmos*, 118, 11,807-811,823, doi:10.1002/2013jd019760, 2013.
- 15 Montzka, S. A., and Fraser, P. J.: *Controlled Substances and Other Source Gases*, Geneva, Switzerland, 1.1-1.83, World Meteorological Organization, 2003.
- Montzka, S. A., Dlugokencky, E. J., and Butler, J. H.: Non-CO₂ greenhouse gases and climate change, *Nature*, 476, 43-50, 2011a.
- Montzka, S. A., Krol, M., Dlugokencky, E., Hall, B., Jockel, P., and Lelieveld, J.: Small Interannual Variability of Global 20 Atmospheric Hydroxyl, *Science*, 331, 67-69, 2011b.
- Moore, C. W., Zielinska, B., Pétron, G., and Jackson, R. B.: Air impacts of increased natural gas acquisition, processing, and use: a critical review, *Environmental Science and Technology* 48, 8349–8359, doi:10.1021/es4053472, 2014.
- Morimoto, S., Aoki, S., Nakazawa, T., and Yamanouchi, T.: Temporal variations of the carbon isotopic ratio of atmospheric methane observed at Ny Ålesund, Svalbard from 1996 to 2004, *Geophysical Research Letters*, 33, doi:10.1029/2005gl024648, 2006.
- 25 Mukhin, V. A., and Voronin, P. Y.: Methane emission from living tree wood, *Russian Journal of Plant Physiology*, 58, 344-350, doi:10.1134/S1021443711020117, 2011.
- Myhre, G., Shindell, D., Bréon, F.-M., Collins, W., Fuglestedt, J., Huang, J., Koch, D., Lamarque, J.-F., Lee, D., Mendoza, B., Nakajima, T., Robock, A., Stephens, G., Takemura, T., and Zhang, H.: Anthropogenic and Natural Radiative Forcing., in: *Climate Change 2013: The Physical Science Basis. Contribution of Working Group I to the Fifth Assessment Report of the Intergovernmental Panel on Climate Change.*, edited by: Stocker, T. F., Qin, D., Plattner, G.-K., Tignor, M., Allen, S. K., Boschung, J., Nauels, A., Xia, Y., Bex, V., and Midgley, P. M., Cambridge University Press, Cambridge, United Kingdom and New York, NY, USA, 2013.
- 30 Naik, V., Voulgarakis, A., Fiore, A. M., Horowitz, L. W., Lamarque, J. F., Lin, M., Prather, M. J., Young, P. J., Bergmann, D., Cameron-Smith, P. J., Cionni, I., Collins, W. J., Dalsøren, S. B., Doherty, R., Eyring, V., Faluvegi, G., Folberth, G. A., Josse, B., Lee, Y. H., MacKenzie, I. A., Nagashima, T., van Noije, T. P. C., Plummer, D. A., Righi, M., Rumbold, S. T., Skeie, R., Shindell, D. T., Stevenson, D. S., Strode, S., Sudo, K., Szopa, S., and Zeng, G.: Preindustrial to present day changes in tropospheric hydroxyl radical and methane lifetime from the Atmospheric Chemistry and Climate Model Intercomparison Project (ACCMIP), *Atmospheric Chemistry and Physics*, 13, 5277-5298, doi:10.5194/acp-13-5277-2013, 40 2013.
- Natchimuthu, S., Sundgren, I., Gålfalk, M., Klemetsson, L., Crill, P., Danielsson, Å., and Bastviken, D.: Spatio-temporal variability of lake CH₄ fluxes and its influence on annual whole lake emission estimates, *Limnology and Oceanography*, doi:10.1002/lno.10222, 2015.
- Neef, L., van Weele, M., and van Velthoven, P.: Optimal estimation of the present-day global methane budget, *Global Biogeochemical Cycles*, 24, doi:10.1029/2009GB003661, 2010.
- 45 Nisbet, E. G., Dlugokencky, E. J., and Bousquet, P.: Methane on the Rise-Again, *Science*, 343, 493-495, doi:10.1126/science.1247828, 2014.
- Nisbet, R. E. R., Fisher, R., Nimmo, R. H., Bendall, D. S., Crill, P. M., Gallego-Sala, A. V., Hornibrook, E. R. C., Lopez-Juez, E., Lowry, D., Nisbet, P. B. R., Shuckburgh, E. F., Sriskantharajah, S., Howe, C. J., and Nisbet, E. G.: Emission of 50 methane from plants, *Proceedings of the Royal Society B-Biological Sciences*, 276, 1347-1354, 2009.



- Olivier, J. G. J., G. Janssens-Maenhout, G., and Peters, J. A. H. W.: Trends in global CO₂ emissions – 2012 Report. Joint Research Centre of the European Commission and the Netherlands Environmental Assessment Agency (PBL), Netherlands, 2012.
- Olivier, J. G. J., and Janssens-Maenhout, G.: CO₂ Emissions from Fuel Combustion - 2012 Edition, IEA CO₂ report 2012, Part III, Greenhouse Gas Emissions, ISBN 978-92-64-17475-7, 2012.
- Olivier, J. G. J., and Janssens-Maenhout, G.: Part III: Total Greenhouse Gas Emissions, of CO₂ Emissions from Fuel Combustion (2014 ed.), International Energy Agency, Paris, ISBN-978-92-64-21709-6, 2014.
- Overduin, P. P., Liebner, S., Knoblauch, C., Günther, F., Wetterich, S., Schirrmeister, L., Hubberten, H.-W., and Grigoriev, M. N.: Methane oxidation following submarine permafrost degradation: Measurements from a central Laptev Sea shelf borehole, *Journal of Geophysical Research - Biogeosciences*, 120, 965-978, doi:10.1002/2014jg002862, 2015.
- Pandey, S., Houweling, S., Krol, M., Aben, I., and Röckmann, T.: On the use of satellite-derived CH₄: CO₂ columns in a joint inversion of CH₄ and CO₂ fluxes, *Atmospheric Chemistry and Physics*, 15, 8615-8629, doi:10.5194/acp-15-8615-2015, 2015.
- Pandey, S., Houweling, S., Krol, M., Aben, I., Chevallier, F., Dlugokencky, E. J., Gatti, L. V., Gloor, M., Miller, J. B., Detmers, R., Machida, T., and Röckmann, T.: Inverse modeling of GOSAT-retrieved ratios of total column CH₄ and CO₂ for 2009 and 2010, *Atmospheric Chemistry and Physics Discussions*, 2016, 1-32, doi:10.5194/acp-2016-77, 2016.
- Pangala, S. R., Moore, S., Hornibrook, E. R. C., and Gauci, V.: Trees are major conduits for methane egress from tropical forested wetlands, *New Phytologist*, 197, 524-531, doi:10.1111/nph.12031, 2013.
- Pangala, S. R., Hornibrook, E. R. C., Gowing, D. J., and Gauci, V.: The contribution of trees to ecosystem methane emissions in a temperate forested wetland, *Global Change Biology*, 21, 2642-2654, doi:10.1111/gcb.12891, 2015.
- Papa, F., Prigent, C., Aires, F., Jimenez, C., Rossow, W. B., and Matthews, E.: Interannual variability of surface water extent at the global scale, 1993-2004, *Journal of Geophysical Research*, 115, D12111, doi:10.1029/2009jd012674, 2010.
- Paris, J.-D., Ciais, P., Nedelec, P., Stohl, A., Belan, B. D., Arshinov, M. Y., Carouge, C., Golitsyn, G. S., and Granberg, I. G.: New insights on the chemical composition of the Siberian air shed from the YAK AEROSIB aircraft campaigns, *Bulletin of the American Meteorological Society*, 91, 625-641, doi:10.1175/2009BAMS2663.1., 2010.
- Parker, R., Boesch, H., Cogan, A., Fraser, A., Feng, L., Palmer, P. I., Messerschmidt, J., Deutscher, N., Griffith, D. W. T., Notholt, J., Wennberg, P. O., and Wunch, D.: Methane observations from the Greenhouse Gases Observing SATellite: Comparison to ground-based TCCON data and model calculations, *Geophysical Research Letters*, 38, L15807, doi:10.1029/2011gl047871, 2011.
- Pathak, H., Li, C., and Wassmann, R.: Greenhouse gas emissions from Indian rice fields: calibration and upscaling using the DNDC model, *Biogeosciences*, 1, 1-11, 2005.
- Patra, P. K., Houweling, S., Krol, M., Bousquet, P., Belikov, D., Bergmann, D., Bian, H., Cameron-Smith, P., Chipperfield, M. P., Corbin, K., Fortems-Cheiney, A., Fraser, A., Gloor, E., Hess, P., Ito, A., Kawa, S. R., Law, R. M., Loh, Z., Maksyutov, S., Meng, L., Palmer, P. I., Prinn, R. G., Rigby, M., Saito, R., and Wilson, C.: TransCom model simulations of CH₄ and related species: linking transport, surface flux and chemical loss with CH₄ variability in the troposphere and lower stratosphere, *Atmospheric Chemistry and Physics*, 11, 12813-812,837, doi:10.5194/acp-11-12813-2011, 2011.
- Patra, P. K., Canadell, J. G., Houghton, R. A., Piao, S. L., Oh, N. H., Ciais, P., Manjunath, K. R., Chhabra, A., Wang, T., Bhattacharya, T., Bousquet, P., Hartman, J., Ito, A., Mayorga, E., Niwa, Y., Raymond, P. A., Sarma, V. V. S. S., and Lasco, R.: The carbon budget of South Asia, *Biogeosciences*, 10, 513-527, doi:10.5194/bg-10-513-2013, 2013.
- Patra, P. K., Saeki, T., Dlugokencky, E. J., Ishijima, K., Umezawa, T., Ito, A., Aoki, S., Morimoto, S., Kort, E. A., Crotwell, A., Ravikumar, K., and Nakazawa, T.: Regional methane emission estimation based on observed atmospheric concentrations (2002-2012). *Journal of Meteorological Society of Japan*, 94, 85-107, doi:10.2151/jmsj.2016-006, 2016.
- Paull, C. K., Brewer, P. G., Ussler, W., Peltzer, E. T., Rehder, G., and Clague, D.: An experiment demonstrating that marine slumping is a mechanism to transfer methane from seafloor gas-hydrate deposits into the upper ocean and atmosphere, *Geo-Marine Letters*, 22, 198-203, doi:10.1007/s00367-002-0113-y, 2002.
- Peischl, J., Ryerson, T. B., Aikin, K. C., de Gouw, J. A., Gilman, J. B., Holloway, J. S., Lerner, B. M., Nadkarni, R., Neuman, J. A., Nowak, J. B., Trainer, M., Warneke, C., and Parrish, D. D.: Quantifying atmospheric methane emissions from the Haynesville, Fayetteville, and northeastern Marcellus shale gas production regions, *Journal of Geophysical Research: Atmospheres*, 120, 2119-2139, doi:10.1002/2014jd022697, 2015.



- Peng, S. S., Piao, S. L., Bousquet, P., Ciais, P., Li, B. G., Lin, X., Tao, S., Wang, Z. P., Zhang, Y., and Zhou, F.: Inventory of anthropogenic methane emissions in Mainland China from 1980 to 2010, *Atmospheric Chemistry and Physics Discussions*, 2016, 1-29, doi:10.5194/acp-2016-139, 2016.
- 5 Peregon, A., Maksyutov, S., Kosykh, N. P., and Mironycheva-Tokareva, N. P.: Map-based inventory of wetland biomass and net primary production in western Siberia, *Journal of Geophysical Research - Biogeosciences*, 113, G1, doi:10.1029/2007jg000441, 2008.
- Peters, W., Jacobson, A. R., Sweeney, C., Andrews, A. E., Conway, T. J., Masarie, K., Miller, J. B., Bruhwiler, L. M. P., Pétron, G., Hirsch, A. I., Worthy, D. E. J., van der Werf, G. R., Randerson, J. T., Wennberg, P. O., Krol, M. C., and Tans, P. P.: An atmospheric perspective on North American carbon dioxide exchange: CarbonTracker, *Proceedings of the National Academy of Sciences of the United States of America*, 104, 18925-18930, doi:10.1073/pnas.0708986104 2007.
- 10 Pétron, G., Karion, A., Sweeney, C., Miller, B. R., Montzka, S. A., Frost, G. J., Trainer, M., Tans, P., Andrews, A., Kofler, J., Helmig, D., Guenther, D., Dlugokencky, E., Lang, P., Newberger, T., Wolter, S., Hall, B., Novelli, P., Brewer, A., Conley, S., Hardesty, M., Banta, R., White, A., Noone, D., Wolfe, D., and Schnell, R.: A new look at methane and nonmethane hydrocarbon emissions from oil and natural gas operations in the Colorado Denver-Julesburg Basin, *Journal of Geophysical Research: Atmospheres*, 119, 6836-6852, doi:10.1002/2013jd021272, 2014.
- 15 Pison, I., Ringeval, B., Bousquet, P., Prigent, C., and Papa, F.: Stable atmospheric methane in the 2000s: key-role of emissions from natural wetlands, *Atmospheric Chemistry and Physics Discussions*, 13, 9017-9049, doi:10.5194/acpd-13-9017-2013, 2013.
- Portmann, R. W., Daniel, J. S., and Ravishankara, A. R.: Stratospheric ozone depletion due to nitrous oxide: influences of other gases, *Philosophical Transactions of the Royal Society of London B: Biological Sciences*, 367, 1256-1264, doi:10.1098/rstb.2011.0377, 2012.
- Poulter, B., Bousquet, P., Canadell, J., Ciais, P., Peregon, A., Saunois, M., Arora, V., Beerling, D., Brovkin, V., Jones, C., Joos, F., Gedney, N., Ito, A., Kleinen, T., Koven, C., MacDonald, K., Melton, J., Peng, C., Peng, S., Schroder, R., Prigent, C., Riley, B., Saito, M., Spahni, R., Tian, H., Taylor, L., Viovy, N., Wilton, D., Wiltshire, A., Xu, X., and Zhang, Z.: 25 Global wetland contribution to increasing atmospheric methane concentrations (2000-2012), *Nature Communications*, 2016, submitted.
- Prather, M. J., Holmes, C. D., and Hsu, J.: Reactive greenhouse gas scenarios: Systematic exploration of uncertainties and the role of atmospheric chemistry, *Geophysical Research Letters*, 39, L09803, doi:10.1029/2012gl051440, 2012.
- 30 Prigent, C., Papa, F., Aires, F., Rossow, W. B., and Matthews, E.: Global inundation dynamics inferred from multiple satellite observations, 1993-2000, *Journal of Geophysical Research-Atmospheres*, 112, D12107, doi:10.1029/2006JD007847, 2007.
- Prinn, R. G., Weiss, R. F., Fraser, P. J., Simmonds, P. G., Cunnold, D. M., Aleya, F. N., O'Doherty, S., Salameh, P., Miller, B. R., Huang, J., Wang, R. H. J., Hartley, D. E., Harth, C., Steele, L. P., Sturrock, G., Midgley, P. M., and McCulloch, A.: A history of chemically and radiatively important gases in air deduced from ALE/GAGE/AGAGE, *Journal of Geophysical Research-Atmospheres*, 105, 17,751-717,792, 2000.
- 35 Prinn, R. G., Huang, J., Weiss, R. F., Cunnold, D. M., Fraser, P. J., Simmonds, P. G., McCulloch, A., Harth, C., Salameh, P., O'Doherty, S., Wang, R. H. J., Porter, L., and Miller, B. R.: Evidence for Substantial Variations of Atmospheric Hydroxyl Radicals in the Past Two Decades, *Science*, doi:10.1126/science.1058673, 2001.
- 40 Prinn, R. G., Huang, J., Weiss, R. F., Cunnold, D. M., Fraser, P. J., Simmonds, P. G., McCulloch, A., Harth, C., Reimann, S., Salameh, P., O'Doherty, S., Wang, R. H. J., Porter, L. W., Miller, B. R., and Krummel, P. B.: Evidence for variability of atmospheric hydroxyl radicals over the past quarter century, *Geophysical Research Letters*, 32, L07809, doi:07810.101029/02004GL022228, 2005.
- Quay, P., Stutsman, J., Wilbur, D., Snover, A., Dlugokencky, E., and Brown, T.: The isotopic composition of atmospheric methane, *Global Biogeochemical Cycles*, 13, 445-461, 1999.
- 45 Quay, P. D., King, S. L., Stutsman, J., Wilbur, D. O., Steele, L. P., Fung, I., Gammon, R. H., Brown, T. A., Farwell, G. W., Grootes, P. M., and Schmidt, F. H.: Carbon isotopic composition of atmospheric CH₄: fossil and biomass burning source strengths, *Global Biogeochemical Cycles*, 5, 25-47, 1991.
- Randerson, J. T., Chen, Y., van der Werf, G. R., Rogers, B. M., and Morton, D. C.: Global burned area and biomass burning emissions from small fires, *Journal of Geophysical Research: Biogeosciences*, 117, G4, doi:10.1029/2012jg002128, 2012.



- Reeburgh, W. S., and Heggie, D. T.: Microbial methane consumption reactions and their effect on methane distributions in freshwater and marine environments, *Limnology and Oceanography*, 22, 1-9, doi:10.4319/lo.1977.22.1.0001, 1977.
- Reeburgh, W. S.: Oceanic Methane Biogeochemistry, *Chemical Reviews*, 107, 486-513, doi:10.1021/cr050362v, 2007.
- Ren, W. E. I., Tian, H., Xu, X., Liu, M., Lu, C., Chen, G., Melillo, J., Reilly, J., and Liu, J.: Spatial and temporal patterns of CO₂ and CH₄ fluxes in China's croplands in response to multifactor environmental changes, *Tellus B*, 63, 222-240, doi:10.1111/j.1600-0889.2010.00522.x, 2011.
- Rhee, T. S., Kettle, A. J., and Andreae, M. O.: Methane and nitrous oxide emissions from the ocean: A reassessment using basin-wide observations in the Atlantic, *Journal of Geophysical Research-Atmospheres*, 114, D12304, doi:10.1029/2008jd011662, 2009.
- Rice, A. L., Gotoh, A. A., Ajie, H. O., and Tyler, S. C.: High-Precision Continuous-Flow Measurement of δ¹³C and δD of Atmospheric CH₄, *Analytical Chemistry*, 73, 4104-4110, doi:10.1021/ac0155106, 2001.
- Rice, A. L., Butenhoff, C. L., Shearer, M. J., Teama, D., Rosenstiel, T. N., and Khalil, M. A. K.: Emissions of anaerobically produced methane by trees, *Geophysical Research Letters*, 37, L03807, doi:10.1029/2009GL041565, 2010.
- Ridgwell, A. J., Marshall, S. J., and Gregson, K.: Consumption of atmospheric methane by soils: A process-based model, *Global Biogeochemical Cycles*, 13, 59-70, doi:10.1029/1998gb900004, 1999.
- Riedel, T. P., Wolfe, G. M., Danas, K. T., Gilman, J. B., Kuster, W. C., Bon, D. M., Vlasenko, A., Li, S. M., Williams, E. J., Lerner, B. M., Veres, P. R., Roberts, J. M., Holloway, J. S., Lefter, B., Brown, S. S., and Thornton, J. A.: An MCM modeling study of nitryl chloride (ClNO₂) impacts on oxidation, ozone production and nitrogen oxide partitioning in polluted continental outflow, *Atmospheric Chemistry and Physics*, 14, 3789-3800, doi:10.5194/acp-14-3789-2014, 2014.
- Rigby, M., Prinn, R. G., Fraser, P. J., Simmonds, P. G., Langenfelds, R. L., Huang, J., Cunnold, D. M., Steele, L. P., Krummel, P. B., Weiss, R. F., O'Doherty, S., Salameh, P. K., Wang, H. J., Harth, C. M., Mühle, J., and Porter, L. W.: Renewed growth of atmospheric methane, *Geophysical Research Letters*, 35, L22805, doi:10.1029/2008gl036037, 2008.
- Rigby, M., Manning, A. J., and Prinn, R. G.: The value of high-frequency, high-precision methane isotopologue measurements for source and sink estimation, *Journal of Geophysical Research-Atmospheres*, 117, doi:10.1029/2011jd017384, 2012.
- Riley, W. J., Subin, Z. M., Lawrence, D. M., Swenson, S. C., Torn, M. S., Meng, L., Mahowald, N. M., and Hess, P.: Barriers to predicting changes in global terrestrial methane fluxes: analyses using CLM4Me, a methane biogeochemistry model integrated in CESM, *Biogeosciences*, 8, 1925-1953, doi:10.5194/bg-8-1925-2011, 2011.
- Ringeval, B., Friedlingstein, P., Koven, C., Ciais, P., de Noblet-Ducoudre, N., Decharme, B., and Cadule, P.: Climate-CH₄ feedback from wetlands and its interaction with the climate-CO₂ feedback, *Biogeosciences*, 8, 2137-2157, doi:10.5194/bg-8-2137-2011, 2011.
- Ringeval, B., Houweling, S., van Bodegom, P. M., Spahni, R., van Beek, R., Joos, F., and Röckmann, T.: Methane emissions from floodplains in the Amazon Basin: challenges in developing a process-based model for global applications, *Biogeosciences*, 11, 1519-1558, doi:10.5194/bg-11-1519-2014, 2014.
- Röckmann, T., Brass, M., Borchers, R., and Engel, A.: The isotopic composition of methane in the stratosphere: high-altitude balloon sample measurements, *Atmospheric Chemistry and Physics*, 11, 13,287-213,304, doi:10.5194/acp-11-13287-2011, 2011.
- Rodgers, C. D.: Inverse methods for atmospheric sounding: theory and practice, *Atmospheric, Oceanic and Planetary Physics*, edited by: World-Scientific, Singapore, London, 240 pp., 2000.
- Rogelj, J., McCollum, D., and Smith, S.: The Emissions Gap Report 2014 - a UNEP synthesis report: Chapter 2. U.N. Environment Programme, Nairobi, Internet: <http://www.unep.org/publications/ebooks/emissionsgapreport2014/>. ISBN: 978-92-807-3413-3., 2014.
- RTI: Updated Research on Methane Oxidation in Landfills, Memorandum to R. Schmeltz (EPA), January 14, 2011, 2011.
- Saad, K. M., Wunch, D., Toon, G. C., Bernath, P., Boone, C., Connor, B., Deutscher, N. M., Griffith, D. W. T., Kivi, R., Notholt, J., Roehl, C., Schneider, M., Sherlock, V., and Wennberg, P. O.: Derivation of tropospheric methane from TCCON CH₄ and HF total column observations, *Atmospheric Measurement Technologies*, 7, 2907-2918, doi:10.5194/amt-7-2907-2014, 2014.
- Saeki, T., Maksyutov, S., Saito, M., Valsala, V., Oda, T., Andres, R. J., Belikov, D., Tans, P., Dlugokencky, E., Yoshida, Y., Morino, I., Uchino, O., and Yokota, T.: Inverse modeling of CO₂ fluxes using GOSAT data and multi-year ground-based observations, *SOLA*, 9, 45-50, 2013.



- Sanderson, M. G.: Biomass of termites and their emissions of methane and carbon dioxide: A global database, *Global Biogeochemical Cycles*, 10, 543-557, doi:10.1029/96gb01893, 1996.
- Santini, M., and Di Paola, A.: Changes in the world rivers' discharge projected from an updated high resolution dataset of current and future climate zones, *Journal of Hydrology*, 531, 768-780, 2015.
- 5 Santoni, G. W., Lee, B. H., Goodrich, J. P., Varner, R. K., Crill, P. M., McManus, J. B., Nelson, D. D., Zahniser, M. S., and Wofsy, S. C.: Mass fluxes and isofluxes of methane (CH₄) at a New Hampshire fen measured by a continuous wave quantum cascade laser spectrometer, *Journal of Geophysical Research: Atmospheres*, 117, D10, doi:10.1029/2011jd016960, 2012.
- Sasakawa, M., Tsunogai, U., Kameyama, S., Nakagawa, F., Nojiri, Y., and Tsuda, A.: Carbon isotopic characterization for the origin of excess methane in subsurface seawater, *Journal of Geophysical Research: Oceans*, 113, C3, doi:10.1029/2007jc004217, 2008.
- 10 Sasakawa, M., Shimoyama, K., Machida, T., Tsuda, N., Suto, H., Arshinov, M., Davydov, D., Fofonov, A., Krasnov, O., Saeki, T., Koyama, Y., and Maksyutov, S.: Continuous measurements of methane from a tower network over Siberia, *Tellus B*, 62, 403-416, doi:10.1111/j.1600-0889.2010.00494.x, 2010.
- 15 Sawakuchi, H. O., Bastviken, D., Sawakuchi, A. O., Krusche, A. V., Ballester, M. V. R., and Richey, J. E.: Methane emissions from Amazonian Rivers and their contribution to the global methane budget, *Global Change Biology*, 20, 2829-2840, doi:10.1111/gcb.12646, 2014.
- Schaefer, H., Fletcher, S. E. M., Veidt, C., Lassey, K. R., Brailsford, G. W., Bromley, T. M., Dlugokencky, E. J., Michel, S. E., Miller, J. B., Levin, I., Lowe, D. C., Martin, R. J., Vaughn, B. H., and White, J. W. C.: A 21st century shift from fossil-fuel to biogenic methane emissions indicated by ¹³CH₄, *Science*, doi:10.1126/science.aad2705, 2016.
- 20 Schepers, D., Guerlet, S., Butz, A., Landgraf, J., Frankenberg, C., Hasekamp, O., Blavier, J. F., Deutscher, N. M., Griffith, D. W. T., Hase, F., Kyro, E., Morino, I., Sherlock, V., Sussmann, R., and Aben, I.: Methane retrievals from Greenhouse Gases Observing Satellite (GOSAT) shortwave infrared measurements: Performance comparison of proxy and physics retrieval algorithms, *Journal of Geophysical Research: Atmospheres*, 117, D10, doi:10.1029/2012jd017549, 2012.
- 25 Schneising, O., Burrows, J. P., Dickerson, R. R., Buchwitz, M., Reuter, M., and Bovensmann, H.: Remote sensing of fugitive methane emissions from oil and gas production in North American tight geologic formations, *Earth's Future*, 2, 548-558, doi:10.1002/2014EF000265, 2014.
- Schroeder, R., McDonald, K. C., Chapman, B., Jensen, K., Podest, E., Tessler, Z., Bohn, T. J., and Zimmerman, R.: Development and evaluation of a multi-year inundated land surface data set derived from active/passive microwave remote sensing data, *Remote Sensing*, 7, 16,668-616,732, doi:10.3390/rs71215843, 2015.
- 30 Schuck, T. J., Ishijima, K., Patra, P. K., Baker, A. K., Machida, T., Matsueda, H., Sawa, Y., Umezawa, T., Brenninkmeijer, C. A. M., and Lelieveld, J.: Distribution of methane in the tropical upper troposphere measured by CARIBIC and CONTRAIL aircraft, *Journal of Geophysical Research: Atmospheres*, 117, D19304, doi:10.1029/2012jd018199, 2012.
- Schuur, E. A. G., McGuire, A. D., Schadel, C., Grosse, G., Harden, J. W., Hayes, D. J., Hugelius, G., Koven, C. D., Kuhry, P., Lawrence, D. M., Natali, S. M., Olefeldt, D., Romanovsky, V. E., Schaefer, K., Turetsky, M. R., Treat, C. C., and Vonk, J. E.: Climate change and the permafrost carbon feedback, *Nature*, 520, 171-179, doi:10.1038/nature14338, 2015.
- 35 Shakhova, N., Semiletov, I., Salyuk, A., Yusupov, V., Kosmach, D., and Gustafsson, Ö.: Extensive Methane Venting to the Atmosphere from Sediments of the East Siberian Arctic Shelf, *Science*, 327, 1246-1250, doi:10.1126/science.1182221, 2010.
- 40 Shakhova, N., Semiletov, I., Leifer, I., Sergienko, V., Salyuk, A., Kosmach, D., Chernykh, D., Stubbs, C., Nicolsky, D., Tumskey, V., and Gustafsson, O.: Ebullition and storm-induced methane release from the East Siberian Arctic Shelf, *Nature Geoscience*, 7, 64-70, doi:10.1038/ngeo2007, 2014.
- Shakhova, N., Semiletov, I., Sergienko, V., Lobkovsky, L., Yusupov, V., Salyuk, A., Salomatov, A., Chernykh, D., Kosmach, D., Panteleev, G., Nicolsky, D., Samarkin, V., Joye, S., Charkin, A., Dudarev, O., Meluzov, A., and Gustafsson, O.: The East Siberian Arctic Shelf: towards further assessment of permafrost-related methane fluxes and role of sea ice, *Philosophical Transactions of the Royal Society of London A: Mathematical, Physical and Engineering Sciences*, 373, doi:10.1098/rsta.2014.0451, 2015.
- 45 Sheng, Y., Smith, L. C., MacDonald, G. M., Kremenetski, K. V., Frey, K. E., Velichko, A. A., Lee, M., Beilman, D. W., and Dubinin, P.: A high-resolution GIS-based inventory of the west Siberian peat carbon pool, *Global Biogeochemical Cycles*, 18, doi:10.1029/2003gb002190, 2004.
- 50



- Shindell, D., Kuylenstierna, J. C. I., Vignati, E., van Dingenen, R., Amann, M., Klimont, Z., Anenberg, S. C., Muller, N., Janssens-Maenhout, G., Raes, F., Schwartz, J., Faluvegi, G., Pozzoli, L., Kupiainen, K., Höglund-Isaksson, L., Emberson, L., Streets, D., Ramanathan, V., Hicks, K., Oanh, N. T. K., Milly, G., Williams, M., Demkine, V., and Fowler, D.: Simultaneously Mitigating Near-Term Climate Change and Improving Human Health and Food Security, *Science*, 335, 183-189, doi:10.1126/science.1210026, 2012.
- 5 Shorter, J. H., Mcmanus, J. B., Kolb, C. E., Allwine, E. J., Lamb, B. K., Mosher, B. W., Harriss, R. C., Partchatka, U., Fischer, H., Harris, G. W., Crutzen, P. J., and Karbach, H.-J.: Methane emission measurements in urban areas in Eastern Germany, *Journal of Atmospheric Chemistry*, 124, 121-140, 1996.
- Simpson, I. J., Thurtell, G. W., Kidd, G. E., Lin, M., Demetriades-Shah, T. H., Flitcroft, I. D., Kanemasu, E. T., Nie, D., Bronson, K. F., and Neue, H. U.: Tunable diode laser measurements of methane fluxes from an irrigated rice paddy field in the Philippines, *Journal of Geophysical Research: Atmospheres*, 100, 7283-7290, doi:10.1029/94jd03326, 1995.
- 10 Simpson, I. J., Rowland, F. S., Meinardi, S., and Blake, D. R.: Influence of biomass burning during recent fluctuations in the slow growth of global tropospheric methane, *Geophysical Research Letters*, 33, 2006.
- Simpson, I. J., Sulbaek Andersen, M. P., Meinardi, S., Bruhwiler, L., Blake, N. J., Helmig, D., Rowland, F. S., and Blake, D. R.: Long-term decline of global atmospheric ethane concentrations and implications for methane, *Nature*, 488, 490-494, doi:10.1038/nature11342, 2012.
- 15 Singarayer, J. S., Valdes, P. J., Friedlingstein, P., Nelson, S., and Beerling, D. J.: Late Holocene methane rise caused by orbitally controlled increase in tropical sources, *Nature*, 470, 82-85, 2011.
- Slater, A. G., and Lawrence, D. M.: Diagnosing Present and Future Permafrost from Climate Models, *Journal of Climate*, 26, 5608-5623, doi:10.1175/JCLI-D-12-00341.1, 2013.
- 20 Smith, L. K., and Lewis, W. M.: Seasonality of methane emissions from five lakes and associated wetlands of the Colorado Rockies, *Global Biogeochem Cycles*, 6, 323-338, 1992.
- Spahni, R., Wania, R., Neef, L., van Weele, M., Pison, I., Bousquet, P., Frankenberg, C., Foster, P. N., Joos, F., Prentice, I. C., and van Velthoven, P.: Constraining global methane emissions and uptake by ecosystems, *Biogeosciences*, 8, 1643-1665, doi:10.5194/bg-8-1643-2011, 2011.
- 25 Stanley, E. H., Casson, N. J., Christel, S. T., Crawford, J. T., Loken, L. C., and Oliver, S. K.: The ecology of methane in streams and rivers: patterns, controls, and global significance, *Ecological Monographs*, doi:10.1890/15-1027, 2016.
- Steele, L. P., Fraser, P. J., Rasmussen, R. A., Khalil, M. A. K., Conway, T. J., Crawford, A. J., Gammon, R. H., Masarie, K. A., and Thoning, K. W.: The global distribution of methane in the troposphere, *Journal of Atmospheric Chemistry*, 5, 125-171, 1987.
- 30 Stocker, B. D., Spahni, R., and Joos, F.: DYP TOP: a cost-efficient TOPMODEL implementation to simulate sub-grid spatiotemporal dynamics of global wetlands and peatlands, *Geoscientific Model Development*, 7, 3089-3110, doi:10.5194/gmd-7-3089-2014, 2014.
- Sugimoto, A., Inoue, T., Kirtibutr, N., and Abe, T.: Methane oxidation by termite mounds estimated by the carbon isotopic composition of methane, *Global Biogeochemical Cycles*, 12, 595-605, doi:10.1029/98gb02266, 1998.
- 35 Sweeney, C., Karion, A., Wolter, S., Newberger, T., Guenther, D., Higgs, J. A., Andrews, A. E., Lang, P. M., Neff, D., Dlugokencky, E., Miller, J. B., Montzka, S. A., Miller, B. R., Masarie, K. A., Biraud, S. C., Novelli, P. C., Crotwell, M., Crotwell, A. M., Thoning, K., and Tans, P. P.: Seasonal climatology of CO₂ across North America from aircraft measurements in the NOAA/ESRL Global Greenhouse Gas Reference Network, *Journal of Geophysical Research: Atmospheres*, 120, 5155-5190, doi:10.1002/2014jd022591, 2015.
- 40 Swinnerton, J. W., and Linnenbom, V. J.: Gaseous Hydrocarbons in Sea Water: Determination, *Science*, 156, 1119-1120, doi:10.1126/science.156.3778.1119, 1967.
- Tarantola, A.: *Inverse problem theory*, edited by: Elsevier, Amsterdam, The Netherlands, 1987.
- Tarnocai, C., Canadell, J. G., Schuur, E. A. G., Kuhry, P., Mazhitova, G., and Zimov, S.: Soil organic carbon pools in the northern circumpolar permafrost region, *Global Biogeochemical Cycles*, 23, doi:10.1029/2008gb003327, 2009.
- 45 Terazawa, K., Ishizuka, S., Sakata, T., Yamada, K., and Takahashi, M.: Methane emissions from stems of *Fraxinus mandshurica* var. *japonica* trees in a floodplain forest, *Soil Biology and Biochemistry*, 39, 2689-2692, doi:10.1016/j.soilbio.2007.05.013, 2007.
- Thoning, K. W., Tans, P. P., and Komhyr, W. D.: Atmospheric carbon dioxide at Mauna Loa Observatory. 2. Analysis of the NOAA GMCC data, 1974,1985, *Journal of Geophysical Research*, 94, 8549-8565, 1989.
- 50



- Thorneloe, S. A., Barlaz, M. A., Peer, R., Huff, L. C., Davis, L., and Mangino, J.: Waste management, in: *Atmospheric Methane: Its Role in the Global Environment*, edited by: Khalil, M., Springer-Verlag, New York, 234–262, 2000.
- Thornton, J. A., Kercher, J. P., Riedel, T. P., Wagner, N. L., Cozic, J., Holloway, J. S., Dubé, W. P., Wolfe, G. M., Quinn, P. K., Middlebrook, A. M., Alexander, B., and Brown, S. S.: A large atomic chlorine source inferred from mid-continental reactive nitrogen chemistry, *Nature*, 464, 271–274, doi:10.1038/nature08905, 2010.
- 5 Tian, H., Xu, X., Liu, M., Ren, W., Zhang, C., Chen, G., and Lu, C.: Spatial and temporal patterns of CH₄ and N₂O fluxes in terrestrial ecosystems of North America during 1979–2008: application of a global biogeochemistry model, *Biogeosciences*, 7, 2673–2694, doi:10.5194/bg-7-2673-2010, 2010.
- Tian, H., Xu, X., Lu, C., Liu, M., Ren, W., Chen, G., Melillo, J., and Liu, J.: Net exchanges of CO₂, CH₄, and N₂O between China's terrestrial ecosystems and the atmosphere and their contributions to global climate warming, *Journal of Geophysical Research: Biogeosciences*, 116, G2, doi:10.1029/2010jg001393, 2011.
- 10 Tian, H., Chen, G., Lu, C., Xu, X., Ren, W., Zhang, B., Banger, K., Tao, B., Pan, S., Liu, M., Zhang, C., Bruhwiler, L., and Wofsy, S.: Global methane and nitrous oxide emissions from terrestrial ecosystems due to multiple environmental changes, *Ecosystem Health and Sustainability*, 1, 1–20, doi:10.1890/ehs14-0015.1, 2015.
- 15 Tian, H., Lu, C., Ciais, P., Michalak, A. M., Canadell, J. G., Saikawa, E., Huntzinger, D. N., Gurney, K. R., Sitch, S., Zhang, B., Yang, J., Bousquet, P., Bruhwiler, L., Chen, G., Dlugokencky, E., Friedlingstein, P., Melillo, J., Pan, S., Poulter, B., Prinn, R., Saunoy, M., Schwalm, C. R., and Wofsy, S. C.: The terrestrial biosphere as a net source of greenhouse gases to the atmosphere, *Nature*, 531, 225–228, doi:10.1038/nature16946, 2016.
- Tiwari, Y. K., and Kumar, K. R.: GHG observation programs in India, Asian GAWgreenhouse gases, 3, Korea Meteorological Administration, Chungnam, South Korea, 2012.
- 20 Tohjima, Y., Kubo, M., Minejima, C., Mukai, H., Tanimoto, H., Ganshin, A., Maksyutov, S., Katsumata, K., Machida, T., and Kita, K.: Temporal changes in the emissions of CH₄ and CO from China estimated from CH₄/CO₂ and CO/CO₂ correlations observed at Hateruma Island, *Atmospheric Chemistry and Physics*, 14, 1663–1677, doi:10.5194/acp-14-1663-2014, 2014.
- 25 Tubiello, F. N., Salvatore, M., Rossi, S., Ferrara, A., Fitton, N., and Smith, P.: The FAOSTAT database of greenhouse gas emissions from agriculture, *Environmental Research Letters*, 8, 015009, doi:10.1088/1748-9326/8/1/015009, 2013.
- Turetsky, M. R., Kotowska, A., Bubier, J., Dise, N. B., Crill, P., Hornibrook, E. R. C., Minkinen, K., Moore, T. R., Myers-Smith, I. H., Nykänen, H., Olefeldt, D., Rinne, J., Saarnio, S., Shurpali, N., Tuittila, E.-S., Waddington, J. M., White, J. R., Wickland, K. P., and Wilmking, M.: A synthesis of methane emissions from 71 northern, temperate, and subtropical wetlands, *Global Change Biology*, 20, 2183–2197, doi:10.1111/gcb.12580, 2014.
- 30 Turner, A. J., Jacob, D. J., Benmergui, J., Wofsy, S. C., Maasackers, J. D., Butz, A., Hasekamp, O., and Biraud, S. C.: A large increase in U.S. methane emissions over the past decade inferred from satellite data and surface observations, *Geophysical Research Letters*, 43, 2218–2224, doi:10.1002/2016gl067987, 2016.
- Tyler, S. C., Rice, A. L., and Ajie, H. O.: Stable isotope ratios in atmospheric CH₄: Implications for seasonal sources and sinks, *Journal of Geophysical Research-Atmospheres*, 112, D3, doi:10.1029/2006JD007231, 2007.
- 35 Umezawa, T., Machida, T., Aoki, S., and Nakazawa, T.: Contributions of natural and anthropogenic sources to atmospheric methane variations over western Siberia estimated from its carbon and hydrogen isotopes, *Global Biogeochemical Cycles*, 26, doi:10.1029/2011gb004232, 2012.
- Umezawa, T., Goto, D., Aoki, S., Ishijima, K., Patra, P. K., Sugawara, S., Morimoto, S., and Nakazawa, T.: Variations of tropospheric methane over Japan during 1988–2010, *Tellus*, B66, doi:10.3402/tellusb.v66.23837, 2014.
- 40 UNFCCC: Common Reporting Format (CRF) tables and annual Inventory Reports (NIRs). United Nations Framework Convention on Climate Change. Online at: http://unfccc.int/national_reports/annex_i_ghg_inventories/national_inventories_submissions/items/7383.php, 2013.
- USEPA: Global anthropogenic non-CO₂ greenhouse gas emissions: 1990–2020. United States Environmental Protection Agency, Washington D.C., 2006.
- 45 USEPA: Office of Atmospheric Programs (6207J), Methane and Nitrous Oxide Emissions From Natural Sources, U.S. Environmental Protection Agency, EPA 430-R-10-001. Available online at <http://nepis.epa.gov/>, Washington, DC 20460, 2010.
- USEPA: Draft: Global Anthropogenic Non-CO₂ Greenhouse Gas Emissions: 1990–2030. EPA 430-R-03-002, United States Environmental Protection Agency, Washington D.C., 2011.
- 50



- USEPA: Global Anthropogenic Non-CO₂ Greenhouse Gas Emissions 1990-2030, EPA 430-R-12-006, US Environmental Protection Agency, Washington DC., 2012.
- USEPA: Draft Inventory of U.S. Greenhouse gas Emissions and Sinks: 1990-2014. EPA 430-R-16-002. February 2016. U.S. Environmental protection Agency, Washington, DC, USA, 2016.
- 5 Valentine, D. W., Holland, E. A., and Schimel, D. S.: Ecosystem and physiological controls over methane production in northern wetlands, *Journal of Geophysical Research*, 99, 1563-1571, 1994.
- Valentini, R., Arneeth, A., Bombelli, A., Castaldi, S., Cazzolla Gatti, R., Chevallier, F., Ciais, P., Grieco, E., Hartmann, J., Henry, M., Houghton, R. A., Jung, M., Kutsch, W. L., Malhi, Y., Mayorga, E., Merbold, L., Murray-Tortarolo, G., Papale, D., Peylin, P., Poulter, B., Raymond, P. A., Santini, M., Sitch, S., Vaglio Laurin, G., van der Werf, G. R., Williams, C. A., and Scholes, R. J.: A full greenhouse gases budget of Africa: synthesis, uncertainties, and vulnerabilities, *Biogeosciences*, 11, 381-407, doi:10.5194/bg-11-381-2014, 2014.
- 10 van der Werf, G. R., Randerson, J. T., Collatz, G. J., Giglio, L., Kasibhatla, P. S., Arellano, A. F., Olsen, S. C., and Kasischke, E. S.: Continental-scale partitioning of fire emissions during the 1997 to 2001 El Nino/La Nina period, *Science*, 303, 73-76, 2004.
- 15 van der Werf, G. R., Randerson, J. T., Giglio, L., Collatz, G. J., Mu, M., Kasibhatla, P. S., Morton, D. C., DeFries, R. S., Jin, Y., and van Leeuwen, T. T.: Global fire emissions and the contribution of deforestation, savanna, forest, agricultural, and peat fires (1997-2009), *Atmospheric Chemistry and Physics*, 10, 11,707-711,735, 2010.
- van Groenigen, K. J., van Kessel, C., and Hungate, B. A.: Increased greenhouse-gas intensity of rice production under future atmospheric conditions, *Nature Climate Change*, 3, 288-291, doi:10.1038/nclimate1712, 2013.
- 20 van Leeuwen, T. T., van der Werf, G. R., Hoffmann, A. A., Detmers, R. G., Rücker, G., French, N. H. F., Archibald, S., Carvalho Jr, J. A., Cook, G. D., de Groot, W. J., Hély, C., Kasischke, E. S., Kloster, S., McCarty, J. L., Pettinari, M. L., Savadogo, P., Alvarado, E. C., Boschetti, L., Manuri, S., Meyer, C. P., Siegert, F., Trollope, L. A., and Trollope, W. S. W.: Biomass burning fuel consumption rates: a field measurement database, *Biogeosciences*, 11, 7305-7329, doi:10.5194/bg-11-7305-2014, 2014.
- 25 Verpoorter, C., Kutser, T., Seekell, D. A., and Tranvik, L. J.: A global inventory of lakes based on high-resolution satellite imagery, *Geophysical Research Letters*, 41, 6396-6402, doi:10.1002/2014gl060641, 2014.
- Vigano, I., van Weelden, H., Holzinger, R., Keppler, F., McLeod, A., and Rockmann, T.: Effect of UV radiation and temperature on the emission of methane from plant biomass and structural components, *Biogeosciences*, 5, 937-947, 2008.
- Voulgarakis, A., Naik, V., Lamarque, J. F., Shindell, D. T., Young, P. J., Prather, M. J., Wild, O., Field, R. D., Bergmann, D., Cameron-Smith, P., Cionni, I., Collins, W. J., Dalsøren, S. B., Doherty, R. M., Eyring, V., Faluvegi, G., Folberth, G. A., Horowitz, L. W., Josse, B., MacKenzie, I. A., Nagashima, T., Plummer, D. A., Righi, M., Rumbold, S. T., Stevenson, D. S., Strode, S. A., Sudo, K., Szopa, S., and Zeng, G.: Analysis of present day and future OH and methane lifetime in the ACCMIP simulations, *Atmospheric Chemistry and Physics*, 13, 2563-2587, doi:10.5194/acp-13-2563-2013, 2013.
- 30 Voulgarakis, A., Marlier, M. E., Faluvegi, G., Shindell, D. T., Tsigaridis, K., and Mangeon, S.: Interannual variability of tropospheric trace gases and aerosols: The role of biomass burning emissions, *Journal of Geophysical Research: Atmospheres*, 120, 7157-7173, doi:10.1002/2014jd022926, 2015.
- 35 Wallmann, K., Pinero, E., Burwicz, E., Haeckel, M., Hensen, C., Dale, A., and Ruepke, L.: The Global Inventory of Methane Hydrate in Marine Sediments: A Theoretical Approach, *Energies*, 5, 2449, 2012.
- Wang, Z., Deutscher, N. M., Warneke, T., Notholt, J., Dils, B., Griffith, D. W. T., Schmidt, M., Ramonet, M., and Gerbig, C.: Retrieval of tropospheric column-averaged CH₄ mole fraction by solar absorption FTIR-spectrometry using N₂O as a proxy, *Atmospheric Measurement Techniques*, 7, 3295-3305, doi:10.5194/amt-7-3295-2014, 2014.
- 40 Wania, R., Ross, I., and Prentice, I. C.: Implementation and evaluation of a new methane model within a dynamic global vegetation model: LPJ-WHyMe v1.3, *Geoscientific Model Development Discussions*, 3, 1-59, 2010.
- Wania, R., Melton, J. R., Hodson, E. L., Poulter, B., Ringeval, B., Spahni, R., Bohn, T., Avis, C. A., Chen, G., Eliseev, A. V., Hopcroft, P. O., Riley, W. J., Subin, Z. M., Tian, H., van Bodegom, P. M., Kleinen, T., Yu, Z. C., Singarayer, J. S., Zurcher, S., Lettenmaier, D. P., Beerling, D. J., Denisov, S. N., Prigent, C., Papa, F., and Kaplan, J. O.: Present state of global wetland extent and wetland methane modelling: Methodology of a model inter-comparison project (WETCHIMP), *Geoscientific Model Development*, 6, 617-641, 2013.
- 45 Wassmann, R., Lantin, R. S., Neue, H. U., Buendia, L. V., Corton, T. M., and Lu, Y.: Characterization of methane emissions in Asia III: Mitigation options and future research needs, *Nutrient Cycling in Agroecosystems*, 58, 23-36, 2000.
- 50



- Whalen, S. C.: Biogeochemistry of Methane Exchange between Natural Wetlands and the Atmosphere *Environmental Engineering Science*, 22, 73-94, doi:10.1089/ees.2005.22.73, 2005.
- Wiedinmyer, C., Tie, X., Guenther, A., Neilson, R., and Granier, C.: Future Changes in Biogenic Isoprene Emissions: How Might They Affect Regional and Global Atmospheric Chemistry?, *Earth Interactions*, 10, doi:10.1175/EI174.1, 2006.
- 5 Wiedinmyer, C., Akagi, S. K., Yokelson, R. J., Emmons, L. K., Al-Saadi, J. A., Orlando, J. J., and Soja, A. J.: The Fire INventory from NCAR (FINN): A high resolution global model to estimate the emissions from open burning, *Geoscientific Model Development*, 4, 625-641, doi:10.5194/gmd-4-625-2011, 2011.
- Wik, M., Thornton, B. F., Bastviken, D., MacIntyre, S., Varner, R. K., and Crill, P. M.: Energy input is primary controller of methane bubbling in subarctic lakes, *Geophysical Research Letters*, 41, 2013GL058510, doi:10.1002/2013gl058510, 2014.
- 10 Wik, M., Thornton, B. F., Bastviken, D., Uhlbäck, J., and Crill, P. M.: Biased sampling of methane release from northern lakes: A problem for extrapolation, *Geophysical Research Letters*, 43, 1256-1262, doi:10.1002/2015gl066501, 2016a.
- Wik, M., Varner, R. K., Anthony, K. W., MacIntyre, S., and Bastviken, D.: Climate-sensitive northern lakes and ponds are critical components of methane release, *Nature Geoscience*, 9, 99-105, doi:10.1038/ngeo2578, 2016b.
- 15 Williams, J. E., Strunk, A., Huijnen, V., and van Weele, M.: The application of the Modified Band Approach for the calculation of on-line photodissociation rate constants in TM5: implications for oxidative capacity, *Geoscientific Model Development*, 5, 15-35, doi:10.5194/gmd-5-15-2012, 2012.
- Winderlich, J., Chen, H., Gerbig, C., Seifert, T., Kolle, O., Lavrič, J. V., Kaiser, C., Höfer, A., and Heimann, M.: Continuous low-maintenance CO₂/CH₄/H₂O measurements at the Zotino Tall Tower Observatory (ZOTTO) in Central Siberia, *Atmospheric Measurement Techniques*, 3, 1113-1128, doi:10.5194/amt-3-1113-2010, 2010.
- 20 Wofsy, S. C.: HIPER Pole-to-Pole Observations (HIPPO): fine-grained, global-scale measurements of climatically important atmospheric gases and aerosols, *Philosophical Transactions of the Royal Society of London A: Mathematical, Physical and Engineering Sciences*, 369, 2073-2086, doi:10.1098/rsta.2010.0313, 2011.
- Woodward, F. I., and Lomas, M. R.: Vegetation dynamics – simulating responses to climatic change, *Biological Reviews*, 79, 643-670, doi:10.1017/s1464793103006419, 2004.
- 25 Woodward, G., Gessner, M. O., Giller, P. S., Gulis, V., Hladyz, S., Lecerf, A., Malmqvist, B., McKie, B. G., Tiegs, S. D., Cariss, H., Dobson, M., Eloegi, A., Ferreira, V., Graça, M. A. S., Fleituch, T., Lacoursière, J. O., Nistorescu, M., Pozo, J., Risnoveanu, G., Schindler, M., Vadineanu, A., Vought, L. B.-M., and Chauvet, E.: Continental-Scale Effects of Nutrient Pollution on Stream Ecosystem Functioning, *Science*, 336, 1438-1440, doi:10.1126/science.1219534, 2012.
- 30 Wooster, M. J., Roberts, G., Perry, G. L. W., and Kaufman, Y. J.: Retrieval of biomass combustion rates and totals from fire radiative power observations: FRP derivation and calibration relationships between biomass consumption and fire radiative energy release, *Journal of Geophysical Research: Atmospheres*, 110, doi:10.1029/2005jd006318, 2005.
- Wuebbles, D. J., and Hayhoe, K.: Atmospheric methane and global change, *Earth-Science Reviews*, 57, 177-210, 2002.
- 35 Wunch, D., Toon, G. C., Blavier, J.-F. L., Washenfelder, R. A., Notholt, J., Connor, B. J., Griffith, D. W. T., Sherlock, V., and Wennberg, P. O.: The Total Carbon Column Observing Network, *Philosophical Transactions of the Royal Society A*, 369, doi:10.1098/rsta.2010.0240, 2011.
- Xu, X., and Tian, H.: Methane exchange between marshland and the atmosphere over China during 1949–2008, *Global Biogeochemical Cycles*, 26, doi:10.1029/2010gb003946, 2012.
- 40 Xu, X. F., Tian, H. Q., Zhang, C., Liu, M. L., Ren, W., Chen, G. S., Lu, C. Q., and Bruhwiler, L.: Attribution of spatial and temporal variations in terrestrial methane flux over North America, *Biogeosciences*, 7, 3637-3655, doi:10.5194/bg-7-3637-2010, 2010.
- Yan, X., Akiyama, H., Yagi, K., and Akimoto, H.: Global estimations of the inventory and mitigation potential of methane emissions from rice cultivation conducted using the 2006 Intergovernmental Panel on Climate Change Guidelines, *Global Biogeochemical Cycles*, 23, doi:10.1029/2008gb003299, 2009.
- 45 Yin, Y., Chevallier, F., Ciais, P., Broquet, G., Fortems-Cheiney, A., Pison, I., and Saunoy, M.: Decadal trends in global CO emissions as seen by MOPITT, *Atmospheric Chemistry and Physics*, 15, 13433-13451, doi:10.5194/acp-15-13433-2015, 2015.
- Yoshida, Y., Kikuchi, N., Morino, I., Uchino, O., Oshchepkov, S., Bril, A., Saeki, T., Schutgens, N., Toon, G. C., Wunch, D., Roehl, C. M., Wennberg, P. O., Griffith, D. W. T., Deutscher, N. M., Warneke, T., Notholt, J., Robinson, J., Sherlock, V., Connor, B., Rettinger, M., Sussmann, R., Ahonen, P., Heikkinen, P., Kyrö, E., Mendonca, J., Strong, K., Hase, F., Dohe,
- 50



- S., and Yokota, T.: Improvement of the retrieval algorithm for GOSAT SWIR XCO₂ and XCH₄ and their validation using TCCON data, *Atmospheric Measurement Techniques*, 6, 1533-1547, doi:10.5194/amt-6-1533-2013, 2013.
- Zavala-Araiza, D., Lyon, D. R., Alvarez, R. A., Davis, K. J., Harriss, R., Herndon, S. C., Karion, A., Kort, E. A., Lamb, B. K., Lan, X., Marchese, A. J., Pacala, S. W., Robinson, A. L., Shepson, P. B., Sweeney, C., Talbot, R., Townsend-Small, A., Yacovitch, T. I., Zimmerle, D. J., and Hamburg, S. P.: Reconciling divergent estimates of oil and gas methane emissions, *Proceedings of the National Academy of Sciences USA* 112, 15597-15602, doi:10.1073/pnas.1522126112, 2015.
- Zhang: Magnitude, spatio-temporal variability and environmental controls of methane emissions from global rice fields: Implications for water management and climate mitigation, *Global Change Biology*, 2016, submitted.
- 10 Zhang, B., and Chen, G. Q.: China's CH₄ and CO₂ Emissions: Bottom-Up Estimation and Comparative Analysis, *Ecological Indicators*, 47, 112-122, doi:10.1016/j.ecolind.2014.01.022, 2014.
- Zhang, T., Barry, R. G., Knowles, K., Heginbottom, J. A., and Brown, J.: Statistics and characteristics of permafrost and ground-ice distribution in the Northern Hemisphere, *Polar Geography*, 23, 132-154, 1999.
- Zhang, X., Myhrvold, N. P., and Caldeira, K.: Key factors for assessing climate benefits of natural gas versus coal electricity generation, *Environmental Research Letters* 9, doi:10.1088/1748-9326/9/11/114022, 2014.
- 15 Zhu, Q., Liu, J., Peng, C., Chen, H., Fang, X., Jiang, H., Yang, G., Zhu, D., Wang, W., and Zhou, X.: Modelling methane emissions from natural wetlands by development and application of the TRIPLEX-GHG model, *Geoscientific Model Development*, 7, 981-999, doi:10.5194/gmd-7-981-2014, 2014.
- Zhu, Q., Peng, C., Chen, H., Fang, X., Liu, J., Jiang, H., Yang, Y., and Yang, G.: Estimating global natural wetland methane emissions using process modelling: spatio-temporal patterns and contributions to atmospheric methane fluctuations, *Global Ecology and Biogeography*, 24, 959-972, 2015.
- Zhuravlev, R. V., Ganshin, A. V., Maksyutov, S., Oshchepkov, S. L., and Khattatov, B. V.: Estimation of global CO₂ fluxes using ground-based and satellite (GOSAT) observation data with empirical orthogonal functions, *Atmospheric and Oceanic Optics*, 26, 507-516, doi:10.1143/s1024856013060158, 2013.
- 25 Zona, D., Gioli, B., Commane, R., Lindaas, J., Wofsy, S. C., Miller, C. E., Dinardo, S. J., Dengel, S., Sweeney, C., Karion, A., Chang, R. Y.-W., Henderson, J. M., Murphy, P. C., Goodrich, J. P., Moreaux, V., Liljedahl, A., Watts, J. D., Kimball, J. S., Lipson, D. A., and Oechel, W. C.: Cold season emissions dominate the Arctic tundra methane budget, *Proceedings of the National Academy of Sciences of the United States of America*, 113, 40-45, doi:10.1073/pnas.1516017113, 2016.
- Zürcher, S., Spahni, R., Joos, F., Steinacher, M., and Fischer, H.: Impact of an abrupt cooling event on interglacial methane emissions in northern peatlands, *Biogeosciences*, 10, 1963-1981, doi:10.5194/bg-10-1963-2013, 2013.
- 30

35

40

**Table 1: B-U models and inventories used in this study.**

B-U models and inventories	Contribution	Time period (resolution)	Gridded	References
EDGAR4.2 FT2010	Fossil fuels, Agriculture and waste, biofuel	2000-2010 (yearly)	X	EDGAR (2013), Olivier et al. (2012)
EDGARv4.2FT2012	Total anthropogenic	2000-2012 (yearly)		EDGAR (2014), Olivier and Janssens-Maenhout (2014), Rogelj et al. (2014)
EDGARv4.2EXT	Fossil fuels, Agriculture and waste, biofuel	1990-2013 (yearly)		Based on EDGARv4.1 (EDGAR, 2010), this study
USEPA	Fossil fuels, Agriculture and waste, biofuel,	1990-2030 (10-yr interval, interpolated in this study)		USEPA (2006, 2011, 2012)
IIASA GAINS ECLIPSE	Fossil fuels, Agriculture and waste, biofuel	1990-2050 (5-yr interval, interpolated in this study)	X	Höglund-Isaksson (2012), Klimont et al. (2016)
FAO-CH ₄	Agriculture, Biomass Burning	Agriculture: 1961-2012 BBG: 1990-2014		Tubiello et al. (2013)
GFEDv3	Biomass burning	1997-2011	X	van der Werf et al. (2010)
GFEDv4s	Biomass burning	1997-2014	X	Giglio et al. (2013)
GFASv1.0	Biomass burning	2000-2013	X	Kaiser et al. (2012)
FINNv1	Biomass burning	2003-2014	X	Wiedinmyer et al. (2011)
CLM 4.5	Natural wetlands	2000-2012	X	Riley et al. (2011)
CTEM	Natural wetlands	2000-2012	X	Melton and Arora (2016)
DLEM	Natural wetlands	2000-2012	X	Tian et al., (2010;2015)
JULES	Natural wetlands	2000-2012	X	Hayman et al. (2014)
LPJ-MPI	Natural wetlands	2000-2012	X	Kleinen et al. (2012)
LPJ-wsl	Natural wetlands	2000-2012	X	Hodson et al. (2011)
LPX-Bern	Natural wetlands	2000-2012	X	Spahni et al. (2011)
ORCHIDEE	Natural wetlands	2000-2012	X	Ringeval et al. (2011)
SDGVM	Natural wetlands	2000-2012	X	Woodward and Lomas (2004), Cao et al. (1996)
TRIPLEX-GHG	Natural wetlands	2000-2012	X	Zhu et al., (2014;2015)
VISIT	Natural wetlands	2000-2012	X	Ito and Inatomi (2012)

5

10



Table 2. Global methane emissions by source type in Tg CH₄ yr⁻¹ from K13 (left columns) and for this work using B-U (middle column) and T-D (right columns). As T-D models cannot fully separate individual processes, only emissions for five categories are provided (see text). Uncertainties are reported as [min-max] range of reported studies. Differences of 1 Tg CH₄ yr⁻¹ in the totals can occur due to rounding errors.

Period of time	K13 B-U	K13 T-D	B-U			T-D		
	2000-2009	2000-2009	2000-2009	2003-2012	2012	2000-2009	2003-2012	2012
NATURAL SOURCES	347 [238-484]	218 [179-273]	382 [255-519]	384 [257-524]	386 [259-532]	234 [194-292]	231 [194-296]	221 [192-302]
Natural wetlands	217 [177-284]	175 [142-208]	183 [151-222]	185 [153-227]	187 [155-235]	166 [125-204]	167 [127-202]	172 [155-201]
Other natural sources				199 [104-297]		68 [21-130]	64 [21-132]	49 [22-68]
Other land sources	112 [43-192]	43 [37-65]		185 [99-272]				
Fresh waters	40 [8-73]			122 [60-180]				
Geological (onshore)	36 [15-57]			40 [30-56]				
Wild animals	15 [15-15]			10 [5-15]				
Termites	11 [2-22]			9 [3-15]				
Wild fires	3 [1-5]			3 [1-5]				
Permafrost soils (direct)	1 [0-1]			1 [0-1]				
Oceanic sources	18 [2-40]			14 [5-25]				
Geological (offshore)	-			12 [5-20]				
Other (incl. hydrates)	-			2 [0-5]				
ANTHROPOGENIC SOURCES	331 [304-368]	335 [273-409]	338 [329-342]	352 [340-360]	370 [351-385]	319 [255-357]	328 [259-370]	347 [262-384]
Agriculture and waste	200 [187-224]	209 [180-241]	190 [174-201]	195 [178-206]	197 [183-211]	183 [112-241]	188 [115-243]	200 [201-213]
Enteric ferm. & manure	101 [98-105] ^a		103 [95-109] ^b	106 [97-111] ^b	107 [100-112] ^b			
Landfills & waste	63 [56-79] ^a		57 [51-61] ^b	59 [52-63] ^b	60 [54-66] ^b			
Rice cultivation	36 [33-40]		29 [23-35] ^b	30 [24-36] ^b	29 [25-39] ^b			
Fossil fuels	96 [85-105]	96 [77-123]	112 [107-126]	121 [114-133]	134 [123-141]	101 [77-126]	105 [77-133]	112 [90-137]
Coal mining	-	-	36 [24-43] ^b	41 [26-50] ^b	46 [29-62] ^b			
Gas, oil, & industry	-	-	76 [64-85] ^b	79 [69-88] ^b	88 [78-94] ^b			
Biomass & biof. burn.	35 [32-39]	30 [24-45]	30 [26-34]	30 [27-35]	30 [25-36]	35 [16-53]	34 [15-53]	35 [28-40]
Biomass burning	-	-	18 [15-20]	18 [15-21]	17 [13-21]			
Biofuel burning	-	-	12 [9-14]	12 [10-14]	12 [10-14]			
SINKS						546^c	548^c	555^c
Total chemical loss	604 [483-738]	518 [510-538]				514^d	515^d	518^d
Tropospheric OH	528 [454-617]							
Stratospheric loss	51 [16-84]							
Tropospheric Cl	25 [13-37]							
Soil uptake	28 [9-47]	32 [26-42]				32 [27-38]	33 [28-38]	36 [30-42]
Sum of sources	678 [542-852]	553 [526-569]	719 [583-861]	736 [596-884]	756 [609-916]	552 [535-566]	558 [540-568]	568 [560-580]
Sum of Sinks	632 [592-785]	550 [514-560]				546^c	548^c	556^c
Imbalance		3 [-4-19]				6^c	10^c	14^c
Atmospheric growth		6				6.0 [4.9-6.6]	10.0 [9.4-10.6]	14.0 []

^a: Manure is now included in Enteric fermentation & manure and not in waste category.

^b: For HASA inventory the breakdown of agriculture and waste (rice, Enteric fermentation & manure, Landfills & waste) and fossil fuel (coal, oil, gas & industry) sources use the same ratios as the mean of EDGAR and EPA inventories.

^c: total sink is deduced from global mass balance and not directly computed.

^d: computed as the difference of global sink and soil uptake.

10

15

**Table 3: Top-down studies used in this study with their contribution to the decadal and yearly estimates. For decadal means, TD Studies have to provide at least 6 years over the decade to contribute to the estimate. All T-D studies provided both total and per categories (including soil uptake) partitioning.**

Model	Institution	Observation used	Time period	Number of inversions	2000-2009	2003-2012	2012	References
Carbon Tracker-CH ₄	NOAA	Surface stations	2000-2009	1	X	X		Bruhwyler et al. (2014)
LMDZ-MIOP	LSCE/CEA	Surface stations	1990-2013	10	X	X	X	Pison et al. (2013)
LMDZ-PYVAR	LSCE/CEA	Surface stations	2006-2012	6		X	X	Locatelli et al. (2015)
LMDZ-PYVAR	LSCE/CEA	GOSAT satellite	2010-2013	3			X	
TM5	SRON	Surface stations	2003-2010	1		X		Houweling et al. (2014)
TM5	SRON	GOSAT satellite	2009-2012	2			X	
TM5	SRON	SCIAMACHY satellite	2003-2010	1		X		
TM5	EC-JRC	Surface stations	2000-2012	1	X	X	X	Bergamaschi et al. (2013), Alexe et al. (2015)
TM5	EC-JRC	GOSAT satellite	2010-2012	1			X	Ishizawa et al. (2016, submitted); Zhuravlev et al. (2013)
GELCA	NIES	Surface stations	2000-2012	1	X	X	X	Patra et al. (2016)
ACTM	JAMSTEC	Surface stations	2002-2012	1	X	X	X	Saeki et al. (2013), Kim et al. (2011)
NIESTM	NIES	Surface stations	2010-2012	1			X	
NIESTM	NIES	GOSAT satellite	2010-2012	1			X	

5

10

15



Table 4: Global, latitudinal, and regional methane emissions in Tg CH₄ yr⁻¹, as decadal means (2000-2009 and 2003-2012) and for the year 2012, for this work using T-D inversions. Global emissions are also compared with K13 for T-D and B-U for 2000-2009. Uncertainties are reported as [min-max] range of reported studies. Differences of 1 Tg CH₄ yr⁻¹ in the totals can occur due to rounding errors.

Period	T-D			B-U
	2000-2009	2003-2012	2012	2000-2009
GLOBAL				
this work	552 [535-566]	558 [540-568]	568 [560-580]	719 [583-861]
<i>Kirschke et al. (2013)</i>	<i>553</i> [526-569]	-	-	<i>678</i> [542-852]
LATITUDINAL				
< 30°N	356 [334-381]	359 [339-386]	360 [341-393]	
30°N-60°N	176 [159-195]	179 [162-199]	185 [164-203]	
60°-90°N	20 [15-25]	21 [15-24]	23 [19-31]	
REGIONAL				
Cent. North America	11 [4-15]	11 [5-15]	11 [6-14]	
Tropical South America	82 [63-99]	84 [65-101]	94 [76-119]	
Temp. South America	17 [12-28]	17 [12-27]	14 [11-18]	
Northern Africa	42 [36-55]	42 [36-55]	41 [36-46]	
Southern Africa	44 [37-55]	44 [37-53]	44 [34-60]	
South East Asia	72 [54-84]	73 [55-84]	74 [66-83]	
India	39 [28-45]	39 [37-46]	38 [27-48]	
Oceania	11 [8-19]	11 [7-19]	10 [7-12]	
Contiguous USA	43 [38-49]	41 [34-49]	41 [33-49]	
Europe	28 [22-34]	28 [21-34]	29 [20-34]	
Central Eurasia & Japan	45 [38-51]	46 [38-54]	48 [38-57]	
China	54 [50-56]	58 [51-72]	58 [42-77]	
Boreal North America	20 [13-27]	20 [13-27]	23 [20-27]	
Russia	38 [32-44]	38 [31-44]	39 [31-46]	
Oceans	7 [0-12]	6 [0-12]	4 [0-13]	

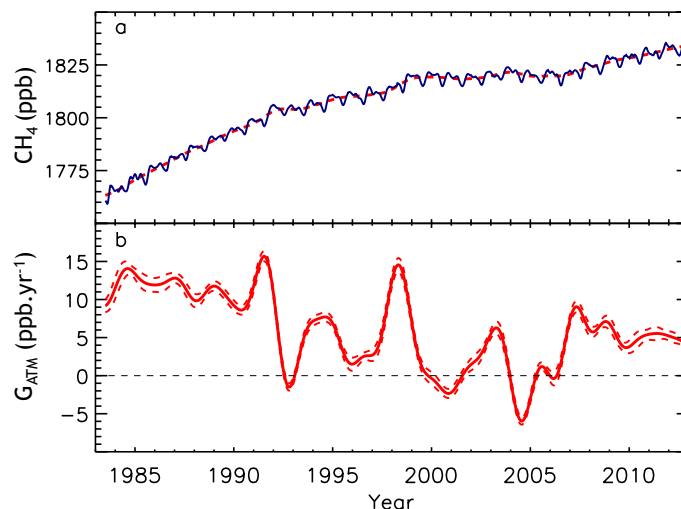


Figure 1: Globally averaged atmospheric CH₄ (ppb) (a) and its annual growth rate G_{ATM} (ppb yr⁻¹) (b) from four measurement programs, National Oceanic and Atmospheric Administration (NOAA), Advanced Global Atmospheric Gases Experiment (AGAGE), Commonwealth Scientific and Industrial Research Organisation (CSIRO), and University of California, Irvine (UCI). Detailed descriptions of methods are given in the supplementary material of K13.

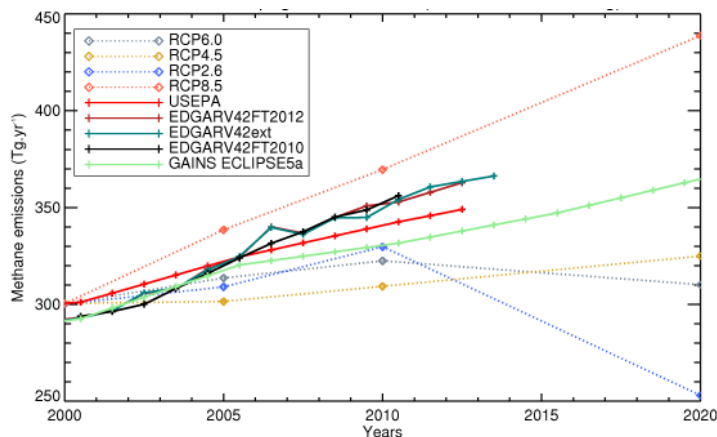


Figure 2: Global anthropogenic methane emissions (excluding biomass burning) from historical inventories and future projections (in Tg CH₄ yr⁻¹). USEPA and GAINS estimates have been linearly interpolated from the 10 or 5-year original products to yearly values. After 2005, USEPA original estimates are projections.

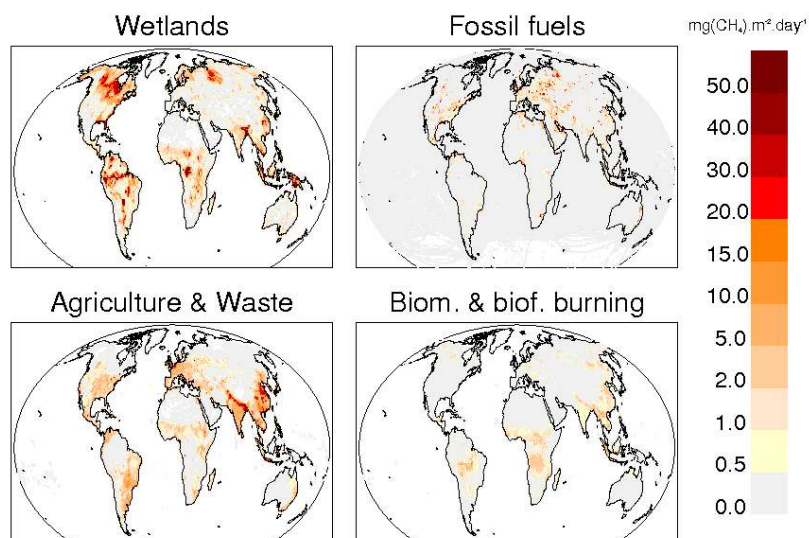


Figure 3: Methane emissions from four source categories: natural wetlands, biomass and biofuel burning, Agriculture and Waste and Fossil fuels for the 2003-2012 decade in $\text{mg CH}_4 \text{ m}^{-2} \text{ day}^{-1}$. The wetland emission map represents the mean daily emission average over the eleven biogeochemical models listed in Table 1 and over the 2003-2012 decade. Fossil fuel and Agriculture and Waste emission maps are derived from the mean estimates of EGDARV42FT2010 and GAINS models. The biomass and biofuel burning map results from the mean of the biomass burning inventories listed in Table 1 added to the mean of the biofuel estimate from EDGARv42FT2010 and GAINS models.

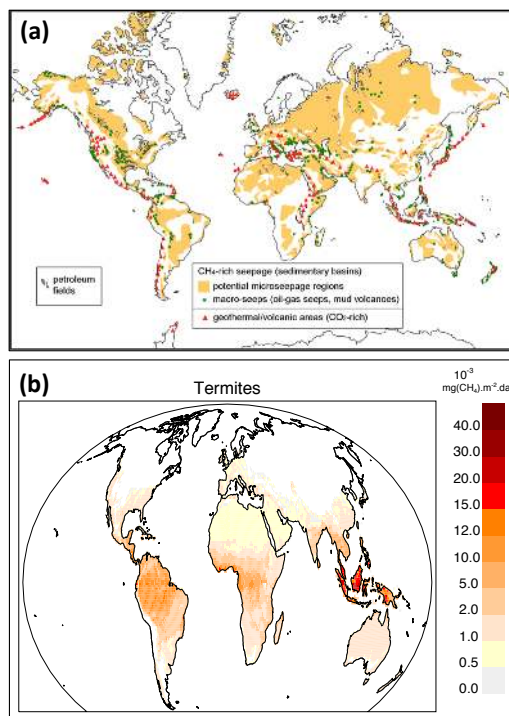


Figure 4: (a) Map of areas and locations for geological emissions of methane related to the different categories mentioned in the text (Sect. 3.2.3) (b) Climatological CH₄ emissions from termites over the period 2000-2007 (Sect. 3.2.4).

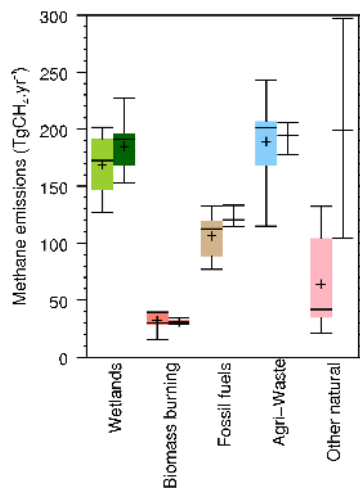


Figure 5: Methane global emissions from the five broad categories (see Sect. 2.3) for the 2003-2012 decade for T-D inversions models (left light coloured boxplots) in Tg CH₄ yr⁻¹ and for B-U models and inventories (right dark coloured boxplots). Median value, first and third quartiles are presented in the boxes. The whiskers represent the minimum and maximum values when suspected outliers are removed (see Sect. 2.2). Suspected outliers are marked with stars when existing. B-U quartiles are not available for B-U estimates. Mean values are represented with “+” symbols, these are the values reported in Table 2.

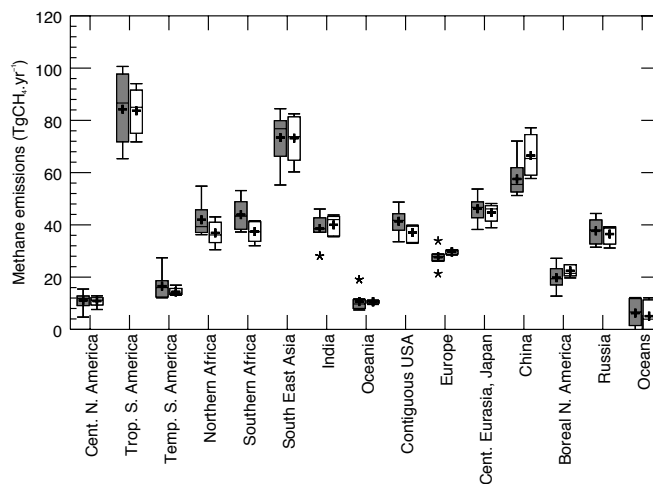


Figure 6: Regional methane emissions for the 2003-2012 decade from top-down inversions (grey) and for the prior estimates used in the inversions (white). Each box plot represents the range of the top-down estimates inferred by the ensemble of inversion approach. Median value, first and third quartiles are presented in the box. The whiskers represent the minimum and maximum values when suspected outliers are removed (see Sect. 2.2). Outliers are marked with stars when existing. Mean values are represented with “+” symbols, these are the values reported in Table 4.

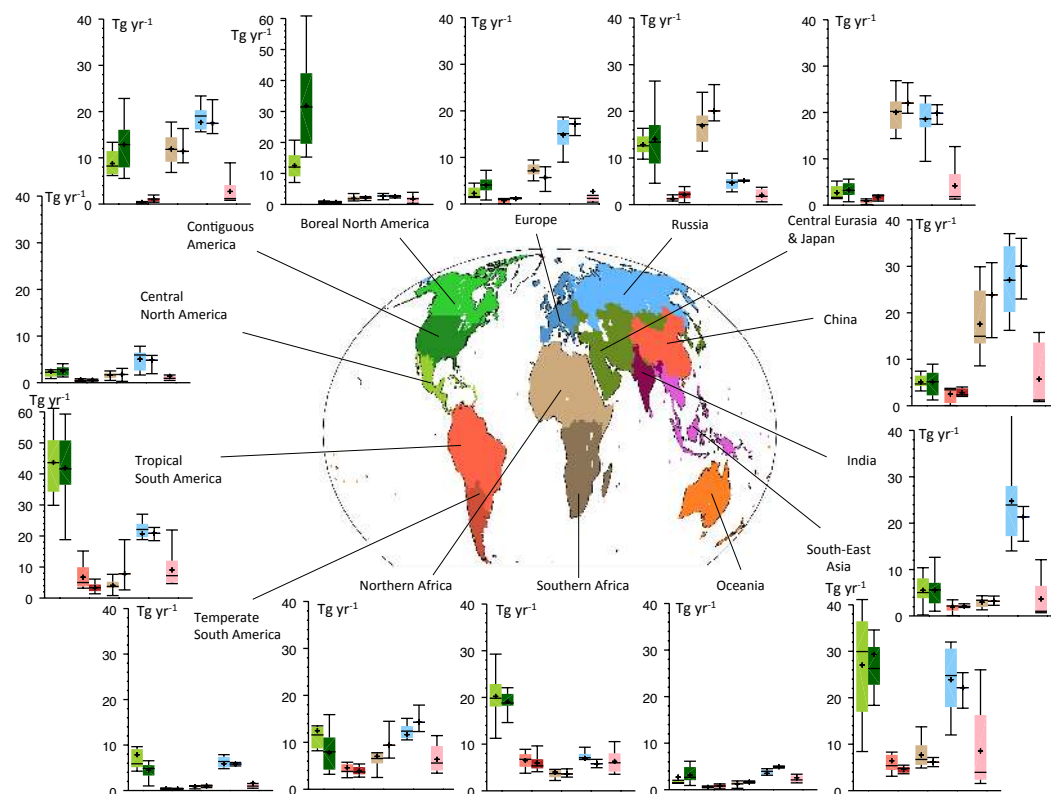


Figure 7: Regional CH_4 budget in $\text{Tg CH}_4, \text{yr}^{-1}$ per category (same as for the global emissions in Fig. 6) and map of the 14 continental regions considered in this study. The CH_4 emissions are given for the five categories from left to right (wetlands, biomass burning, fossil fuels, agriculture and waste, and other natural). TD estimates are given by the left dark coloured boxes and BU estimates by the right light coloured boxes.